CHAPTER ONE

Introduction

1.1 Background:

Achieving higher quality and lower cost of textiles is a basic strategy for retailers and producers around the world over the past decade. Furthermore, wide adoption of quality management standards such as ISO 9000 requires the standardization and automation of design, production, and quality control of textile products. As a computational power growing almost daily at lower costs, measurement and digital imaging in the textile industry is facing new opportunities and unprecedented challenges. Improving the quality of yarn and fabric is the main focus of the new challenge. All yarns are inherently prone to periodic and random variations. However, the effects of variation on the resulting fabric are difficult to predict due to limitations in measurement technology, computation and especially unpredictable mapping from yarn to fabric. Although there are several studies (Peirce, 1937, Suh & et. al, 2003) suggesting where a yarn may be located in a fabric, in reality the fabrication process is far from ideal. Until recently, non-uniformity of fabric appearance has been assessed by the standard yarn board that shows yarn variations. In addition to traditional yarn boards, fabric samples were often produced by actual weaving or knitting, although this is expensive and time consuming. Extensive research work has been carried out by many researchers in the past to develop a system for characterizing numerous fabric properties, some through the introduction of quality indices and others by new methods of measurement using time series analysis, Fourier transform, and wavelets (E. J. Wood,1990 , Pourdeyhimi &Spivak, 1991, Zweigle,1997 ,

Arkady , 1998 , Arkady,1999 , Sule & Bardhan , 1999 and Akio et.al , 2001) However, these measures are of limited capacity to evaluate the features of irregular fabric. Methods such as the Kawabata System (KES) and fabric assurance by simple testing (FAST) have been developed for the rating of fabric's mechanical properties and used widely by fabric manufacturers and testers. These systems combine objective measurements with subjective rating methods and produce indices that may be useful when comparing fabrics. In addition to these various indices and methods, a few yarn quality testing instruments are nowadays equipped with devices for obtaining information on yarn properties on-line or off-line and then mapping them into weave or knit fabric structures in order to help the manufacturer visualize the final product. A quick review of the literature indicates that methods for analyzing yarn irregularity using spectrograms, correlograms, and variance-length curves are advanced. They are widely accepted by yarn manufacturers. On the other hand, widely accepted standardized methods are not available for fabrics. There are several possible reasons why irregularities have not been defined or measured properly in the past for woven, knitted, and nonwoven fabrics. These reasons can be summarized as follows;

- Difficulty in measuring the properties of two-dimensional fabric at reasonable cost;
- Difficulty in mapping from yarn to fabrics;
- Difficultly in interpreting the information obtained through the measurement sensors.

Therefore, the first goal of this research was to suggest a method for characterization of knitted fabric irregularity and the second goal was to

develop a theoretical approach for estimating knitted fabric irregularity based on yarn irregularity measurements.

Although in this study, fabric irregularity is defined in terms of mass distribution, the theory and practical applications of yarn irregularity analysis methods are examined and then ways to expand or carry over some of these ideas into analysis of fabric mass uniformity are proposed. Since, the major factor affecting fabric appearance is the yarn irregularity, it was important to understand the causes of yarn irregularity and the methods for analyzing them. With this methodology, it is hoped not only understand the yarn formation, especially the random fiber arrangement and the twist distribution within the yarn, but also to expand or carry over some of the yarn irregularity analysis methods to characterize fabric irregularity.

1.2. Yarn irregularity:

Yarn evenness is an important property that must be studied and identified accurately and improved because it affects directly on a regular basis, the cloth and its general appearance, which definitively determines acceptability. It is a measure of the level of variation in yarn linear density or mass per unit length. In other words, it refers to the variation in yarn count along its length. A yarn with poor evenness will have thick and thin places along its length, while an even yarn will have little variation in mass or thickness along length. While a yarn may vary in many properties, evenness is the most important quality aspect of a yarn, because variations in other yarn properties are often a direct result of yarn count irregularity. It is well known that twist tends to accumulate at the thin places in a yarn, so irregularity in yarn linear density will cause variations in twist along the

yarn length. This preferential concentration of twist in thin places along a yarn also exacerbates the variations in yarn diameter or thickness, which often adversely affects the appearance of the resultant fabrics. An irregular yarn will also vary in strength along the yarn. The importance of irregularity arises from the following factors:

- Irregularity has a profound influence on appearance of yarn and fabric. More regular the yarn, better will be the appearance and aesthetic value of the product. As a result, better sale value can be achieved.
- Regularity contributes to a smoother feel. In apparel and most of other textiles, smoothness is the most desired characteristic. Sale value of fabric is dependent, among other things, on smoothness.
- Regular yarns will have fewer weak places and, as yarn breaks at weakest place, it will have a better strength. Better strength realization from fibre can be achieved if regularity of yarn is improved. It is for this reason mills, which produce more regular yarn, are able to produce a yarn of much higher strength from the same cotton
- Because of the lower incidence of weak places, fewer end breaks are encountered with regular yarns in weaving preparatory, weaving and knitting. Efficiency in these processes is improved leading to higher productivity.
- Fabric defects and rejections are critically influenced by irregularity of yarns. Periodic and quasi periodic irregularities in yarn result in warp way streaks and weft bars in woven fabrics leading to fabric rejections. Yarn defects like slubs, crackers, long thick places and

long thin places downgrade the fabric and cause considerable value loss. Mills which produce more regular yarns therefore get better realization and contribution and as a result higher profitability.

1.2.1 Yarn Irregularity Sources:

The regularity of a yarn fundamentally depends on fibers and their arrangement within the yarn (Warren & Moon, 2005). The causes of irregularity are:

1. Random fiber arrangement and fiber-length: the fibers constituting the yarn are arranged in a completely random way during blending, carding, doubling, roving, and spinning processes. Therefore all the fibres have the same chance of being found at any selected place in the yarn. Therefore the fiber length variation causes irregularity in yarn cross-section.

2. Effect of drafting waves: In drafting process the short fibers move in groups causing non-random wave-like patterns called drafting waves, which are responsible for periodic thin and thick places over a yarn length (B. P. Saville , 2000).

3. Twist variation: Fundamentally spun yarn production involves twisting of a random fiber array. Twisting tends to condense the yarn structure into an irregular close-packed polygonal shape, but the cross-section still possesses a concave-convex irregular shape (J. W. S. Hearle etc all, 1969). In addition, there is a complex relationship between yarn diameter, twist, and mass. Therefore, it is hard to predict the effect of twist on yarn structure. For example, twist is not constant but accumulated in the thinnest

parts of the yarn. Therefore, high twist compresses thin places and exaggerates the variations in the apparent diameter (Alberto, 1952).

4. Foreign elements existence: Neps are caused by foreign elements, immature fibres, and insufficient and improper cleaning during preparation processes. These faults are usually random and visible to the human eye. They are detected by many evenness-testing instruments. When a cross-section deviation exceeds a preset value, the instrument classifies the imperfection as either a nep, or a thin or thick place. The standard levels are as follows, +200%, -50% and +50%, respectively. The length of the fault is usually in the order of a few centimeters (Uster Tester 4-SX, 2004). A yarn's neps, thin places, and thick places can significantly affect the appearance of a woven or knitted fabric. While the thin and thick places do not lead to processing difficulties, neps on the other hand, do, particularly in knitting (T. Vijayakumar, 2003).

1.2.2 Yarn irregularity measurement:

There are many ways of measuring yarn irregularity:

1.2.2.1 Visual examination:

Yarns to be examined are wrapped onto a matt black surface in equally spaced turns so as to avoid any optical illusions of irregularity. The blackboards are then examined under good lighting conditions using uniform non-directional light. Generally the examination is subjective but the yarn can be compared with a standard if one is available; the ASTM produces a series of cotton yarn appearance standards. Motorized wrapping machines are available; in these the yarn is made to traverse steadily along the board as it is rotated, thus giving a more even spacing (B. P. Saville, 2000**)**.

1.2.2.2 Cut and weigh methods:

This method consists of cutting consecutive lengths of the yarn and weighing them. The mass of each consecutive length of yarn is plotted on a graph as shown in Figure1.1, a line showing the mean value can then be drawn on the plot. The scatter of the points about this line will then give a visual indication of the unevenness of the yarn. The further, on average, that the individual points are from the mean line, the more uneven is the yarn (B. P. Saville, 2000**)**

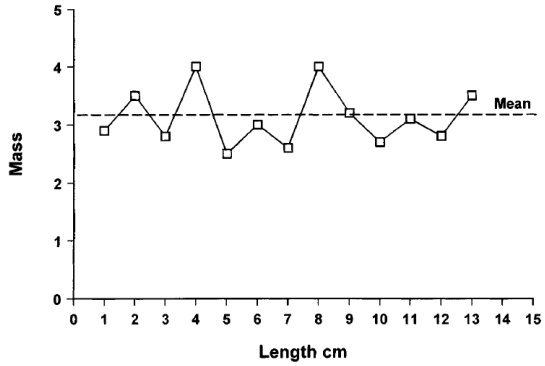

Figure.1.1: The variation of weight of consecutive 1 cm lengths of yarn.

A mathematical measure of the unevenness is required which will take account of the distance of the individual points from the mean line and the number of them. There are two main ways of expressing this in use: The average value for all the deviations from the mean is calculated and then expressed as a percentage of the overall mean (percentage mean deviation, PMD). This is termed U% by the Uster Company and is given in equation (1.1).

$$U = \frac{V}{\bar{x}} \qquad (1.1)$$

Where

$\bar{x}$ the average of absolute differences between the mean mass,

V the deviations from the mean

The standard deviation is calculated by squaring the deviations from the mean and this is then expressed as a percentage of the overall mean (coefficient of variation, CV %) see equation (1.2).

$$CV = \frac{\sigma}{\bar{x}} \qquad (1.2)$$

This measurement is in accordance with standard statistical procedures. When the deviations have a normal distribution about the mean the two values are related by the following equation:

$$CV = 1.25\ PMD. \qquad (1.3)$$

1.2.2.3 Uster evenness tester:

The Uster evenness tester measures the thickness variation of a yarn by measuring capacitance. The yarn to be assessed is passed through two parallel plates of a capacitor whose value is continuously measured electronically. The presence of the yarn between the plates changes the capacitance of the system which is governed by the mass of material between the plates and its relative permittivity (dielectric constant). If the relative permittivity remains the same then the measurements are directly related to the mass of material between the plates. For the relative permittivity of a yarn to remain constant must consist of the same type of fibre and its moisture content must be uniform throughout its length. The presence of water in varying amounts or an uneven blend of two or more fibres will alter the relative permittivity in parts of the yarn and hence appear as unevenness. The Uster Tester III is a capacitive type of tester for slivers and yarns. It provides a CV (%), a spectrogram, and a CV (L) curve.

The field length L can be adjusted by timing the capacitive reading and the speed of the tested material. For yarns, L typically defaults to 8 mm intervals. The latest model, Uster 4-SX, is capable of measuring yarn diameter and hairiness with dual light beams perpendicular to each other. This design reduces shape error caused by irregular yarn cross-sections (I. S. Tsai & W. C. Chu, 1996). Note that the CV (%) was provided directly as opposed to U% (= mean irregularity) in earlier models (B. P. Saville, 2000**).**

1.2.2.4 Zweigle G 580:

This instrument measures yarn evenness by a fundamentally different method from the mass measuring system of the Uster instrument. Instead of capacitance measurements it uses an optical method of determining the yarn diameter and its variation. In the instrument an infra-red transmitter and two identical receivers are arranged. The yarn passes at speed through one of the beams, blocking a portion of the light to the measuring receiver. The intensity of this beam is compared with that measured by the reference receiver and from the difference in intensities a measure of yarn diameter is obtained. The optical method measures the variations in diameter of a yarn and not in its mass. For a constant level of twist in the yarn the mass of a given length is related to its diameter by the equation;

$$\text{Mass} = C^* d$$

Where

C is a constant,

d the diameter of the yarn

However, in practice the twist level throughout a yarn is not constant (B P Saville, 2000**)**. Therefore the imperfections recorded by this instrument differ in nature from those recorded by instruments that measure

mass variation. However, the optical system is claimed to be nearer to the human eye in the way that it sees faults. Because of the way yarn evenness is measured, this method is not affected by moisture content or fibre blend variations in the yarn. The G 585/G 588 yarn testing modules use an infrared light sensor operating with a precision of 1/100 mm over a measuring having a length of 2 mm and at a sampling interval of 2 mm also. The speed of measurement may be selected on a graduated scale between 100 and 400 m/min. The sensor is unaffected by the aging of the light source, extraneous light, contamination, temperature, and humidity. It is unaffected by such yarn characteristics as color, conductivity, or luster. The defects are classified in respect of their length and their variation in diameter. The system provides a CV (%), a CV (L) curve, a histogram that shows diameter distribution and a spectrogram that shows wavelengths of the periodic defects in the yarn. It was reported that (KET-80 Evenness Tester, 2004) the measurements of G-580 should not be compared with the readings of Uster due to the following reasons:

- Different principles of measurement (optical determination of diameter, capacitive determination of mass variations);
- Different test zone lengths (integration stages), USTER 8 mm,G 585/G 588 2 mm;

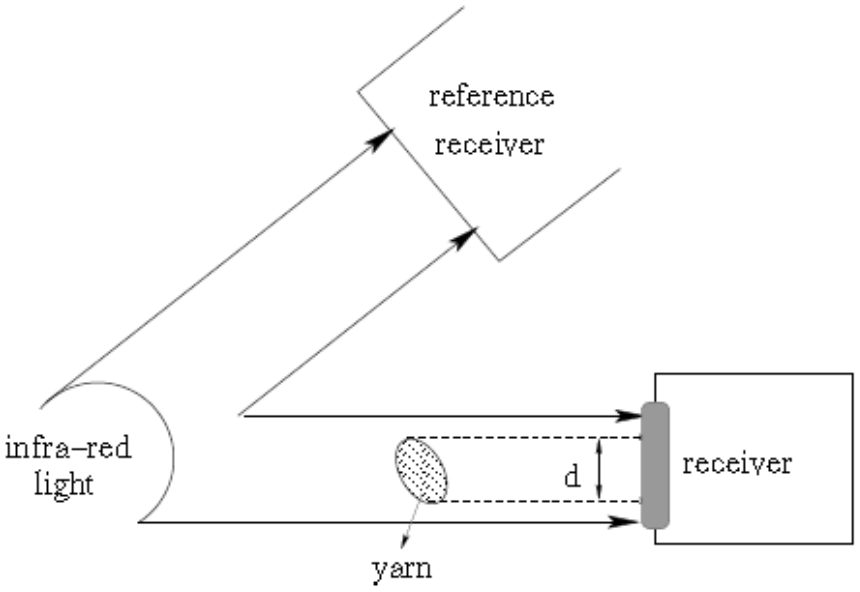

Figure 1.2: Zweigle G-580 yarn evenness tester

1.2.2.5 Lawson-Hemphill EIB:

Lawson-Hemphill EIB® is an optical system with a line-scan camera. It scans every 0.5 mm with a speed of 100 m/min. The diameter is defined to be the distance between the pixels near a user-set threshold level. Because optical readings are from a single angle, they are subject to shape errors. The yarn vibration is prevented by guiding the yarn through a measurement zone. In addition, the Constant Tension Transport (CTT) unit prevents variations that might be introduced by irregular yarn tension.

1.2.2.6 Keisokki KET-80 and Laserspot:

Keisokki KET-80 and Laserspot (KET-80 Evenness Tester, 2004) are two types of evenness testers based on capacitive and optical measurement principles, respectively. Like Uster Tester III, KET-80 provides a U% and CV (%), a CV (L) curve, and a spectrogram. It also provides a deviation rate, a DR%, which is defined as the percentage of the summed-up length of all partial irregularities exceeding the preset cross-sectional level to the test length. In practice, however, the yarn signal is

primarily processed by the moving average method for a certain reference length. As a result, long-term irregularities are likely to be detected. The Laserspot evenness and hairiness instrument uses laser beam and is based on the Fresnel diffraction principle. With this principle the yarn core is separated from hairs, allowing yarn diameter and hairiness to be measured at the same time. See Figure 1.3.

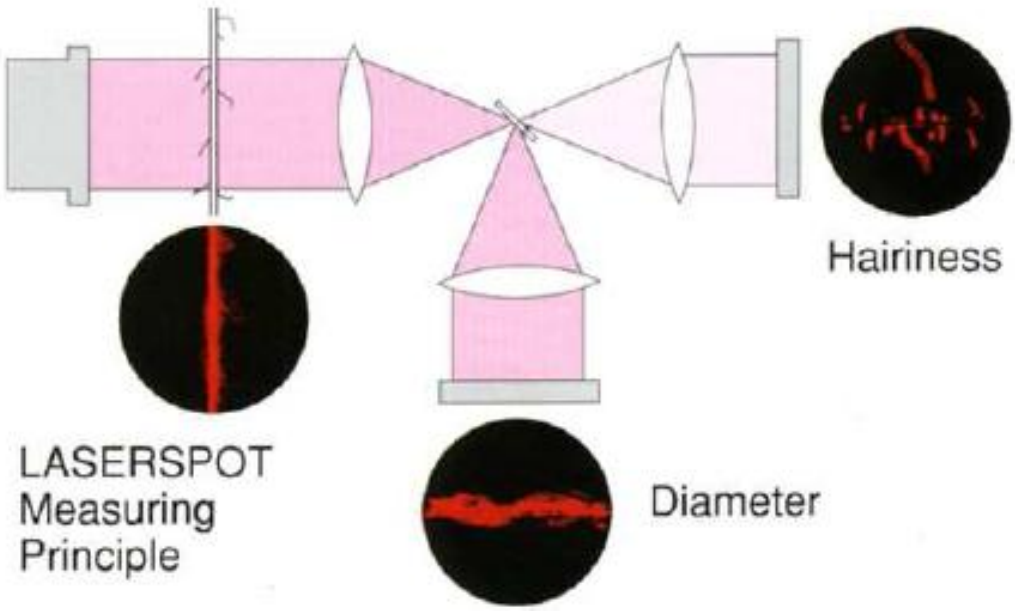

Figure 1.3: Yarn evenness testing with Fresnel Principle [Keissokki, 2004]

1.2.2.7 Flying Laser Spot Scanning System:

The Flying Laser Spot Scanning System (You Huh and Moon, 2003) consists of three parts: the sensor head, the specimen feeding device, and the data analysis system. When an object is placed in the scanning area, the flying spot generates a synchronization pulse that triggers the sampling. The width between the edge of the first and the last light segment determines the diameter of the yarn. Depending on the spot size and specimen feeding speed, the measurement values may vary. Therefore, it is important to calibrate the system for the feeding speed and the spot size.

1.2.2.8 Time-series modeling and spectral analysis:

A discrete time series is a set of time-ordered data obtained from observations of some phenomenon over time. If at each time a single quantity is observed, the resulting set is called a scalar or univariate time series. If at each time several related quantities are observed, this corresponds to a vector or multivariate time series (Eric, 2004). The fundamental aim of time series analysis is to understand the parameters of the observed data to forecast future values of the observations. Since one-dimensional yarn signals and two-dimensional surface signals are usually correlated among their observations, textile structures can be represented with datasets of time-series. Three commonly used linear time series models - Autoregressive, AR, Moving Average, MA, and Autoregressive Moving Average, ARMA - are summarized briefly below.

1.2.2.9 Linear time series models:

The fundamental assumption of time series modeling is that the value of the series at time, t, depends only on its previous values (deterministic part) and on a random disturbance (stochastic part) (Eric, 2004). The dependence of X (t) on the previous p values is assumed to be linear and can be written as

$$X_t = \emptyset_1 X_{t-1} + \emptyset_2 X_{t-2} + \cdots + \emptyset_p X_{t-p} + \widetilde{Z}_t \qquad (1.4)$$

Where $\emptyset_1, \emptyset_2, \ldots, \emptyset_p$ are real constants and $\widetilde{Z}_t$ is often referred to as the error at time t. This error usually has two components, a zero-mean uncorrelated random variable, Z_t, and a zero-mean white noise process, θZ, that is,

$$\widetilde{Z}_t = Z_t + \theta_1 Z_{t-1} + \theta_2 Z_{t-2} + \cdots + \theta_q Z_{t-q} \qquad (1.5)$$

The constants$\emptyset_1,\ \emptyset_2,\ \ldots, \emptyset_p$ and $\theta_1,\ \theta_2,\ \ldots, \theta_q$ are called AR and MA coefficients, respectively. Combining Equations 1.4 and 1.5 yields

$$X_t - \emptyset_1 X_{t-1} - \emptyset_2 X_{t-2} - \cdots - \emptyset_p X_{t-p} = Z_t + \theta_1 Z_{t-1} + \theta_2 Z_{t-2} + \cdots + \theta_q Z_{t-q} \quad (1.6)$$

This defines a zero-mean autoregressive moving average (ARMA) process of orders p and q, or ARMA (p; q). ARMA, however, has a short-term memory and therefore may not be suitable for expressing long-term seasonal periods, which is usually the case for yarn signals.

1.2.2.10 Spectrogram:

A spectrogram helps to recognize and analyze periodic faults in a sliver, roving, and yarn by representing the mass variations in the frequency domain in a way similar to time-series analysis. If a yarn with a periodic fault is analyzed using a spectrogram, the wavelength of the a periodic fault calculated using equation (1.7).

$$\text{Frequency} = \frac{\text{wavelength}}{\text{material}-\text{speed}} \quad (1.7)$$

Therefore, in textiles, a direct representation of wavelength is preferred over the frequency domain. In a spectrogram, the X-axis represents the wavelengths and Y-axis represents the amplitude of the faults as shown in Figure 1.4. Often a logarithmic scale is given for the X-axis to cover the maximum range of wavelengths. In general, the periodic defects could be sinusoidal or non-sinusoidal. The sinusoidal defects are usually caused by rotating parts such as drafting rollers and are easier to detect. However, the non-sinusoidal defects are harder to detect and difficult to comment on (Mario, 1994). Based on the characteristics of the period, these defects can be divided into categories as being symmetrical,

asymmetrical, or impulsive. In addition, depending upon the wavelength of the periodic fault, the mass variations are classified as

- Short-term variation (wavelength ranges from 1 cm to 50cm);
- medium-term variation (wavelength ranges from 50cm to 5 m);
- Long-term variation (wavelength longer than 5 m).

If yarns with periodic variations in the range of 1 cm to 50 cm lie next to each other and repeat a number of times within the fabric width, a fabric defect called the moiré effect may be formed. This effect is particularly striking to the naked eye if the finished product is observed at a distance of approximately 50 cm to 1 m.

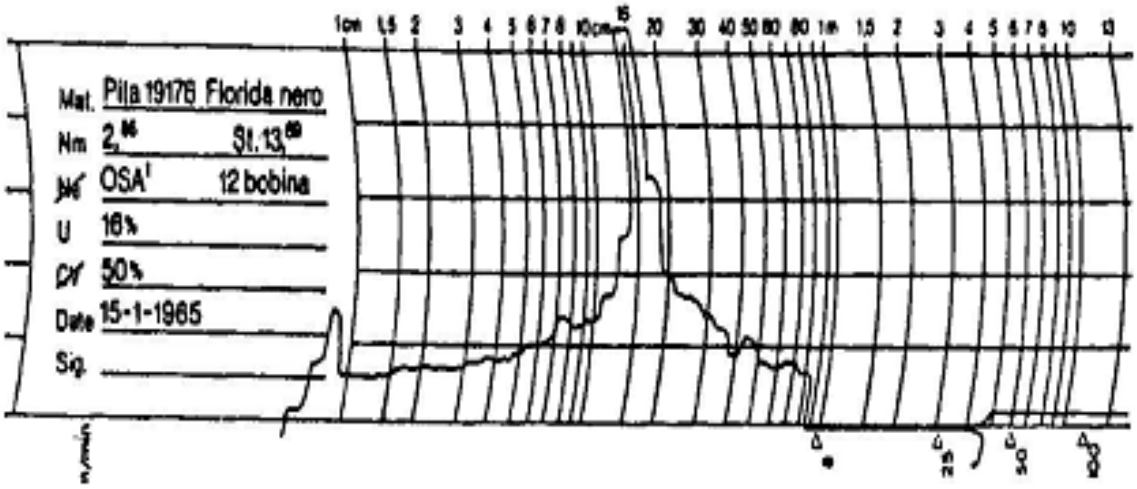

Figure 1.4: Spectrogram of a yarn (R. Further**, 1982)**

Periodic mass variations in the range of 50 cm to 5 m are not recognizable in every case. Faults in this range are particularly effective if the width of the cloth is the integral (or near integral) number of the periodic fault wavelength. In such cases, weft stripes in woven and rings in knitted fabrics are likely to appear.

Periodic mass variations with wavelengths longer than 5 m can result in quite distinct cross-stripes in woven or knitted fabrics. This is because

the wavelength of the periodic fault will be longer than the width of the woven fabric or the circumference of the knitted fabric. In addition the longer the wavelength is the wider the width of these cross-stripes. Such faults are easily recognizable in finished products, particularly when they are observed from distances further away than 1 m. A periodic mass variation in fiber assembly does not always affect the CV (%) of the yarn significantly. Nevertheless, such a fault will detract from the appearance quality of a fabric especially after dyeing. The degree to which a periodic fault can affect the finished product is dependent on its intensity, the width and type of the woven or knitted fabric, the fiber material, the yarn count, and the dye up-take of the fiber. A considerable number of trials have shown that the height of the peak above the basic spectrum should not over-step 50% of the basic spectrum height at the wavelength position where the peak is observed.

A periodic fault, which occurs at some stage during the spinning process, is lengthened by subsequent drafting. For instance, if the front roller of the second draw frame is eccentric, then by knowing the number of drafts in the following processes, the position of the peak in the spectrogram of the yarn measurement can be calculated. Similarly, from the position of the peak in the spectrogram, the location of the defective part can be located using the wavelength reading at the peak and the speed of the rollers (T. Vijayakumar, 2003).

1.2.2.11 Correlogram:

A correlogram is the plot of the correlation coefficient, ρ(L), as a function of distance, L. A yarn correlogram shows how readings of yarn signals that are, for instance, L apart are correlated with each other. Normally, as L changes, the ρ (L) may vary as demonstrated in Figures 1.5

and 1.6. However, the correlogram is often a damped harmonic curve for a yarn. This usually indicates the existence of 'quasi-periodic' wave in the signal (Townsend & Cox, 1951). On the other hand, an undamped sinusoidal curve indicates a strong periodic motion. It was suggested that a correlogram could be derived from the fiber length distribution by assuming that fibers are randomly distributed in the yarn [Spencer-Smith & Todd, 1941).

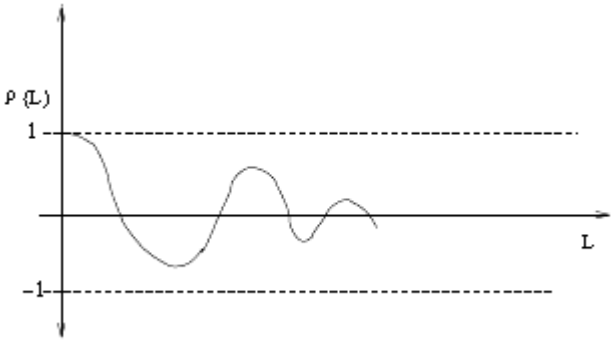

Figure 1.5: Damped correlogram

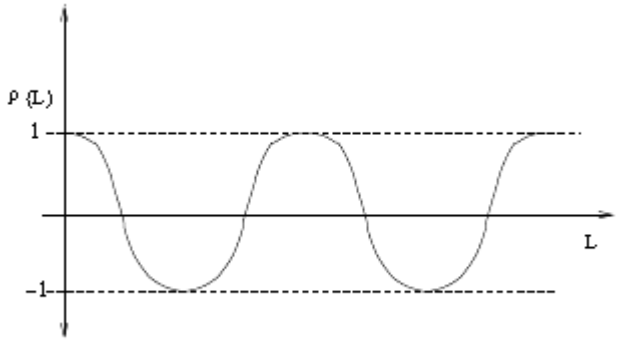

Figure 1.6: Undamped correlogram

1.2.2.12 Variance-length curves:

The variance length curve is produced by calculating the CV for different cut lengths and plotting it against the cut length on log-log paper. A perfect yarn would produce a straight line plot. The curve is a useful tool for examining long-term non-periodic variations in a yarn. The better is the

evenness of the yarn the lower is the curve and the steeper is the angle it makes to the cut length axis. This is shown in Figure. 1.7 where the variance length curve for an actual cotton yarn is compared with a curve for an ideal yarn. The measured curve deviates from the theoretical curve in the region where there is long-term variation in the yarn. The variance length curve of a poor fibre assembly lies above the curve of a good fibre assembly as is shown in Figure 1.8 where the poor yarn diverges from the good yarn at the longer cut lengths.

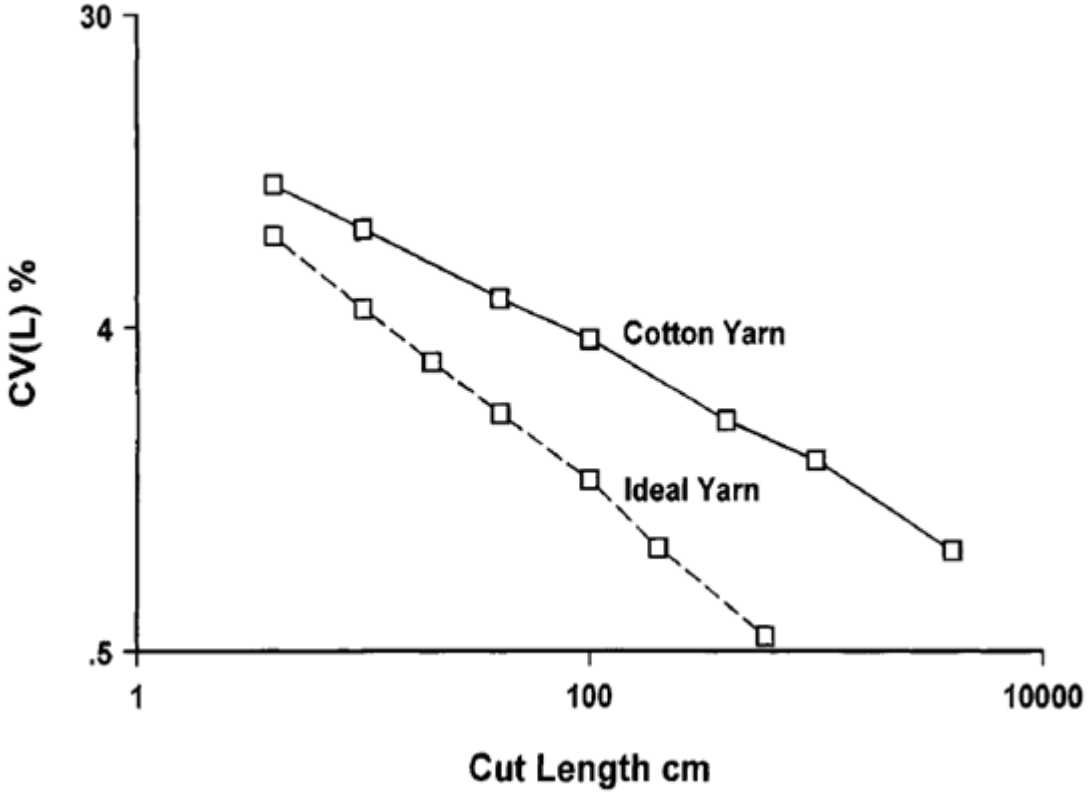

Figure 1.7 Variance length curves for cotton and ideal yarns

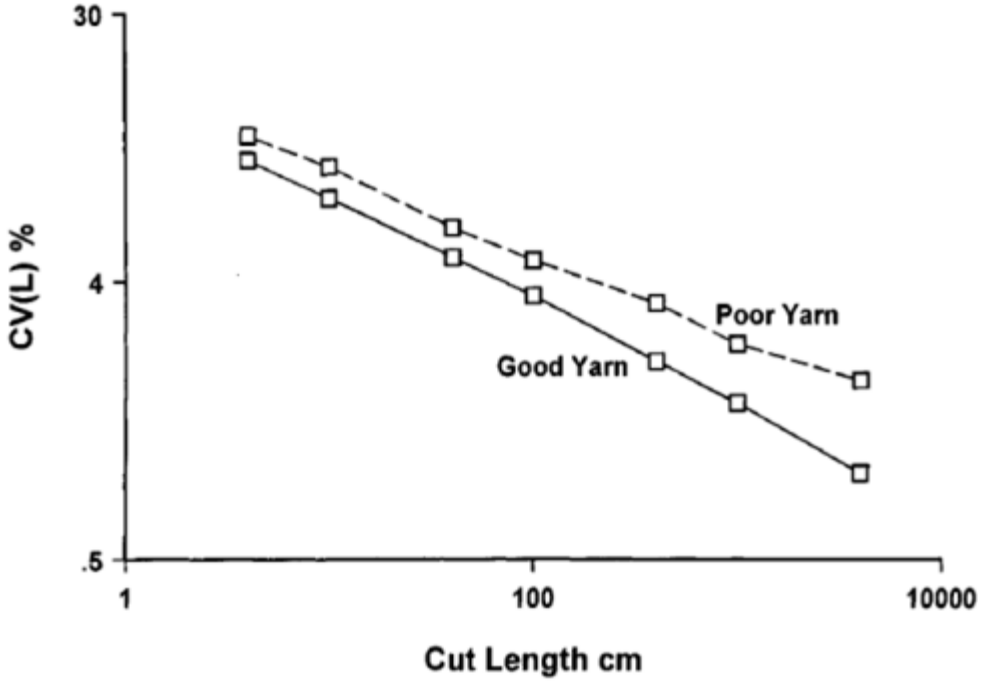

Figure 1.8 Variance length curves for poor and good yarns

1.3. Fabric irregularity:

1.3.1 Fabric irregularity causes:

The appearance of fabrics is affected by the irregularity of yarns and fabric production process problems. Irregular yarn will have an uneven strength and will likely to disturb the fabric production process because of frequent breakage. The fabric defects caused by irregular yarns may be grouped in two categories: random and periodic fabric irregularities. While random fabric irregularities may occur at any location in a fabric, periodic irregularities may create visible patterns in certain directions (Saville, 2000).

1.3.1.1 Random irregularities:

Random yarn irregularity may cause rough fabric appearance. Cloudiness, rough, fuzziness is a fabric condition characterized by a hairy appearance due to broken fibers or uneven twist. Irregular reed marks are

due to cracks between warp ends at random intervals for short distances. Missing or faulty yarns are visible at a portion of the fabric. Holes, cuts, knots or slubs are local defects mainly caused by mechanical problems.

1.3.1.2 Periodic fabric irregularities:

Bárre is a striped effect in a fabric caused by a series of picks, which have apparent difference in color or luster that is repeated at intervals in the warp direction. See Figure 1.9. Warp streak is characterized by a narrow bar running warp-wise and has difference in color from neighboring ends. Filling bar is a weft that runs parallel with the picks and that is different in material, linear density, twist, and luster from the adjacent wefts. Diamond bar/Moiré is caused by sinusoidal periodic thickness variations in weft yarn whose wavelength is less than twice the width of the cloth (Catling, 1958, Foster, 1952). See Figure 1.9. Figure 1.10 shows the influence of the wavelength on the visibility of a periodic defect on fabric. Reed marks, unlike irregular reed marks, occur in regular intervals and run along the pick. Skewing, bowing, non-symmetric placements are usually caused by excessive tension in fabrication.

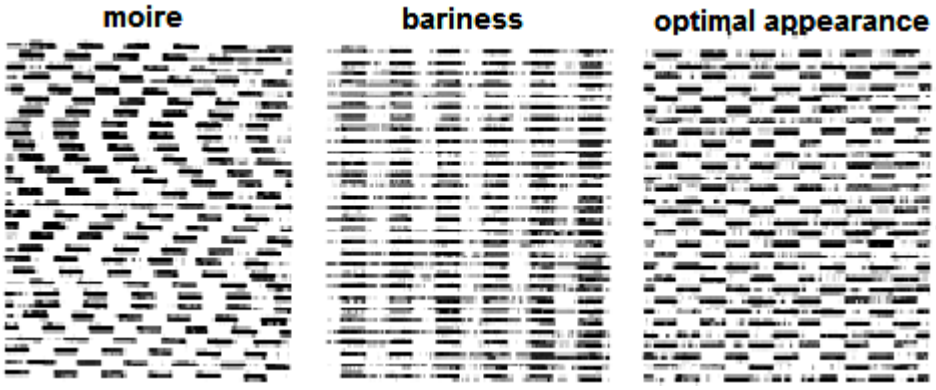

Figure 1.9: Appearance of some fabric defects (Saville, 2000)

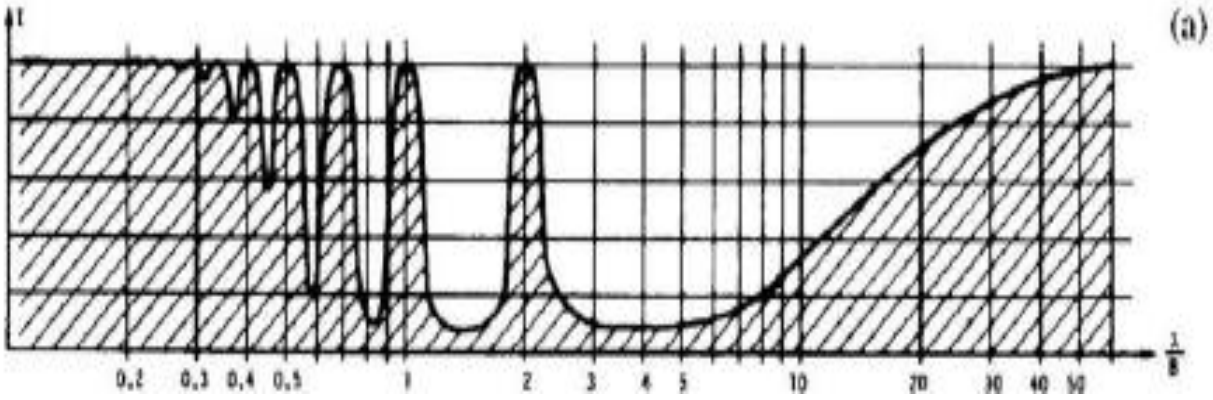

Figure 1.10: Influence of wavelength on visibility (Saville, 2000)

1.3.2. Fabric irregularity measurement:

It was suggested that the quality of fabric can be predicted from the coefficient of variation, the CV (%), of the yarn that is used (Wegener, 1986, Moyer, 1992). However, in industry, the evaluation of fabrics is still commonly done by the experts through eye and hand judging. This is primarily due to the fact that the CV (%) is grossly insufficient to predict the features of irregularities, since it is not location specific within the fabric. Several researchers in the past tried to characterize numerous fabric properties, some through introduction of quality indices and others by new methods of measurement using time series, Fourier transform, and Wavelets. Consequently, methods such as the Kawabata System (KES) (Sule & Bardhan , 1999), fabric assurance by simple testing (FAST), and the Total Quality Index (Snyder, 2000) have been proposed for total appearance rating. Nowadays yarn quality testers are equipped with devices for obtaining information on yarn properties on-line or off-line and then mapping them into weave or knit fabric structures in order to help visualize the final product (Zweigle, 1997, Avishai & Filiz, 2001 and Moon et al, 2003).

1.3.2.1 Kawabata system and FAST:

The operation of these systems includes the measurement of certain fabric properties and the interpretation of the data to predict the tailorability, appearance, feel, and handle (Sule & Bardhan, 1999). Kawabata system suggests several indices, such as the Total Appearance Value (TAV) and Total Hand Value (THV), for fabric properties. These indices are calculated by combining measurements made on several parameters, some of which are: elongation, linearity, tensile energy, resilience, shear stiffness, hysteresis, bending rigidity, compressional energy, thickness, roughness, and friction. Depending on the requirements, importance is attached to properties affecting feel, handle, and appearance. Due to the complexity and expensiveness of the instrument, some mills use FAST (fabric assurance simple testing), which is simpler and less expensive.

1.3.2.2 Fabric visualization commercial systems:

Until recently, no commercial system existed for predicting or visualizing fabric qualities directly from the yarn diameter or mass measurements taken on-line. There are now several systems, such as CY ROS ®, USTER ®, EXPERT ® and OASY S ®, that visualize yarn and fabric qualities through various types of images created directly from the yarn profiles captured from certain measurement sensors.

However, these systems are not completely satisfactory because of the way the yarn data are converted into fabric images. These images also require subjective visual judgment in the absence of a quantitative measure. More importantly, none of the existing systems maps or fingerprints the quality of a woven or knitted fabric for an entire roll. Therefore, there exists no method for judging and ranking the visual or physical qualities of

fabric rolls produced from a given machine at different time points or from different yarns, or from more than one machine. Other difficult technical issues include how to define and measure yarn signals optically, capacitively or optic-capacitively. The optical method or the capacitive method currently being used is known to be grossly inadequate due to distortion of actual yarn images within a fabric. Until recently, no technology existed for fusing the two independent datasets (capacitive and optical readings). Now there are commercial systems for making more than one measurement within a given tester (Uster Tester 4-SX using OM sensors, Keisokki opto-capacitive dual sensor system).

1.4. Objectives:

The objectives of this research are:

- To develop a model for determination of knitted fabric irregularity from yarn irregularity measurements;
- To develop a prediction model for the rating of the knitted fabric based on yarn quality; and
- To suggest a model for the generation of more deterministic yarn data.
- To measure the affect of yarn irregularity in fabric irregularity.

CHAPTER TWO

Literature Review

2.1 Introduction:

The unevenness of yarn may occur in the form of twist irregularity, diameter irregularity, and mass irregularity. While yarn irregularity may have a direct impact on its weight, permeability, and strength distributions, it may also indirectly impact the appearance, for example, by causing variation in the dye absorption behavior of the yarn.

This chapter highlights a number of studies that were carried out in the subject of thread and fabric uniformity and how they were measured and appreciated.

2.2 Yarn irregularity:

2.2.1 Fiber arrangement:

In the past many researchers investigated the irregularity of spun yarns under several assumptions. It was often suggested that the random fiber arrangement and the drafting of shorter fibers are the main causes of yarn mass irregularity. Martindale, 1945, reported that the fibers are randomly arranged through blending, carding, doubling, roving, and spinning. His model was based on the fact that the probability of a fiber crossing a given yarn cross-section is proportional to the length of the fiber. He gave the probability (P) of a fiber crossing a given cross-section by the following equation;

$$P = n / N$$

Where

n is the average number of fibers in the yarn cross-section.

N the total fibre in yarn cross-section

As *P* is very small, coefficient of variation (CV) of yarn was then expected as:

$$CV = \frac{100}{\sqrt{n}}.$$

Martindale then a assume that a yarn cross-section contains a group of (m) fibers with the lengths i_1, i_2, $i_3 \ldots i_m$, each group having n_1, $n_2 \ldots n_m$ fibers, where

$$\sum_{r=1}^{m} n_r = n$$

He showed that the standard deviation (σ) of the number of fibers in a yarn cross-section is still $\sqrt{n}$ as follows:

$$\sigma_n^2 = \sum_{r=1}^{m} \sigma_r^2 = \sum_{r=1}^{m} n_r = n$$

Grosberg, 1956 showed that the fiber length and the yarn irregularity are correlated; therefore, one can calculate the yarn irregularity from the mean fiber length, diameter, and yarn count. His experiments show that for a given fiber diameter, an increase in the mean fiber length would result in a decreasing coefficient of variation, perhaps as a result of improved orientation. Martindale finally divided the variation of yarn into variation caused by the non-uniform fiber cross-section area and the non-constant number of fibers in the yarn cross-section. He assumed that the number of fibers in the yarn cross-section has a mean *n* and variance σ_n^2 where each fiber has a mean cross-section area $\bar{A}$ and variance σ_A^2 . He obtained the variance of yarn, σ_Y^2 , as follows:

$\sigma_Y^2 = \bar{A}^2 \sigma_Y^2 + n\sigma_A^2 = n\bar{A}^2 + n\sigma_A^2 = n\bar{A}^2(1 + \frac{\sigma_A^2}{\bar{A}^2}) = n\bar{A}^2(1 + 0.00001CV^2(A))$

Note that $\mathrm{CV_A} = 100\frac{\sigma_A}{A}$ and therefore $\sigma_A = \frac{A \times \mathrm{CV_A}}{100}$

And defined the limit irregularity of a yarn as

$$\mathrm{cv(Y)} = \frac{100\sqrt{n}\bar{A}\sqrt{1 + .0001\mathrm{cv(A)}^2}}{n\bar{A}}$$

$$= \frac{100\sqrt{1+0.0001\mathrm{cv}^2(\mathrm{A})}}{\sqrt{n}} \qquad (2.1)$$

A third component, configuration of fibers, was considered later (Dyson, 1974, Mishu , Moon , and Subhash, 1990) in the analysis of yarn irregularity as a result of random fiber arrangement. The irregularity was given as the variation of local linear density, T(x):

$$\mathrm{T(x)} = n(x)m_t(x)m_s(x) \qquad (2.2)$$

Where *n(x)* is the number of fibers, m_t(x) is the mean local linear density, and m_s(x) is the mean local fiber orientation. Assuming independence between these three components and using the additive rule of variances, the yarn CV (%) was given as (Mishu , Moon , and Subhash, 1990)

$$\mathrm{cv}^2(T) = \mathrm{cv}^2(n) + \mathrm{cv}^2(m_t) + \mathrm{cv}^2(m_s) \qquad (2.3)$$

2.2.2 Effect of drafting waves:

(Balls, 1928) pointed out that fibers move in groups causing non-random wave-like patterns. He called them drafting waves, and showed that they are responsible for periodic thin and thick places over a yarn. He

suggested that they are often caused by improper draft zone settings, eccentric top rollers, improper top roller pressures, and high percentages of short fibers in the material. Foster, 1945 investigated the effect of drafting wavelength on yarn irregularity and noticed that neither the wave nor the amplitude was constant. During the drawing process, three things were happening: drafting was increasing irregularity, the fibers were being parallelized and, the irregularities were reduced by doubling. While the amplitude of the drafting wave increased with the increasing draft, the effect of doubling was to reduce the period of the drafting wavelength. He finally concluded that the irregularities in a cotton yarn are mostly made up of drafting waves introduced at the spinning frames rather than the draw frames. Although the drafting waves introduced in earlier steps are small in amplitude, they are responsible for long-term variations. In addition, the wavelength of a periodic fault would grow in the subsequent drafting. According to Foster, the stretching during winding at the speed and ring frames were also important causes of count variations. In one study, (Foster, 1945) suggested that when the fiber's mid-point reaches a certain point, the fiber changes speed from the back roller speed to the front roller speed. This point was called the change point, was said to be located somewhere between the two rollers, and was perhaps responsible for the drafting waves. Several researchers including (Cox and Ingham, 1950) investigated the effect of change location on the irregularity of yarns and proposed various estimation models. An important conclusion of yarn irregularity studies is that evenness deteriorates during processing. There are two reasons for this (Vijayakumar, 2003):

- The number of fibers in the cross section steadily decreases; therefore, uniform arrangement of the fibers becomes more difficult.

- Each drafting operation increases the unevenness by adding a certain amount of irregularity to the irregularity of a finished yarn. The resultant irregularity at the output of any spinning process stage is equal to the square root of the sum of the squares of the irregularities of the material and the irregularity introduced in the process.

Mathematically stated, if CV_o is the CV(%) of output material, CV_i is the CV(%) of input material, and CV_p is the irregularity introduced by the machine, then

$$CV_o = \sqrt{CV_i + CV_p}$$

Sung and Suh, 2002 proposed a technique for separating the input variance and the process variance when a roving is produced from a sliver by a conventional drafting process in ring spinning. They demonstrated that a spline method and a cross-spectrum analysis could be used to estimate the density profiles of roving from slivers. This provided a mean to separate out the input variances from the process variances.

2.2.3 Effect of twist variation:

Spun yarn production fundamentally involves twisting of a random fiber array. Twisting tends to concentrate the yarn structure into an irregular close-packed polygonal shape (Hearle & Grosberg, 1969), but the cross-section still possesses a concave-convex irregular shape. Over time, many studies have modeled yarn as a cylinder with a circular cross-section. With the advances in image analysis, (Tsai and Chu, 1996) showed that the cross-sections of ring-spun and open-end-spun yarns are better approximated as an ellipse with an irregular outline. The eccentricities of the best-fit ellipses for ring-spun and open-end-spun yarns were obtained as 0:40 and 0:36, respectively, indicating that the cross-sectional shape of

open-end-spun yarns are more circular than the ring-spun yarns. This resulted from the smaller linear density and yarn twist of ring-spun yarns.

2.3 Measurement of yarn irregularity:

2.3.1 Coefficient of Variation:

Uster® defined yarn irregularity, U (%), as the average of absolute differences between the mean mass $\bar{x}$, and the measured mass readings, x, as follows:

$$U = \frac{\frac{1}{n-1}\sum_{i=1}^{n}|x_i - \bar{x}|}{\frac{1}{n}\sum_{i=1}^{n} x_i} \qquad (2.4)$$

Where *n* is the number of readings. Although U (%) has been widely used, the coefficient of variation, CV (%), has now widely been accepted as a measure of expressing yarn irregularity due to ease of statistical manipulation. Using the same symbols given in equation (2.4), it is defined mathematically by;

$$CV = \frac{\sqrt{\frac{1}{n-1}\sum_{i=1}^{n}(x_i - \bar{x})^2}}{\frac{1}{n}\sum_{i=1}^{n} x_i} \qquad (2.5)$$

If normal distribution is assumed, then it can be shown mathematically that CV (%) and U (%) are related by equation2.6.

$$\text{CV} = \sqrt{\frac{\pi}{2}}\, U\,. \qquad (2.6)$$

Extending the definition of CV (%), (Martindale, 1945) introduced the concept of limit irregularity, CV_{lim}. The index of irregularity was defined as

the ratio between the measured irregularity (Equation 2.5) and the limit irregularity (Equation 2.1) and is given by;

$$I = \frac{CV_{eff}}{CV_{lim}}$$

Note that the closer the value to unity the more regular the yarn would be. Although CV(%) is simple to obtain and interpret, it does not provide any information on the medium and long term yarn variations. Due to the significance of these variations on fabric irregularity, the measurement methods discussed below are developed for yarn evenness testing.

2.3.2 Time-series modeling and spectral analysis:

Linear time series models:

Sung and Such, 2002 captured signals from slivers and fit them with the ARMA model to predict the future behavior of the rovings and yarns. Although the signals did not show any obvious trends or cyclic patterns, the time series analysis made it possible to extract patterns as a function of time. In addition to ARMA, Spectral analysis, which is based on Fourier series, has been applied to analyze periodic yarn mass variations. This computation involves breaking up a yarn signal, Y (t), into a set of frequency components by inverse discrete Fourier transform. The original sequence Y (t) can be represented as a combination of N different frequencies f as

$$Y(t) = \frac{1}{N}\sum_{k=1}^{N} U_N\left(\frac{2\pi k}{N}\right) e^{-\frac{i2\pi kt}{N}} \qquad (2.7)$$

The parameter $U_N(2\pi k/N)$ corresponds to the amplitude of the signal at angular frequency $w_k = 2\pi k/N$. However, in practice, for a given signal, the power spectrum is used to obtain a plot of the portion of a

signal's power (energy per unit time) falling within given frequency bins (Eric, 2004). It is given by

$$P_y(t) = \int_{-\infty}^{\infty} [Y(t) - \bar{y}]\, \boldsymbol{e^{-i2\pi ft\, dt}} \qquad (\mathbf{2.8})$$

Spectrogram & Correlogram:

(Townsend and Cox, 1951) demonstrated that the correlogram could not always be derived from the fiber length distribution because the assumption that the fibers are distributed randomly is untrue. However, they acknowledged that the fiber length distribution must nevertheless influence the correlogram, that is; the greater the fiber length, the greater the value of L at which ρ (L) converges to zero. Even though the contribution of quasi-periods to the visual appearance of yarns and fabrics was not so clear to (Townsend and Cox, 1951) they suggested that the correlogram is probably the best method of detecting quasi-periods in yarn signals. Acknowledging that no single measure is sufficient to assess all features of the yarn irregularity, (Townsend and Cox, 1951) felt that the V (L) relation is a more appropriate measure of yarn irregularity.

2.3.3 Variance-length curves:

Townsend and Cox,1951 showed that the relationship between the mean standardized variance, V (L), and the length within which V (L) is measured leads to indices characterizing types of irregularity that may be of practical importance. When analyzing the causes of irregularity they preferred to deal with the square of the CV (%), namely relative variance, instead of CV (%) itself. This was because a moderately small addition of irregularity has a small effect on the total coefficient of variation, CV(%). They proposed two variance-length curves, namely B(L) and V(L), to

illustrate the relationship between the length L and the standardized deviation. While B (L) was defined to be the standardized variance between the means of lengths L, V (L) was defined to be the mean standardized variance within lengths L of yarn. These definitions may be expressed mathematically as follows:

$$B(L_i) = \frac{\sqrt{\sum_{k=1}^{n_i}[x_{ki} - \bar{x_i}]^2}}{n_i} \qquad (2.9)$$

Where

B (L_i) is the variance between sections of i^{th} length cut;

x_{ki} is the value of the k^{th} section for i^{th} length cut;

$\bar{x_i}$ is the mean value of the yarn property for i^{th} length cut;

n_i is the number of yarn segments for i^{th} length cut.

$$V(L_i) = \frac{\sum_{k=1}^{n_i} V(x_{ki})}{n_i}$$

Where

$V(L_i)$ is the i^{th} length variance;

$V(x_{ki})$ is the variance of the property for k^{th} segment;

n_i is the number of yarn segments for i^{th} length cut.

Townsend and Cox, 1951 pointed out that

$$V(L) + B(L) = V(\infty) \qquad (2.10)$$

Where V (∞) is the overall standardized variance from the simple theory of analysis of variances. Consequently, they provided the general shapes of V (L) and B (L) as shown in Figure 2.1. The B (L) curve starts with an initial value of B (∞) at small lengths. It falls rapidly at first and then more slowly to an asymptotic value of zero at longer lengths. On the other hand, the V (L) curve starts with an initial value close to zero at small lengths and

increases to a limiting value V (1) as additional length introduces more opportunity for variation to arise (Kim,1998).

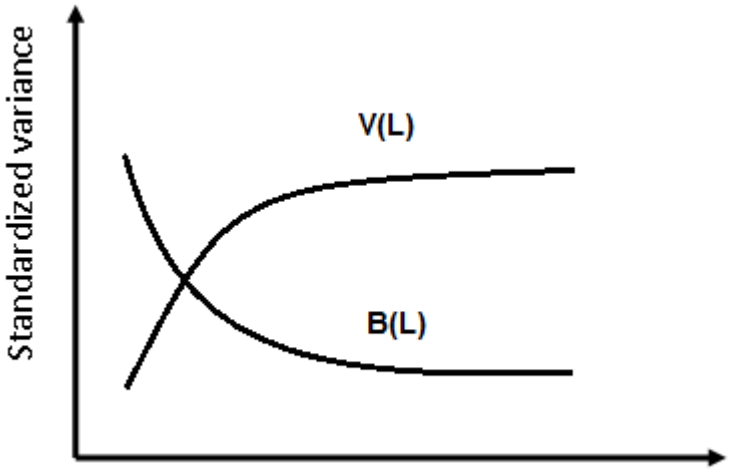

Figure 2.1: General shapes of V (L) and B (L)

Townsend and Cox, 1951 classified the yarns to have either short or long term variation, based on the rapidity of approach to V (∞). They mentioned that the gradient at the origin of these curves as well as the scatter of variances about their mean could be a discriminating tool for yarns. Townsend and Cox, 1951 gave the relationship between the correlogram and the V(L) curve as shown below:

$$V\ (L) = V\ (\infty)\left[1 - \frac{2}{L^2}\int_0^L (L-U)\rho(u)du\right] \qquad (2.11)$$

Where ρ (u) is the coefficient indicating the correlation between points u apart on the yarn, V (L) is the mean standardized variance within lengths L of yarn, and V (∞) is the overall standardized variance. They suggested that variance-length curves may be obtained faster from the correlogram of yarns using Equation 2.10.

In a follow up study, Breny, 1953 combined the results of Townsend and Cox, 1951, Martindale, 1945 and Spencer-Smith and Todd, 1941 in order to determine V (L) curve using only the following quantities:

- The fiber length distribution;
- The mean fiber diameter and its dispersion and;
- The yarn count.

Letting l_m be the maximum fiber length and assuming ρ (u) = 0 for $u > l_m$; V (L) curve was derived as

$$V(L) = \frac{2\big(V(\infty)\big)}{L^2}\int_0^{i_m}(L-u)[1-\rho(u)]du$$

$$+\frac{2\big(V(\infty)\big)}{L^2}\int_0^{i_m}(L-u)du = V(\infty)(1-\frac{A}{L}+\frac{B}{L^2}) \quad (2.12)$$

Where A and B are determined experimentally or theoretically from fiber length distribution. Breny, 1953 conducted experiments to verify the validity of the model, however, by assuming fibers with same length. Suh, 1976 statistically derived the most generic expression for the fiber mass contained in length interval L of a fiber array of known thickness as a function of fiber length distribution. Noting that yarn irregularity is the variation of the length aggregate of all fibers S_T (L) within L, he derived S_T (L) as a function of fiber length distribution, average number of fibers and length interval L. He then derived coefficient of variation of yarn as

$$CV\,[S_T\,(L)] = \frac{\sqrt{V\,ar[S_T\,(L)]}}{E[S_T\,(L)]} \quad (2.13)$$

Suh's, 1976 investigated the effect of average fiber length and the number of fibers from the total irregularity of the yarn. The expressions obtained for uniform fiber length were compatible with the time-series expression .He also showed that when L = 0 and the fiber diameter is

uniform, the expression simplifies to the one obtained by Martindale, 1945. Finally he showed that an increase in L results in a decrease in CV (%) as expected. Some connection between the variance-length curve and fractal theory was reported. It was suggested that fractal dimension could be calculated from a variance-length curve by taking the logarithm of the curve to obtain a quality index for quantifying irregularity of yarns (Kim, 1998).

2.4. Mass, diameter and twist relationships of yarns:

2.4.1 Geometric descriptors of yarn and coordinate system:

If yarn is assumed to be circular in cross-section, then the unit twist (T) may be given as $\pi d \tan(\theta)$ where d is the diameter of the yarn and θ is the twist angle as shown in Figure 2.2.

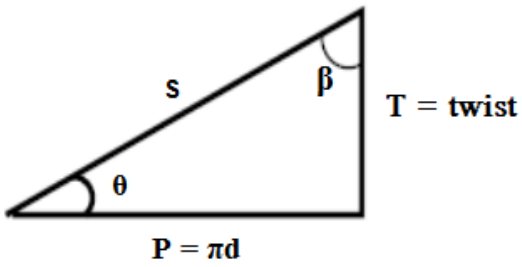

Figure 2.2: Twist triangle

On the other hand, (Lieve, 1997) in cylindrical coordinates the twist angle, $\tan(\theta)$, may be given as, $rd\theta/dz$. In addition to twist angle, migration angle,φ, of a single fiber shown in Figure 2.3 may be given as:

$$tan(\varphi) = dr/dz \qquad (2.14)$$

Combining the twist angle θ and the migration angle φ, Lieve, 1997 suggested the coordinate system of a fiber as,

$$\frac{dF}{dz} = \left(\frac{dr}{dz}, \frac{rd\theta}{dz}, 1\right) \qquad (2.15)$$

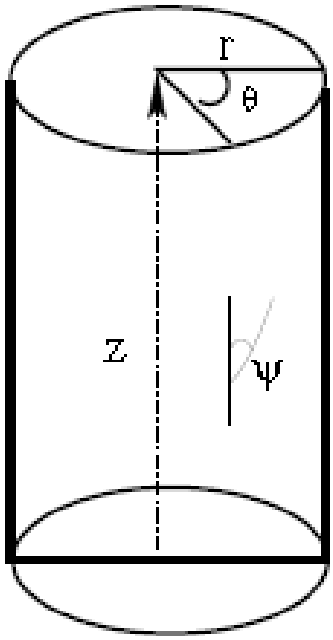

Figure 2.3: Yarn fiber in cylindrical coordinates

2.4.2 Twist and fiber strand interactions:

Cybulska, 1999 by using image analysis evaluated yarn thickness, hairiness, and twist. He assumed a cylindrical yarn with a variable diameter where the fibers are laid along the helix curves characterizing the twist on the surface. The projection of helix to the image plane was given by;

$$y - y_0 = \frac{d}{2} sin(b_1 x + b_0) \qquad (2.16)$$

Where

y_0 denotes the y-coordinate of the yarn axis,

d is the local diameter of the yarn core, and

b_1 characterizes the spiral lead. The value of tan(β) was calculated as the slope of the tangent to the helix at point (x_0; y_0) as follows:

$$tan(\beta) = \frac{b_1 d}{2} cos(b_1 x + b_0) = \frac{b_1 d}{2} \qquad (2.17)$$

Finally he calculated the twist of a yarn using Equation 2.18 and by estimating the parameters of Equation 2.16 from the best-fit sine curve of the projected yarn image.

$$\frac{1}{T} = \frac{tan(\beta)}{\pi d} = \frac{b_1}{2\pi} \qquad (2.18)$$

The results show that the twist varies along a yarn and concentrates in the thin places of the yarn. Benslimane and Lachkar also estimated the level of twist by finding the best-fit sine curve using Equation 2.16 and genetic based inverse voting Hough transform. Genetic algorithms were used in image space to overcome the memory and computational requirements of Hough transform in parameter space. Using genetic algorithms, a set of best-fit curves was preserved and the others were eliminated in a way similar to natural selection. However, Tsai and Chu, 1996 using image analysis techniques showed that the cross-sections of spun yarns are better approximated as ellipses. This was achieved by measuring yarn cross-sections rotated during the test so that the angle of intersection between the emitted light beam and the fixed axis of the yarn cross-section varies continuously. The eccentricities of the best-fit ellipses for ring-spun and open-end spun yarns were obtained as 0.40 and 0.36, respectively, indicating that the cross-sectional shapes of open-end-spun yarns more circular than the ring-spun yarns. This was contributed to the smaller linear density and yarn twist of ring-spun yarns. In order to account for the irregular outline of yarn, shape error factor (SEF) was introduced. It was simply given as the ratio of the actual area to the approximated ellipse's area such as shown in Figure 2.4.

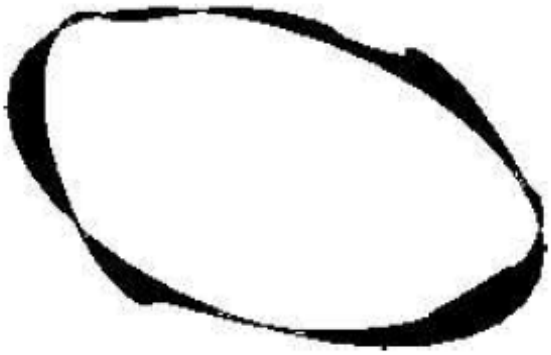

Figure 2.4: Shape Error Factor (SEF)

SEF was given by;

$$SEF = \frac{\frac{\pi}{2}\sum_{i=1}^{n} v_i}{\sum_{i=1}^{n} \pi\, ab} \times 100 \qquad (2.19)$$

Where πab is the area of the best-fit ellipse of a yarn cross-section, *n* is the number of yarn cross-section readings, and *v* is the area difference. Since, the second moment of a best-fit ellipse equals to that of the cross-sectional shape. The radii a and b were given by

$$a = \left(\frac{4}{\pi}\right)^{1/4} \left(\frac{I_{max}^3}{I_{min}}\right)^{1/8} \qquad (2.20)$$

and

$$b = \left(\frac{4}{\pi}\right)^{1/4} \left(\frac{I_{min}^3}{I_{max}}\right)^{1/8} \qquad (2.21)$$

Where I_{min} and I_{max} are the greatest and least moments of inertia, respectively (Pourdeyhimi &Sobus, 1993).

In Equation 2.19, the dividend was multiplied by $\frac{\pi}{2}$ to translate absolute irregularity to coefficient of variation with the assumption that the area difference is distributed normally.

Tsai and Chu, 1996 suggested that the cross-sectional shapes of ring-spun and open-end spun were not identical due to different yarn formation

mechanisms. The greater the yarn twist and linear density (Tex), the smaller was the ellipticity of the yarn cross-section. In addition, the SEF was greater for ring-spun yarns than open-end-spun yarns owing to the greater ellipticity of the former. Furthermore, the SEF can be applied to both spun yarns because of the low variance (0.005) of the eccentricities between the various cross-sections of the yarns. On the other hand, several researchers (Peirce, 1937, Barella, 1950) investigated the relationship between yarn count and diameter with the assumption that the yarn is cylindrical and its linear density is known. While studying the effect of twist on yarn diameter and contraction, (Barella, 1950) derived the diameter in terms of yarn count N (Tex) and yarn density (δ) as

$$d = 2\sqrt{\frac{N}{1000\pi\delta}} \qquad (2.22)$$

He suggested that when there is no slippage, the yarn density would be equal to fiber density if a force is applied at breaking levels. At that point, the diameter may be called the critical diameter. The relationship between the diameter and force was given by $d_f = d_o - K\sqrt{F}$. In this relation, *K* is a constant that depends on the yarn type, and d_o and d_f are the diameters of the yarn under no tension and under force, respectively. Taking into account the effect of twist on yarn count through contraction, Barella obtained contraction, *C*, as

$$C = 100\left(1 - \frac{1}{\sqrt{1 + tan^2\theta}}\right) \qquad (2.23)$$

Where θ is the twist angle. Correcting diameter for contraction yields

$$d = \sqrt{\frac{\sqrt{1 + \pi\gamma 10^{-2}T^2}}{N_\pi(a + bT)}} \qquad (2.24)$$

In this equation, T is unit twist, and γ is yarn density and may be given by:

$$\gamma = c_1 + c_2 T.$$

The constants c_1 and c_2 are experimentally determined for a given yarn. A theoretical relationship between mass and diameter was derived by Kim et al, 2000 as, *CV (diameter) ≈ 0.5 * CV (mass).* It was assumed that yarn cross-sections are circular, the yarn linear density is uniform, and mass (m) and diameter (d) are normally distributed, $N(\mu, \sigma^2)$. By definition, the CV (%) of mass m is

$$CV\ (m)\ = \frac{\sqrt{V\ ar(m)}}{E(m)} \qquad (2.25)$$

Since $m = \rho\pi d^2/4$, the expected value and variance of the mass is given respectively by

$$E(m)\ =\ E(\frac{\rho\pi d^2}{4})\ = \frac{\rho\pi\left(V\ ar(d) +\ E^2(d)\right)}{4}$$

$$= \frac{\rho\pi}{4}(\sigma^2\ + \mu^2) \qquad (2.26)$$

$$V\ ar(m) =\ V\ ar\left(\frac{\rho\pi d^2}{4}\right) = \frac{\rho^2\pi^2}{16} = \left(E(d^4) - E^2(d^2)\right)$$

$$= \frac{\rho^2\pi^2}{16}(4\mu^2\sigma^2 + 2\sigma^4) \qquad (2.27)$$

Substituting Equations 2.26 and 2.27 into Equation 2.25 yields

$$CV\ (m)\ = \frac{CV\ (d)\sqrt{4\ +\ 2CV^{\,2}(d)}}{CV^2\ (d) +\ 1} \qquad (2.28)$$

The Maclaurin expansion of Equation 2.28 yields

$$CV\ (m) =\ 2CV\ (d) + \frac{3}{4CV^3}(d) + \frac{23}{16CV^5}(d)\ ...\ \approx\ 2CV\ (d) \qquad (2.29)$$

In other words, the measured mass CV(%) would be twice the measured diameter CV(%) for a circular yarn.(Barella, 1952) showed that in practice,

however, the variation in diameter is higher than the theoretical approximated one. He suggested that this must be due to the influence of twist on yarn diameter irregularity. He conducted the following three experiments on yarn:

- tension increased and length kept constant;
- Twist increased and length kept constant;
- Twist increased and yarn allowed to contract.

  And observed a decreased in apparent diameter CV (%) for the three experiments conducted. He explained the decreases in CV (%) by the following theories:

- In the first case, the tension effected thick places more than the thin places and had a regulating effect;
- In the second case, the increase in twist caused an increase in tension and had a regulating effect;
- In the third case, the tension was constant and the redistribution of twist occurred. This in turn increased the regularity of the yarn.

Barella finally concluded that mass irregularity causes twist irregularity and in turn exaggerates the yarn irregularity. However, his analysis did not take into account the effect of measurement principle and field length. Kim et al, 2000 investigated the effect of measurement field length on yarn evenness by comparing the CV(%) of the measurement obtained from three sensors with different measurement principles. These sensors were: a capacitance sensor with an 8 mm sensing zone; an optical sensor with a 2 mm sensing zone; and a laser scanner with a 1 mm effective sensing zone. They derived the theoretical CV (%) of capacitive and optical sensors by partitioning the measurement field length of the capacitive to the one of the

optical as $M = m_1 + m_2 + m_3 + m_4$ and assuming independence between partitions. Equation 2.28 was then modified as

$$CV\ (M) = \frac{\sqrt{V\ ar(m_1 + m_2 + m_3 + m_4)}}{E(m_1 + m_2 + m_3 + m_4)} = \frac{\sqrt{4V\ ar(m)}}{4E(m)}$$
$$= 0.5CV\ (m) \qquad (2.30)$$

Substituting Equation 2.29 into Equation 2.30 yield *CV (M) = CV (d)*, which means that the CV (%) measured by the optical sensor would be as high as the CV(%) measured by the capacitive sensor. Although measured CV (%) s were in agreement with the theoretically calculated ones for both the optical and the capacitive sensors, the measured CV(%) obtained for the laser scanner was lower than the theoretically calculated one. This was explained by the diminishing effect of correlation between yarn readings of 1 mm apart for the laser scanner.

2.5 Instruments for yarn irregularity measurement:

They are two types of yarn irregularly measurements systems, one based on capacitive and the other based on optical used in the textile industry. Using capacitive measurement, the irregularity of yarn is detected from the variations in electric capacitance generated by the movement of yarn sample that passes through the gap of a fixed air condenser. Using the photoelectric measurement, the irregularity is measured from the fluctuation of the light intensity or shadow on the sensor caused by the beam of light passing across the yarn cross-section see Figure 2.5.

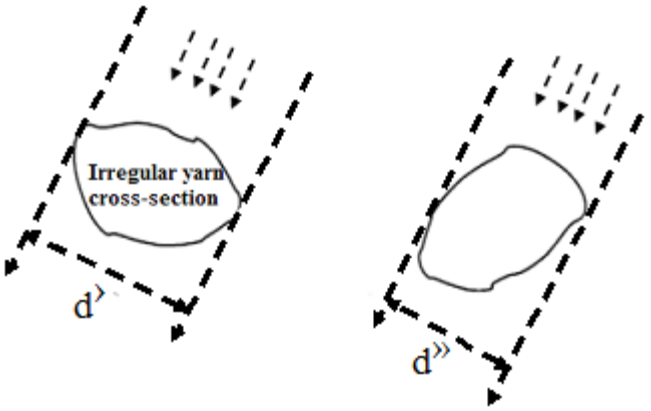

Figure 2.5: Emitted light for a yarn with irregular cross-section

Two main factors, the inhomogeneous radiant intensity of the emitted light source and the irregular yarn cross-section, are likely to cause error in the measurement of yarn evenness by the photoelectric method (Tsai and Chu, 1996). The effect of an irregular yarn cross-section on yarn evenness measurement is demonstrated in Figure 2.5. For the same cross-sectional area, the projected diameters $d_{\rangle}$ and $d_{\rangle\rangle}$ are not equal because of the orientation of the yarn. Furthermore Tsai and Chu, 1996 showed that the problem of orientation could be solved if two photoelectric instruments with two incident beams are placed perpendicular to each other. They demonstrated this by first calculating the measured area from the projected diameter assuming single incident light beam as shown in Figure 2.6. The measured area, A_o, is a function of and the semi-major and semiminor axises, *a* and *b* as given below:

$$A_o = \frac{\pi d^2}{4} = \frac{\pi(b^2 + a^2 \tan^2 \varphi)}{1 + \tan^2 \varphi} \qquad (2.31)$$

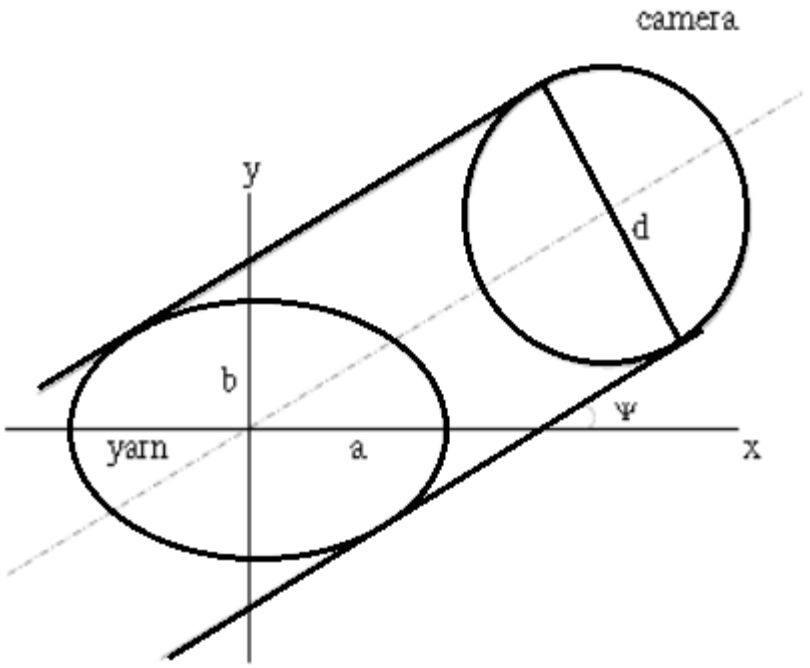

Figure 2.6: Projected yarn diameter using single camera

Then they compared the actual area to the projected area and plotted the difference as an error. As one expects the error was maximum when the major or minor axes were perpendicular to the light beam. They next introduced another camera into their model as shown in Figure 2.7. The measured area was calculated theoretically by adding the projected areas of the two cameras and dividing the result by 2. The measurement error was plotted for various values of α ($0 \leq \alpha \leq \pi$). It was shown that when two light beams are perpendicular to each other, in other words when $\alpha = \pi/2$, the error was zero, indicating that the measured area was exact and independent of the camera or the orientation of the yarn. Huh and Suh, 2003 suggested that if the variations in yarn diameter are correlated, then the sampling interval in optical systems may also affect the measured signal. They observed that the higher the sampled data were correlated with each other, the higher were the mean thickness and the CV (%).

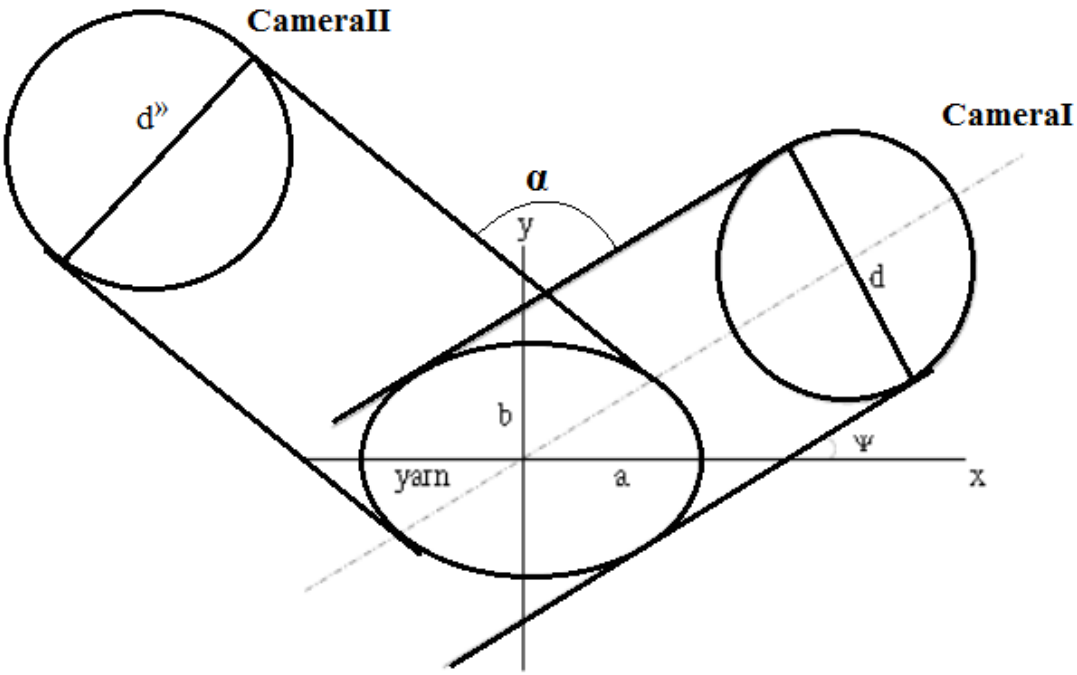

Figure 2.7: Projected yarn diameter using two cameras

This suggested that the mean and standard deviation of the measured thickness decreases as the yarn speed increases. They concluded that in order to reach the randomness of yarn thickness variation, the yarn must be sampled at further than 2 mm intervals. The advantages and disadvantages of capacitive and optical systems are listed in Table 2.1. Because of the advantages of optical systems, they are preferred over capacitive ones (Booth, 1977, Mukhopadhyay, 2002).

Table 2.1: Comparison of yarn irregularity measurement systems

System	Advantage	Disadvantage
Optical	• Sees like eye. • Suitable for hairiness determination. • More sensitive to diameter variations. • The fiber material does not affect measurement due to conductivity.	• Discrete sampling causing lower resolution. • Irregular shape of yarn cross-section. • Inhomogeneous radiant intensity. • Sensitive to vibrations during measurement.
Capacitive	• Continues sampling	• Sensitive to temperature and humidity. • Not suitable for hairiness calculation. • Sensitive to fiber material.

2.6. Wavelet-stochastic hybrid model for yarn diameter simulation:

Fundamental problems of on-line yarn monitoring systems are the storage and handling of vast amounts of data. Kim et al, 1998 developed a system for characterization of yarn properties (mass, diameter) using a wavelet-stochastic hybrid method. According to the method developed only the essential statistical information and significant events are recorded, and vast amounts of normal data are filtered out. While the stochastic models facilitate detection and identification of the spinning faults, wavelet analysis allows the compact representation of the necessary information with up to a 99.9% data reduction rate. It was shown that a variety of virtual yarns could be generated with the algorithm developed for data reduction.

Data screening and reduction:

The spun yarn was considered an assembly of fiber with random thick places and neps. The parameters of these imperfections were the amplitude of the fault, the length of the fault, and the arrival time of these faults. For the arrival time of these faults, the Poisson process was chosen. The Gamma and generalized Pareto distribution functions were chosen for the length and the amplitude of the thick places, respectively (Kim et al, 1998): The procedure for data screening and reduction was as follows:

- Capture yarn diameter signals until a base parameter set is formed;
- Capture yarn diameter signals continuously in a block and estimate the parameters of the block;
- Compare the parameters of the block with the base parameter set;
- If there is a significant change, record the location of the current block along with its parameters, before compressing them using wavelet transform;
- Otherwise discard the current block data; and
- Continue processing from step 2 as needed.

Snyder et al, 2000, tried to develop a fabric quality rating system using wavelet methods and *CY ROS*® in conjunction with human judgment. Yarn signals captured from a traditional evenness tester were first broken down into twelve sub-signals using wavelet decomposition and multi-resolution analysis (MRA) with successively decreasing frequencies. The variance profiles of these twelve sub-signals were then obtained and compared with various yarns having specific fabric defects. The correlation between the defects and these sub-signals is determined and used to develop visual

quality rating system in conjunction with subjective (human) evaluations of *CY ROS*® fabric images.

2.7 Fabric appearance and irregularity:

Farger et al, 1950, studied the effects of yarn irregularity in dyeing and finishing. They examined the effect of weight irregularity, twist irregularity, and the fiber characteristic variation. Their study showed that:

- The yarn mass variation effects the weight distribution and cover of fabrics, which in turn may affect the dyeability and the finishing behavior of fabrics. This was because liquors used in processing penetrate differently depending on the accessibility of the material.
- The yarn twist variation causes packing density variation, which in turn effects the penetration of liquids. In addition, highly twisted portions of the yarn are raised more slowly than the portions of low twist, and this causes variations along the cloth causing wasting, puckering, and pile variations.
- The variation in fiber characteristics is responsible for irregular natural shade.

Prevention of defects that occur during weaving or knitting, in other words, during the fabric production process, requires on-line monitoring of the raw fabric. On the other hand, the yarn related defects could be prevented by inspecting the yarns as thoroughly as possible. While most of the defects may be identified right after fabric production, some yarn related irregularities appear after dyeing and finishing.

2.7.1 The analysis of fabric appearance and uniformity:

Surface-variation function:

Wegener, 1986 introduced a surface variation function to estimate the irregularity of the textile surfaces. He suggested that the variance-area relation of fabrics characterizes the variation of a property in its dependence on the measured area similar to variance-length relation of linear fiber assemblies. Analogous to within and between length variations of variance-length curves, internal and external surface variation function, as well as a total coefficient of variation, were discussed in his paper. He pointed out that the surface variation function can be satisfied for different properties of a fabric such as mass, thickness, reflectivity, absorption, and air and water permeability. However, he suggests that mass distribution acquires practical importance due to following reasons:

- Mass per unit area is often used in irregularity measurement of textile fabrics;
- The mass for unit area and its scatter are experimentally easy to determine.

The surface coefficient of variation CB (A) of the masses Gi(g) of N square fabric samples of area A (cm^2) was determined as follows:

$$CB(A) = \frac{100}{\bar{G}} \sqrt{\frac{1}{N-1}\sum_{i=1}^{N}(G_i - \bar{G})^2} \qquad (2.32)$$

Where G_i = mass of the i^{th} sample of size A within the fabric,

$\bar{G}$= average mass of samples of area size A, and

N = total number of fabric samples with size A.

Defining the ideal weaving process as a process in which the yarns are uniformly spaced, the thick and thin places in the yarn are randomly

distributed in the fabric, the yarn tension and weaving conditions are constant, and the fabric contains no faults, Wegener, 1986 suggested that the irregularity of warp yarn and weft yarn and the deviation from an ideal manufacturing process causes fabric mass variations. As with between length variation curves, between area variation curves decrease as section size or cover increases. This can be explained by the doubling law but in two dimensions and is given by

$$CB^2(A) = \frac{CB^2(L_1)z_1\left(\frac{e_1T\overline{G_1}}{e_2T\overline{G_2}}\right) + CB^2(L_2)z_2}{\sqrt{A}\left[z_1\left(\frac{e_1T\overline{G_1}}{e_2T\overline{G_2}}\right) + z_2\right]^2} \qquad (2.33)$$

Where A is the sub-sample area of a square fabric,

CB (L_i) is the length variation of yarn i,

L_i is the extended sample length of the part of yarn i in the fabric,

e_i is the crimp % of yarn i,

z_i is the thread density of yarn i,

$T\overline{G_i}$ is the count of yarn i, and

i=1, 2 yarn 1 and yarn 2, respectively.

For a fabric having the same structure in the warp and weft directions, the indices of quantities *z*, *e*, $T\overline{G}$, and CB (L) can be omitted in Equation 2.32 and the surface variation function simplifies to;

$$CB^2(A) = \frac{CB^2(L)}{2z\sqrt{A}} \qquad (2.34)$$

As seen from Equation 2.33, CB2 (A) is less than CB2(L) by the factor of thread density and sample area. Consequently, the CB (A) curve has greater negative slope than the CB(L) curve for small values of L and A.

Therefore CB(A) approaches zero faster than CB(L) as shown in Figure 2.8.

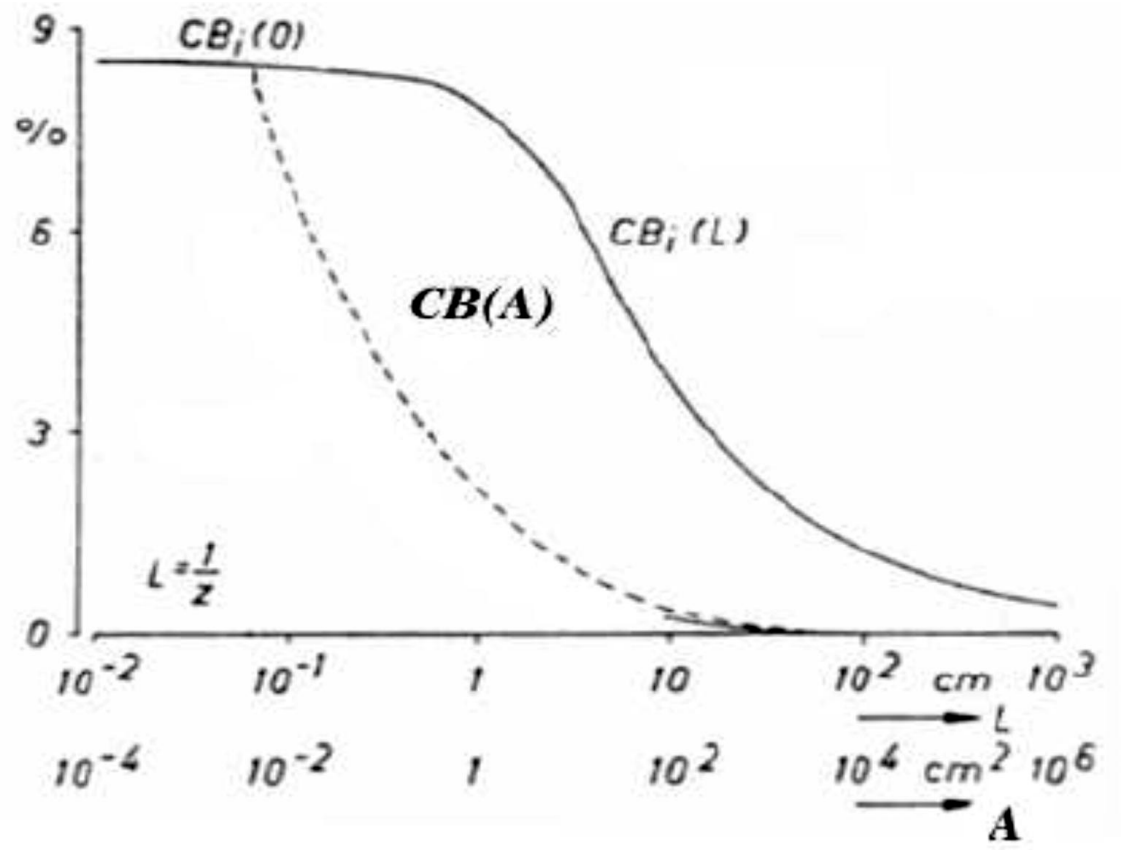

Figure 2.8: CB (L) and CB (A) of a fabric (Wegener, 1986)

Wegener conducted experiments that showed that the observed CB(A) in a real weaving process was higher than the theoretically calculated one. He stated that the reasons for this disagreement were:

- Non-uniform thread spacing;
- Non-random distribution of thick and thin places in the fabric;
- Tension differences and faults (knots).

It was suggested that the surface coefficient of variation contains irregularity contributions of warp and weft and is given by the following equation;

$$CB(A) = \sqrt{\frac{V\ ar_w(A) + V\ ar_p(A)}{\bar{X}_w + \bar{X}_p}} \qquad (2.35)$$

Where $\bar{X}_w$ and $\bar{X}_p$ are the mean masses of individual warp and weft contributions.

Therefore $\bar{X}_w + \bar{X}_p = \bar{G}$, and Var_w (A) and Var_p (A) are the variance contributions of individual warp and weft masses.

Wegener finally derived the surface variation function for an ideal knitting process assuming single-yarn system and setting warp-thread density to zero as follows:

$$CB^2(A) = \frac{CB^2(L_s)}{z_s\sqrt{A}} \qquad (2.36)$$

Where z_s = stitch density of fabric,

L_s = is the yarn length in a row of stitches.

As in woven fabrics, he observed that the surface variation function of a knitted fabric was also higher than the theoretically calculated one.

2.8. Variance-area curves:

Han et al, 2002 developed two prediction models for fabric quality based on 2-D and 3-D electronic fabric images. These fabric images were obtained by mapping yarns into specific locations in a 2-D matrix array. They suggested two types of variance-area curves, CV (A) and CB (A) curves, to quantitatively judge the fabric quality in its dependence on the measured area. It was shown that the variance-area curves approach their limits asymptotically as the unit area increases similarly to the variance-length curves. They also demonstrated that a larger CB (A) value implies a greater appearance variation especially in the form of scattered fabric non-uniformity such as cloudiness and bárre. Finally they investigated the

invariance property of the variance-area curves within a fabric by arranging the weft yarns to either random or specific locations within the fabric. They concluded that as long as the original yarn data sets remain the same, the variance-area curves would be identical regardless of the way weft yarns are arranged.

2.9. Anisotropy of 2-D texture images:

C. T. J. Dodson, 1996, investigated the uniformity and anisotropy of 2-D texture images of structures such as paper, nonwoven materials, and medical images. Dodson, 2000 gave definitions of anisotropy and isotropy as follows, respectively: the random field is anisotropic if adjacent pixels have a stronger correlation along one direction than another direction; if the correlation between grey-levels decreases equally in all directions, then the random field is isotropic. In addition, Dodson et al, 1996 suggested an index called anisotropy for the quantification of anisotropy in 2-D structures. According to his approach, an ellipse was fitted to a number of variance-between-area readings at different angles. The anisotropy index was then defined to be the function of eccentricity of the best-fit ellipse for each unit area size. If the correlation between the points of a fabric decreases equally as a result of isotropy, then the ellipse will be a circle, and if they are highly correlated then the ellipse will be highly elliptic. However, since a woven fabric is made of mainly two groups of yarns, warp and weft, it may not be necessary to investigate other directions.

2.10 Summary:

Extensive research work, such as the introduction of quality indices, time series analysis, Fourier transform, and Wavelets have been carried out to develop systems for signal for woven fabric characterizing and

numerous fabric and yarn properties. Several authors (Wegener, 1986, Moyer, 1992] suggested that the quality of fabric can be predicted from the CV (%) of the yarns that are used within the fabric. However, the CV (%) is grossly insufficient to predict the features of irregularities, as it is not location specific within the fabric. In addition to the CV (%), several methods are developed to evaluate fabric qualities that are based on the actual fabric. The Kawabata System (KES) (Sule &Bardhan, 1999) and fabric assurance by simple testing (FAST) are among the ones that are industrially accepted. They provide indices for quantification of various fabric qualities. Recognizing the difficulty in assessing fabric irregularities from a single number, it was suggested that the aesthetics and appearance qualities of fabrics could be visualized with the information obtained on yarn properties without having to weave or knit a fabric. This prediction is usually achieved by collecting on-line or off-line mass and/or diameter information of yarns and simply mapping them into a 2-D matrix, such as shown in Figures 2.9 and 2.10, through a simulation technique (Nevel & Avsar, 2001, Suh et all, 2003). While the existing visualization methods (CY ROS ®, etc.) do not quantify irregularity, the fabric evaluation systems (KES ®, FAST ®) on the other hand provide an index for quantifying quality.

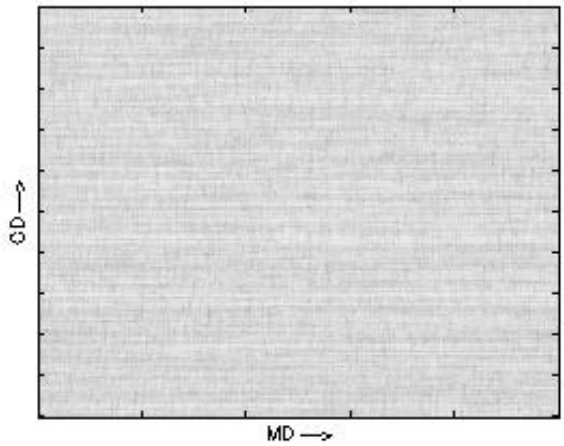

Figure 2.9: Mapping of yarn signal into a woven fabric

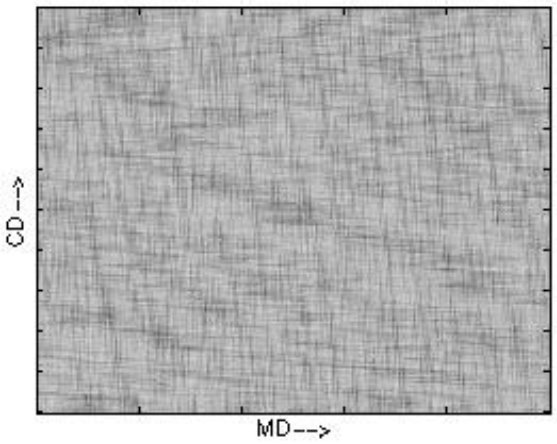

Figure 2.10: Mapping of yarn signal for another woven fabric

However, information on the irregularity features of fabrics cannot be obtained from a single number. Townsend and Cox, 1951 suggested that the relationship between the coefficient of variation and the length within which the variance is measured leads to indices characterizing the types of yarn irregularity that have practical importance. They characterized the uniformity of the yarn along the yarn axis, and expanded the CV (%), a

point estimate, to a series of numbers expressible in two curves also known as variance-length curves. They showed that the variance-length curves provide a much more powerful method for discriminating the irregularity features of the spun yarns than any other method. Wegener, 1986 introduced the surface variation function, which is determined by partitioning the 2-D fabric into subsections and calculating the mass variation between these sections. In addition, he derived the relationship between variance-length and the surface-variation function for square unit-areas. He finally concluded that the surface-variation of a fabric could be estimated from the variance-length relationship of the yarns that are used; therefore, it is not necessary to obtain the surface variation function of a fabric. Fundamental problems of on-line yarn monitoring systems are the storage and handling of vast amounts of data. Kim et al, 1998 developed a system for characterization of yarn properties (mass, diameter) using a wavelet-stochastic hybrid method. According to the method developed only the essential statistical information and significant events are recorded and a vast amount of normal data is filtered out. While the stochastic models facilitate detection and identification of the spinning faults, wavelet analysis allows the compact representation of the necessary information. It was shown that a variety of virtual yarns could be generated with the algorithm developed for data reduction. Generation of vast amounts of simulated yarn data, however, requires a better understanding of yarn geometry. Most studies, which describe the geometry of yarn and fabrics, assume a circular cross section for the yarn. With advances in image processing and computing, it was demonstrated that the shapes of yarn cross-sections could be better approximated as ellipses (Tasi & Chu, 1996). However, the interactions between the twist and the elliptic cross-section of

the yarn, the distribution of eccentricity, and the orientation of the major axes with respect to the twist of the yarn have not yet been addressed. Attempts have been made to estimate the twist of yarn by finding the slope of this best-fit sine curve of the fibers laid on the surface (Cybulska, 1999). Because yarn has an elliptic cross-section, the sine curve approximation must be revised in order to improve this estimation.

CHAPTER THREE

Material and Method

3.1 Design of experiments for determination of yarn evenness:

3.1.1 Equipment:

The experiments were carried out on the Uster Evenness Tester3. It measures mass variations along the length of a fibre assembly. A photo of the Uster tester 3 is shown in Figure 3.1. It is based on the capacitance principle as depicted in Figure3.2. The two capacitors detect the mass variations or weight per unit length variations of the fibre assembly running between them. These variations are transformed into a proportional electrical signal. The signal processing unit will process this signal, and work out the U% and CV% value, as well as other useful information concerning the mass variations.

Figure3.1: Aphoto of Uster evenness tester3(Zellweger)

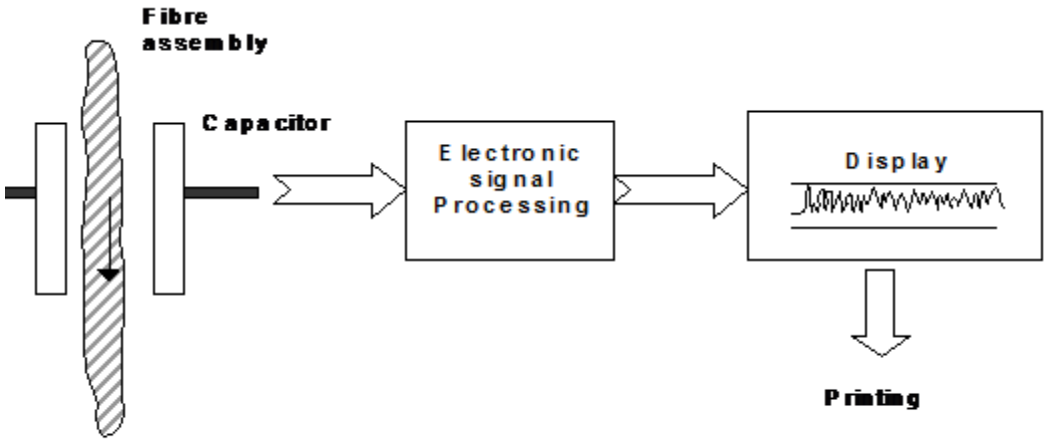

Figure 3.2.: Principle of Uster Evenness Tester

The Uster evenness tester provides a considerable amount of information on the evenness of a fibre assembly, including:

1. Single overall results:

These include the U% and CV% values, the index of irregularity (I), as well as the number of imperfections (thin place, thick place, and neps). All those parameters are expressed as single numbers, which are easy to use, particularly in a mill situation. These single values provide an overall picture of yarn evenness. However, if the results are bad, the causes of the poor results cannot be identified from these single values.

Um — Irregularity (U) of the mass with a cut length of approximately 1 cm (measuring field length). In other words, this is the U value one could get from cutting the yarn into approximately 1 cm sections and weighing those short sections.

CVm — Coefficient of variation of mass with a cut length of approximately 1 cm. This is the CV most often quoted in yarn specification and commercial transactions. It is the effective CV used for calculating the index of irregularity.

CVm(1m) Coefficient of variation of mass with a cut length of 1 m, simulating the CV that can be obtained from cutting the yarn into 1 m sections and weighing those sections. The same applies to CVm (10m) and CVm (100m). It should be noted that as the measured length increases, the irregularity reduces.

Index The index of irregularity (I) value, which is always greater than one as indicated in the print-out.

Thin places (-50%)

Number of places that have mass reductions of 50% or more with respect to the mean value. Note that (-50%) is the standard sensitivity level used in the test. If a different sensitivity level (-40%, -50%, -60%) is used, the result would have been different. The number of thin places has a significant impact on yarn strength.

Thick palces (+50%)

Number of places that have mass increases of 50% or more with respect to the mean value. Note that (+50%) is the standard sensitivity level used in the test. If a different sensitivity level (+35%, +70%, +100%) is used, the result would have been different.

Neps (+280%)

Number of places that have mass increases of +280% or more with respect to the mean value and a reference length of 1mm. Note that +200% is the sensitivity level normally used in the test. The results would have been dThese short thick places in a yarn are often the results of vegetable matter or entangled fibres.

S Standard deviation of results

Q95% 95% confidence interval of the mean value

(note that the thin places, thick places, and neps are called imperfections.)

2. Diagram:

A diagram is simply a trace of mass (linear density) variations along a fibre assembly. For instance, if a long length of yarn is dissected into many very short sections and then weigh each section; many mass readings (x_i) will be obtained as shown in Figure 3.3

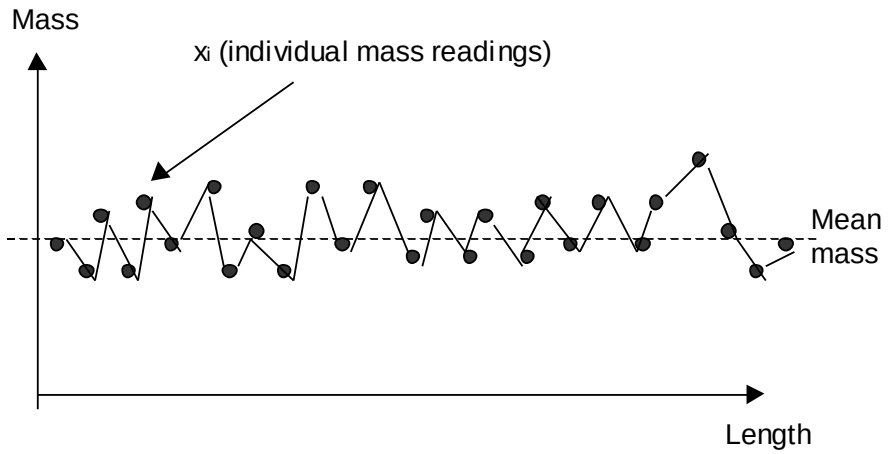

Figure 3.3: Manually constructed diagram of mass variation

From this diagram, many useful statistics parameters such as (mean, CV etc) can be obtained.

Atypical diagram obtained from the Uster evenness tester is shown in Figure 3.4 .The diagrams can help to identify extreme thin and thick places, slow changes in the mean mass value, step changes in the mean value, periodic mass variations of long wave length etc.

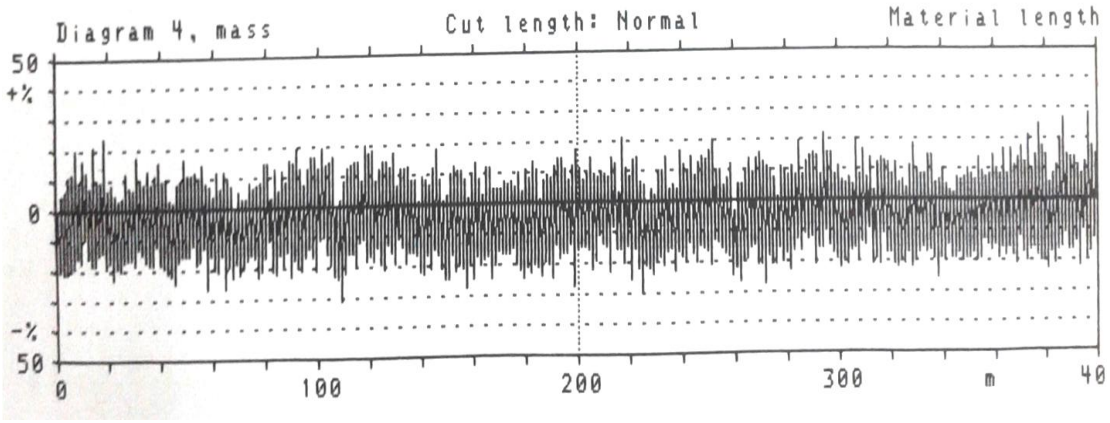

Figure 3.4: Uster tester diagram of mass variation

All the necessary adjustments for the Uster are given in table3.1

Table 3.1: uster3 adjustments

Sample No.	V (m/min)	Time (min)	Slot/yarns	Yarn tension (%)	Imperfections	No. of tests
1	400	1	3	50	Short staple	10
2	400	1	4	37.5	Short staple	5
3	400	1	3	50	Short staple	5
4	400	1	3	50	Short staple	5
5	400	1	4	25	Short staple	5
6	400	1	4	50	Short staple	10
7	400	1	4	37.5	Short staple	10

- All the details can be displayed or printed out.
- All the measurements of the yarn evenness were carried out at SAMTEX FACTORY (Al Hasahisa)

3.1.2 Yarn conditioning:

For all the experimental work given in this thesis, the yarns used are stored for at least 24 hours in a standard atmospheric condition i.e Rh 65 ± 2% and T= 27 ± 2°C except where otherwise stated .

3.1.3 Yarn properties:

Seven different types of yarns are used in this resarch. These yarns are the most common yarns used to produce knitted fabrics in Sudan.. The measured yarn properties are given in table 3.2. The yarn diameter is calculated using the equation given below:

$$d = \frac{1}{28\sqrt{Ne}} \qquad \text{(Booth, 1977)}$$

Where *d* is yarn diameter in inch.

Ne is yarn count.

Table 3.2: measured yarns properties

Sample No.	Material & Spinning Type	Yarn count Ne	Yarn diameter mm	Yarn twist TPM	Evenness		Appearance (visual inspection)
					Cv%	U	
1	p/v (65/35)% Ring	14	0.242443	650	10.65	8.48	Grade A
2	Cotton Ring	24	0.185166	958	19.68	15.42	Grade B
3	p/c (50/50)% Ring	15	0.234213	530	8.84	7.03	Grade B
4	p/v (65/35)% Ring	15	0.234213	570	10.39	8.24	Grade A
5	Polyester Ring	30	0.165633	870	14.5	11.52	Grade A
6	Cotton Ring	16	0.226797	717	13.89	10.98	Grade A
7	Cotton Open end	20	0.202844	780	13.74	10.81	Grade B

3.1.4 Techniques used to determine yarn appearance:

The visual examination method described in Chapter One section 1.1.2, is used to determine the yarn appearance.

3.2. Design of experiments for the production of fabric samples:

3.2.1. Equipment:

Passap Doumatic 80 Knitting machine Fig 3.5 is used to produce a plain knitted fabric from each yarn ample.

The main parts of the machine are illustrated by the numbers shown in figure 3.5 and are as follows:

1) The needles: front and back row, each having 179 needles.

2) The needles scale: a numbering scale starting from the centre of the bed. All needles are numbered to facilitate countering of the stitches.

3) The knob for lowering the front bed is situated at the right hand side underneath the front bed .To lower the front bed; it is pulled to the right. To return bed to its normal position the front bed is pressed and the knob is pulled up to the left simultaneously.

4) The locks (front lock &back lock): they are the most important parts of the machine. They carry the counter to count the number of rows, feeders and cams operating the needles.

5) The yarn guides: they guide the yarn to unwind smoothly and easily from the supply cones.

6) The color changer: it selects the required yarn color automatically.

7) The racking handle: it serves to move the back bed sideways in relation to the front bed – in either direction.

8) The racking indicator: the metal indicator is situated at the bottom to the left of the front bed. It indicates the direction of the racking movement.

9) The blocking rail: It is used to lock and release the pusher in order to change their positions.

10) The edge springs: There are four edge springs .Two on each bed. They must always be placed on the edge of the needles while they are in working position, with their latches closed.

11) The trip cam for the row counter: it operates the row counter each time the lock moves across it.

12) The clip of the guide sheet: it serves to hold the guide sheet or any other notes during knitting.

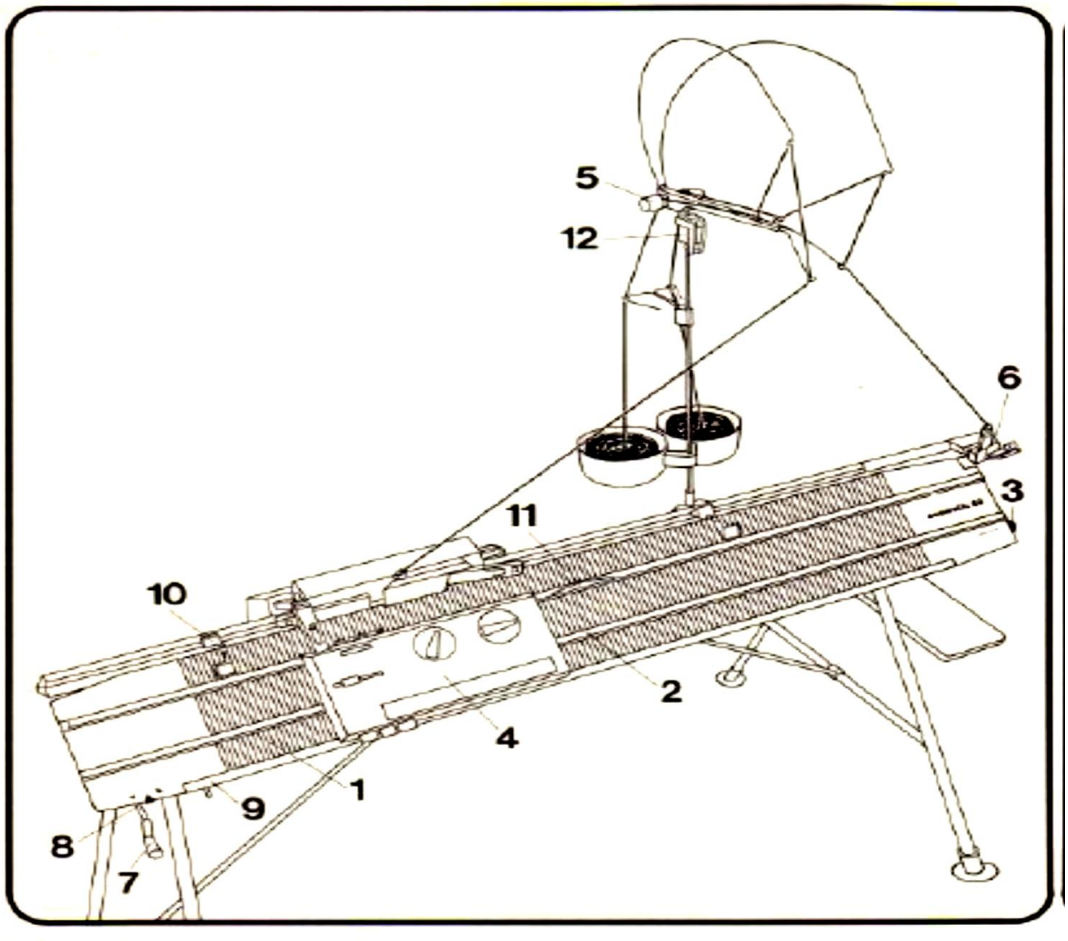

Figure3.5: Passap duomatic machine.

3.2.2. Experimental conditions and procedure:

The adjustment and the setting of the knitting machine used to produce the fabric samples are as follows;

- Rule needles: follow rule needles.
- Stitch size: 3
- N-X Laver: N
- Stripers: orange.
- Feeder: one feeder
- Raking handle: down

3.2.3. Fabric samples properties and specifications:

From each yarn type a double ribbed knitted fabric is produced. The specifications of the knitted fabric samples are given in table 3.3. The sample numbers given in table 3.3 correspond to the sample numbers given in table 3.2.

Table 3.3: the knitted Fabric Specifications

SAMPLE No.	YARN USED	KNITTED FABRIC TYPE	COURSE LENGTH (cm)	STITCH LENGTH (cm)	STITCH DENSITY (stitch/cm^2)	FABRIC APPEARANCE
1	p/v (65/35)%	Interlock	110	0.92	30	G
2	Cotton	Interlock	110	0.92	29	M
3	p/c (50/50)%	Interlock	110	0.92	28	G
4	p/v (65/35)%	Interlock	110	0.92	29	G
5	Polyester	Interlock	110	0.92	28	G
6	Cotton	Interlock	110	0.92	30	G
7	Cotton	Interlock	110	0.92	28	G

3.2.4. Technique used to determine the fabric CV:

The cut and weigh method is used to determine the fabric CV. The CV of each knitted fabric type is determined. For each knitted fabric sample 100 tests are performed. For each test the knitted fabric sample is taken in such a way that it consists 18 courses. Therefore the length of the yarn used is nearly 20 m. From each knitted fabric type a total of 1800 courses (equivalent to 2000 m yarn being consumed) is tested.

3.2.5. Technique used to determine the fabric appearance:

The Uster statistics is used to determine the knitted fabric appearance. The grading system given by the Uster statistics is based on the as follow:

Appearance (u%)	Classification
12.6	Good (G)
12.7-14.7	Medium (M)
14.8.18.0	Acceptable (MS)
>18.0	Unacceptable (SS)

CHAPTER FOUR

Result and Discussion

This chapter shows the results obtained for the yarn tests and the knitted fabric analysis.

4.1. The yarn:

4.1.1. Yarn irregularities:

For each yarn sample the irregularity is tested using Uster3 Tester. The mass diagram and the coefficient of variation are obtained.

Sample 1:

As mentioned before for yarn "sample 1" ten tests are performed. The results are given in table 4.1 and their spectrograms mass wavelength is shown in Appendix A. The figure consists of ten diagrams. Each diagram shows the mass variations for 400 meter length of yarn.

Table 4.1 total result for Ne 14 polyester/viscose (65/35) yarn

Test No	Um %	CVm %	Thin - 40%	Thin -50%	Thick +35%	Thick +50%	Nebs +200%	Nebs +280%	Hairiness (-)
1	**8.84**	**10.09**	**1**	**0**	**9**	**0**	**0**	**0**	**6.54**
2	**8.68**	**10.81**	**4**	**0**	**14**	**3**	**2**	**2**	**6.21**
3	**8.74**	**10.97**	**5**	**0**	**14**	**0**	**2**	**0**	**6.37**
4	**8.43**	**10.57**	**0**	**0**	**13**	**1**	**2**	**1**	**6.25**
5	**8.43**	**10.59**	**3**	**0**	**13**	**3**	**4**	**1**	**6.16**
6	**8.69**	**10.92**	**6**	**0**	**12**	**4**	**2**	**2**	**5.97**
7	**8.37**	**10.54**	**6**	**0**	**9**	**1**	**1**	**1**	**5.85**
8	**8.45**	**10.61**	**7**	**0**	**10**	**1**	**2**	**1**	**5.98**
9	**8.67**	**10.92**	**10**	**0**	**14**	**5**	**4**	**3**	**5.81**
10	**8.35**	**10.58**	**2**	**0**	**18**	**3**	**2**	**0**	**5.91**
Mean value	**8.48**	**10.65**	**11/km**	**0/km**	**32/km**	**5/km**	**5/km**	**3/km**	**6.10**
CVb (%)	**2.46**	**2.49**	**68.8**	**8.0**	**21.9**	**82.3**	**57.0**	**90.4**	**4.83**
0.95% +/-	**0.15**	**0.19**	**5**	**0**	**5**	**3**	**2**	**2**	**8.18**

As can be seen from table 4.1and figure 4.1 the yarn shows very good evenness based on the Uster statistics 2013 recommendations.

Sample 2:

As mentioned before for yarn sample 2 five tests are performed. The results are given in table 4.2 and their spectrograms mass wavelength is shown in Appendix B. The figure consists of five diagrams. Each diagram shows the mass variations for 400 meter length of yarn.

Table 4.2 total result for Ne 24 cotton yarn

Test No	Um %	CVm %	Thin -40%	Thin -50%	Thick +35%	Thick +50%	Nebs +200%	Nebs +280%	Hairiness (-)
1	**15.20**	**19.37**	**560**	**73**	**927**	**274**	**205**	**52**	**7.98**
2	**15.03**	**19.09**	**518**	**40**	**889**	**247**	**201**	**57**	**7.88**
3	**15.63**	**20.05**	**606**	**70**	**1004**	**331**	**215**	**59**	**7.94**
4	**15.60**	**19.96**	**641**	**76**	**1093**	**350**	**252**	**85**	**7.91**
5	**15.66**	**19.92**	**602**	**62**	**1091**	**358**	**319**	**92**	**7.89**
Mean value	**15.42**	**19.68**	**1464/km**	**160/km**	**2502/km**	**780/km**	**596/km**	**178/km**	**7.90**
CVb (%)	**1.87**	**2.15**	**8.1**	**22.6**	**9.3**	**15.7**	**20.7**	**22.9**	**0.91**
0.95% +/-	**0.36**	**0.53**	**147**	**45**	**289**	**152**	**153**	**50**	**0.09**

As can be seen from table 4.2 and the spectrograms the yarn has a high CVm, thick- and-thin places and neps which lead to high irregularity and lower evenness.

Sample 3:

As mentioned before for yarn sample 3 five tests are performed. The results are given in table 4.3 and their spectrograms mass wavelength shows the mass variations for 400 meter length of yarn.

Table 4.3 total result for Ne 15 polyester/cotton (50/50) yarn

Test No	Um %	CVm %	Thin -40%	Thin -50%	Thick +35%	Thick +50%	Nebs +200%	Nebs +280%	Hairiness (-)
1	**7.20**	**9.06**	**0**	**0**	**12**	**1**	**2**	**2**	**7.65**
2	**6.98**	**8.78**	**0**	**0**	**3**	**1**	**2**	**0**	**7.68**
3	**6.94**	**8.71**	**0**	**0**	**3**	**0**	**0**	**0**	**7.69**
4	**7.05**	**8.86**	**0**	**0**	**6**	**0**	**2**	**0**	**7.65**
5	**6.99**	**8.81**	**0**	**0**	**3**	**0**	**0**	**0**	**7.60**
Mean value	**7.03**	**8.84**	**0/km**	**0/km**	**14/km**	**1/km**	**3/km**	**1/km**	**7.65**
CVb (%)	**1.45**	**1.50**	**0.0**	**0.0**	**72.4**	**0.0**	**91.3**	**0.0**	**0.46**
0.95% +/-	**0.13**	**0.16**	**0**	**0**	**12**	**2**	**3**	**3**	**0.04**

As can be seen from the table 4.3 and the spectrograms the yarn has a very low CVm, thick-and-thin places and neps which lead to high degree of evenness.

Sample 4:

As mentioned before for yarn "sample 4" five tests are performed. The results are given in table 4.4 and their spectrograms mass wavelength are shown in Appendix D. The figure consists of five diagrams. Diagram shows the mass variations for 400 meter length of yarn.

Table 4.4 total result for Ne 15 polyester/viscose (65/35) yarn

Test No	Um %	CVm %	Thin -40%	Thin -50%	Thick +35%	Thick +50%	Nebs +200%	Nebs +280%	Hairiness (-)
1	**7.95**	**10.03**	**2**	**0**	**12**	**4**	**7**	**3**	**6.17**
2	**8.34**	**10.52**	**3**	**0**	**17**	**3**	**8**	**1**	**5.72**
3	**8.34**	**10.49**	**4**	**0**	**13**	**2**	**7**	**2**	**6.05**
4	**7.70**	**9.71**	**0**	**0**	**10**	**4**	**4**	**2**	**6.02**
5	**8.85**	**11.21**	**2**	**0**	**22**	**2**	**6**	**3**	**6.28**
Mean value	**8.24**	**10.39**	**6/km**	**0/km**	**37/km**	**8/km**	**16/km**	**6/km**	**6.05**
CVb (%)	**5.32**	**5.47**	**67.4**	**0.0**	**32.2**	**33.3**	**23.7**	**38.0**	**3.48**
0.95% +/-	**0.54**	**0.71**	**5**	**0**	**15**	**3**	**5**	**3**	**0.26**

As can be seen from the table 4.4 and the spectrogram the yarn has a low CVm, thick places, thin places and neps which indicate that the yarn has a very good degree of evenness based on the Uster statistics 2013 recommendation.

Sample 5:

As mentioned before for yarn sample 5 five tests were performed. The results are given in table 4.5 and their spectrograms mass wavelength is shown in Appendix E. The figure consists of five diagrams. Diagram shows the mass variations for 400 meter length of yarn.

Table 4.5 total result for Ne 30 polyester yarn

Test No	Um %	CVm %	Thin -40%	Thin -50%	Thick +35%	Thick +50%	Nebs +200%	Nebs +280%	Hairiness (-)
1	**11.55**	**14.53**	**69**	**1**	**63**	**7**	**6**	**1**	**6.65**
2	**11.57**	**14.51**	**68**	**1**	**61**	**4**	**7**	**1**	**6.23**
3	**11.41**	**14.40**	**90**	**6**	**69**	**7**	**8**	**2**	**6.14**
4	**11.47**	**14.42**	**77**	**9**	**92**	**10**	**13**	**4**	**6.67**
5	**11.59**	**14.64**	**54**	**0**	**86**	**6**	**14**	**6**	**6.52**
Mean value	**11.52**	**14.50**	**179/km**	**8/km**	**185/km**	**17/km**	**24/km**	**7/km**	**6.44**
CVb (%)	**0.66**	**0.66**	**18.4**	**115.0**	**18.9**	**31.9**	**38.0**	**77.4**	**3.78**
0.95% +/-	**0.09**	**0.12**	**41**	**12**	**43**	**7**	**11**	**7**	**0.38**

As can be seen from table 4.5 and figure 4.5 the yarn has a low CVm, thick places & thin places and neps which indicate that the yarn has a very good evenness based on the Uster statistics 2013 recommendation.

Sample 6:

As mentioned before for yarn sample6 ten tests were performed. The results are given in table 4.6 and their spectrograms mass wavelength is shown in appendix F. The figure consists of ten diagrams. Diagram shows the mass variations for 400 meter length of yarn.

Table 4.6 total result for Ne 16 cotton yarn

Test No	Um %	CVm %	Thin - 40%	Thin -50%	Thick +35%	Thin +50%	Nebs +280%	Hairiness (-)
1	**10.77**	**13.58**	**35**	**0**	**72**	**3**	**0**	**7.58**
2	**10.77**	**13.61**	**45**	**0**	**79**	**4**	**0**	**7.58**
3	**10.99**	**13.86**	**41**	**0**	**81**	**6**	**0**	**7.43**
4	**10.94**	**13.85**	**34**	**0**	**81**	**7**	**1**	**7.29**
5	**11.38**	**14.42**	**38**	**0**	**89**	**5**	**2**	**7.04**
6	**11.08**	**13.99**	**45**	**0**	**82**	**5**	**1**	**6.84**
7	**11.04**	**13.92**	**38**	**0**	**55**	**5**	**2**	**7.17**
8	**10.74**	**13.62**	**30**	**0**	**59**	**12**	**0**	**7.47**
9	**10.75**	**13.63**	**31**	**1**	**91**	**7**	**1**	**6.78**
10	**11.36**	**14.38**	**49**	**1**	**69**	**4**	**2**	**7.01**
Mean value	**10.98**	**13.89**	**96/km**	**0/km**	**190/km**	**14/km**	**2/km**	**7.22**
CVb (%)	**2.19**	**2.21**	**16.4**	**0.0**	**15.8**	**43.6**	**97.3**	**4.10**
0.95% +/-	**0.17**	**0.22**	**11**	**1**	**21**	**5**	**2**	**0.21**

As can be seen from the table 4.6 and the spectrogram the yarn has a medium CVm , thick-and-thin places and neps indicate that the yarn has an acceptable evenness based on the Uster statistics 2013 recommendation.

Sample 7:

As mentioned before for yarn sample 7 ten tests are performed. The results are given in table 4.7 and their spectrograms mass wavelength is shown in appendix G consists of ten diagrams. Diagram shows the mass variations for 400 meter length of yarn.

Table 4.7 total result for Ne 20 cotton yarn

Test No	Um %	CVm %	Thin - 40%	Thin -50%	Thick +35%	Thin +50%	Nebs +280%	Hairiness (-)
1	**10.38**	**13.12**	**38**	**0**	**106**	**7**	**1**	**5.95**
2	**10.47**	**13.32**	**45**	**2**	**116**	**6**	**4**	**5.83**
3	**10.83**	**13.70**	**41**	**0**	**108**	**8**	**1**	**5.75**
4	**11.41**	**14.36**	**59**	**1**	**114**	**10**	**2**	**5.13**
5	**10.70**	**13.68**	**43**	**0**	**113**	**8**	**5**	**5.63**
6	**10.61**	**13.47**	**57**	**0**	**100**	**5**	**2**	**5.55**
7	**11.35**	**14.54**	**67**	**2**	**118**	**14**	**8**	**5.41**
8	**10.81**	**13.84**	**56**	**2**	**102**	**7**	**6**	**5.61**
9	**10.85**	**13.74**	**60**	**1**	**99**	**11**	**2**	**5.36**
10	**10.68**	**14.60**	**47**	**0**	**115**	**7**	**5**	**5.43**
Mean value	**10.81**	**13.74**	**128/km**	**2/km**	**273/km**	**21/km**	**9/km**	**5.56**
CVb (%)	**3.12**	**3.16**	**18.9**	**114.9**	**6.5**	**32.2**	**65.7**	**4.37**
0.95% +/-	**0.24**	**0.31**	**17**	**2**	**13**	**5**	**4**	**0.17**

As can be seen from the table 4.7 and the spectrogram the yarn has a low CVm , thick places, thin places and neps indicate that the yarn has a good evenness based on the Uster statistics 2013 recommendation.

From results obtained it can be seen that the polyester and cotton yarns show lower regularity than blended yarns. The polyester /viscous and polyester/cotton blended yarns show a high regularity than the polyester and cotton yarns. Furthermore, fine yarns are more regular than coarse yarns.

4.1.2. Yarn diameter:

The actual yarn diameter was determined as follows:

From the spectrogram diagrams, the deviation in the yarn mass from the mean was determined. The measured yarn diameter was calculated using the following equation:

$$\text{Actual yarn diameter} = d\,(1 + \text{deviation \%})$$

The diameter in millimeters for each yarn type was calculated. The results are given in appendix H. For each yarn type 100 tests were performed. For each test the sample length was 20 meters. Therefore from each yarn type a total of 2000 meters was tested.

4.1.3 Yarn diameter spectrograms:

The spectrograms for each yarn sample were drawn and are shown below. Figure 4.1 shows the variations in the yarn diameter for sample1. As can be seen from the figure the trend the curve behavior is similar to the mass diagram curve for yarn sample1shown in Appendix A

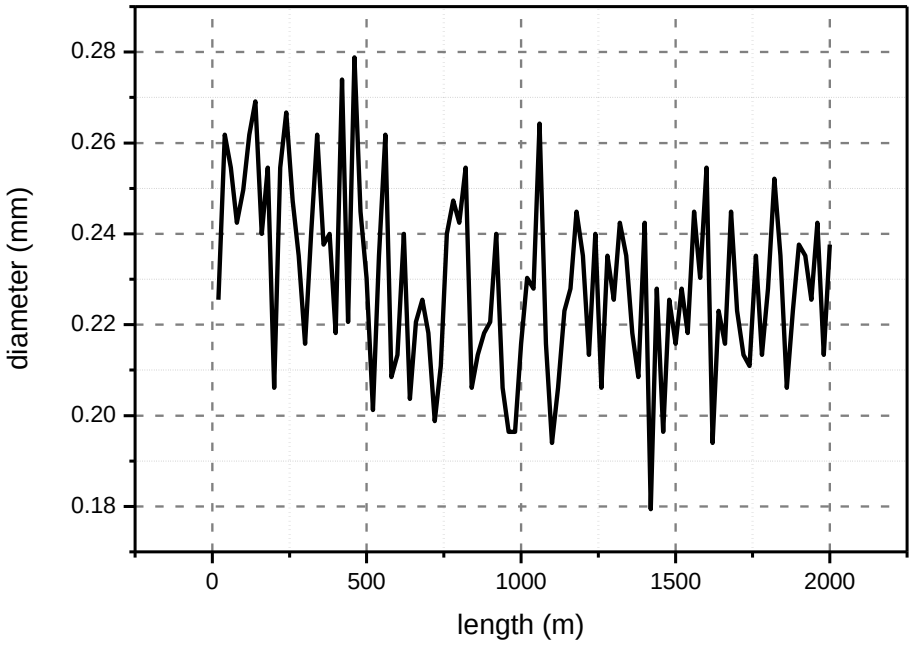

Figure 4.1: The variations in the yarn diameter for Ne 14, polyester/viscose (65/35) blended yarn.

Figure 4.2 shows the spectrogram for the variations in the yarn diameter for sample 2. The curve behavior is nearly similar to the mass diagram curve for sample 2. See Appendix B

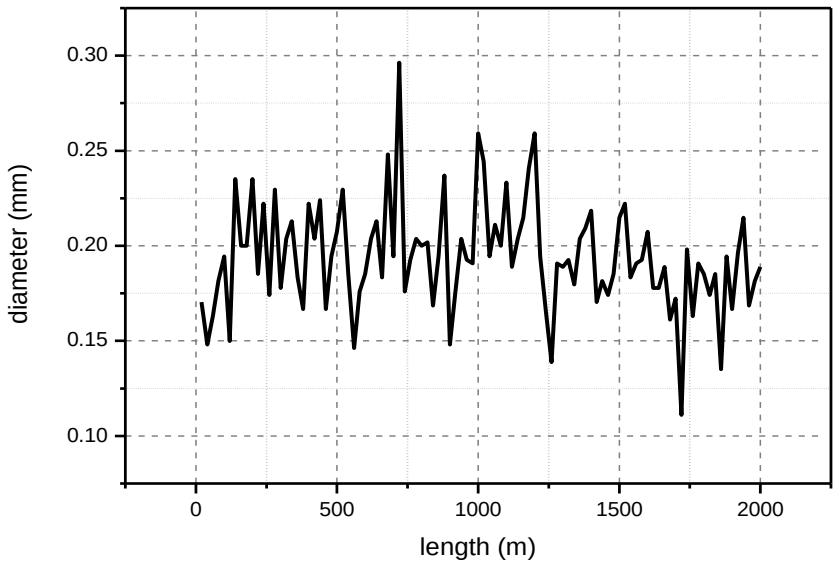

Figure 4.2: The variations in the yarn diameter for Ne 24, cotton yarn.

Figure 4.3 shows the spectrogram for yarn sample 3 diameter. The curve behavior seems to be the same as the mass diagram curve of yarn sample 3.

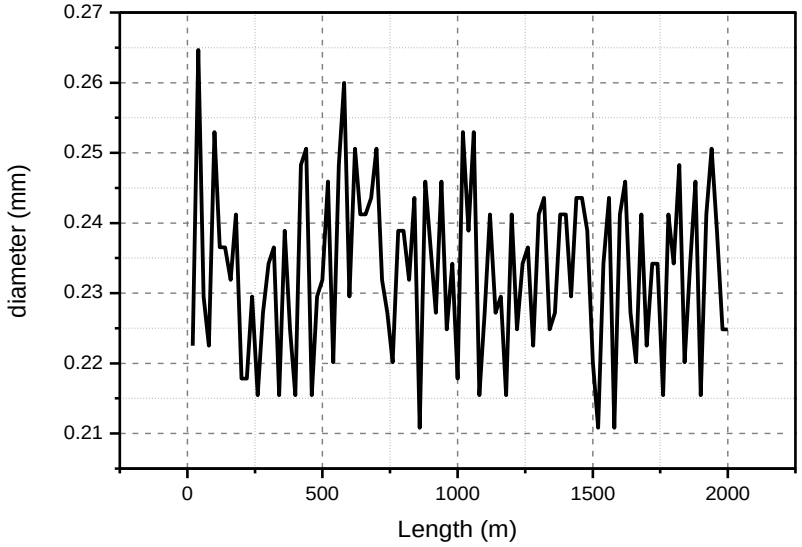

Figure 4.3: The variations in the yarn diameter for Ne 15 polyester/cotton (50/50) blended yarn.

Figures 4.4, 4.5, 4.6 and 4.7 show the spectrogram of variations in yarn diameter for sample 4, 5, 6 and 7 respectively. The curve behavior for both samples is nearly the same as the mass diagram curve of both samples.

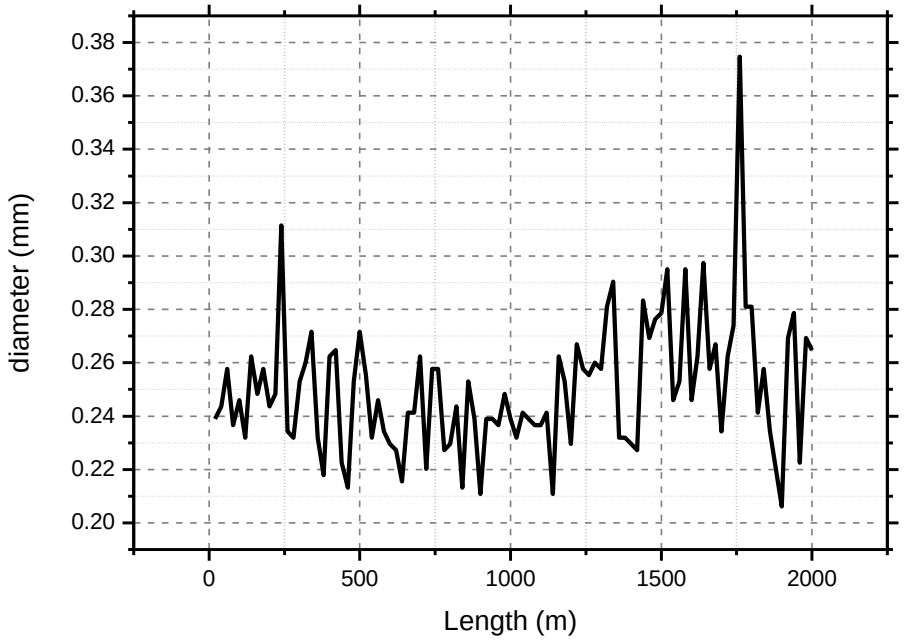

Figure 4.4: The variations in the yarn diameter for Ne 15 polyester/ viscose (65/35) % blended yarn.

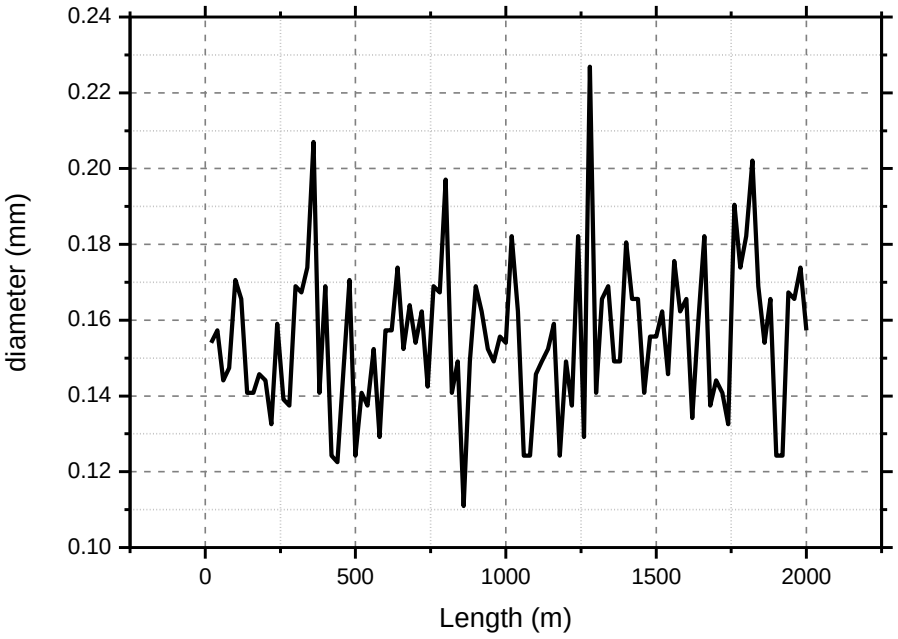

Figure 4.5: The variations in the yarn diameter for 30Ne polyester yarn.

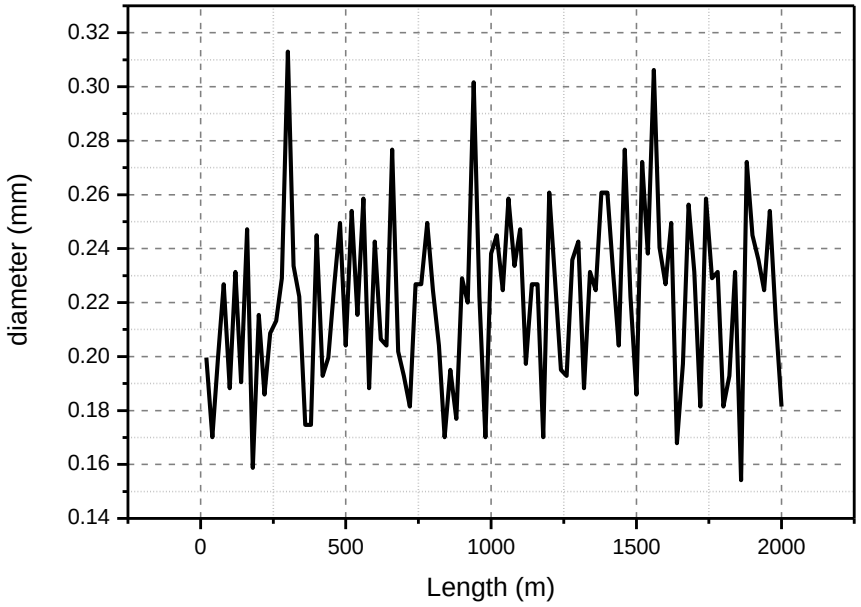

Figure 4.6: The variations in the yarn diameter for Ne 16 cotton yarn.

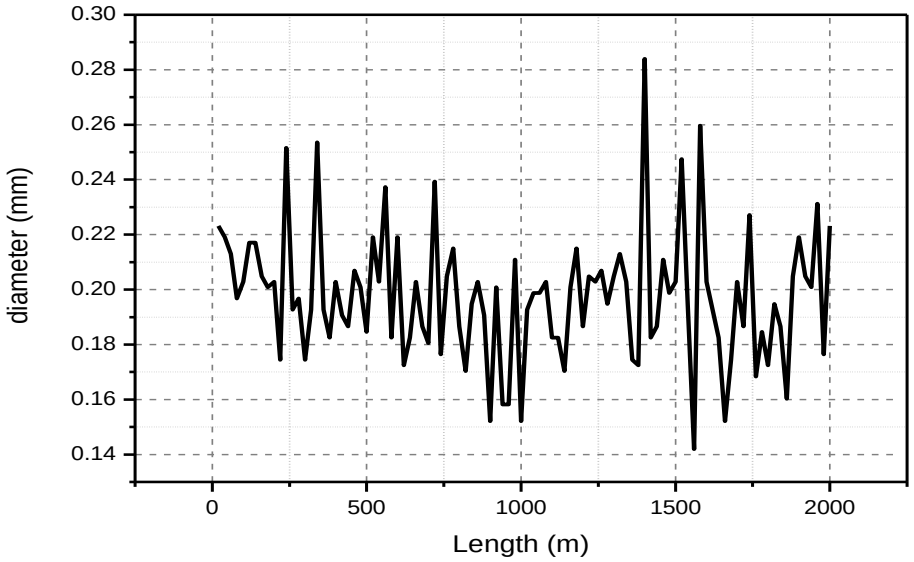

Figure 4.7: The variations in the yarn diameter for Ne 20 cotton yarn.

4.2. Knitted fabric:

From each yarn sample an interlock knitted fabric was produced.

4.2.1 Fabric analysis:

Sample 1:

Figure 4.8 shows the image of fabric knitted from yarn sample1. As can be seen from the image the produced fabric is more regular.

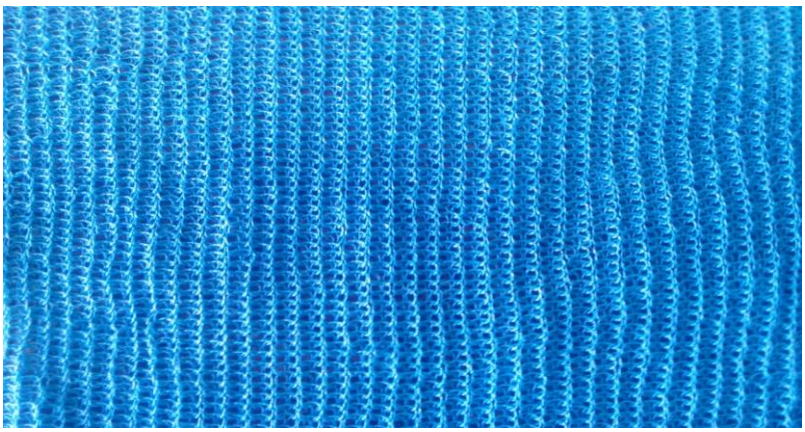

Figure 4.8: Image of fabric1, knitted from yarn sample1

Sample 2:

Figure 4.9 shows image of the fabric knitted from yarn sample 2. From the image, it is clear that the fabric is irregular and shows some faults, cloud area and hairiness. This is attributed to the irregularity of the yarn (sample 2) used to knit the fabric.

Figure 4.9: Image of fabric 2 knitted from yarn sample 2

Sample 3:

Figure 4.10 shows image of the fabric knitted from yarn sample 3. From the image, it is clear that the fabric is regular and shows good appearance.

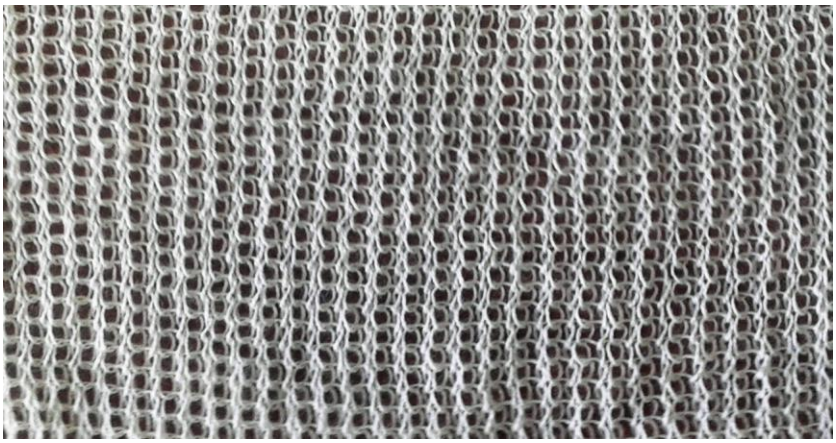

Figure 4.10: Image of fabric 3 knitted from yarn sample 3

Sample 4:

Figure 4.11 shows image of fabric knitted from yarn sample 4. From the image, it is clear that the fabric is regular and show good appearance.

Figure 4.11: Image of fabric 4 knitted from yarn sample 4

Sample 5:

Figure 4.12 shows image of fabric knitted from yarn sample 5. From the image, it is clear that the fabric show some cloud area and it is accepted.

Figure 4.12: Image for fabric 5 knitted from yarn sample 5

Sample 6:

Figure 4.20 shows image of fabric knitted from yarn sample 6. From the image, it is clear that the fabric is regular and shows good appearance.

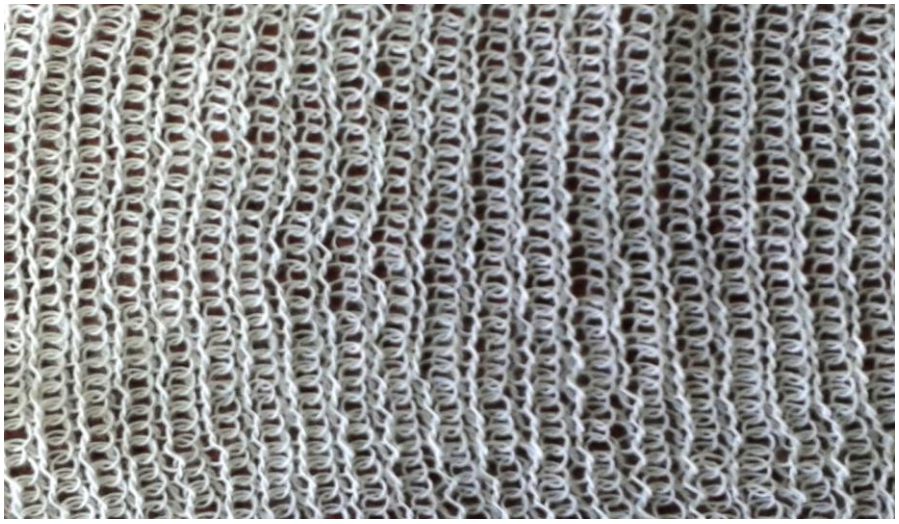

Figure 4.13: Image for fabric 6 knitted from yarn sample 6

Sample 7:

Figure 4.14 shows image of fabric knitted from yarn sample 7. From the image, it is clear that the fabric is regular and shows good appearance.

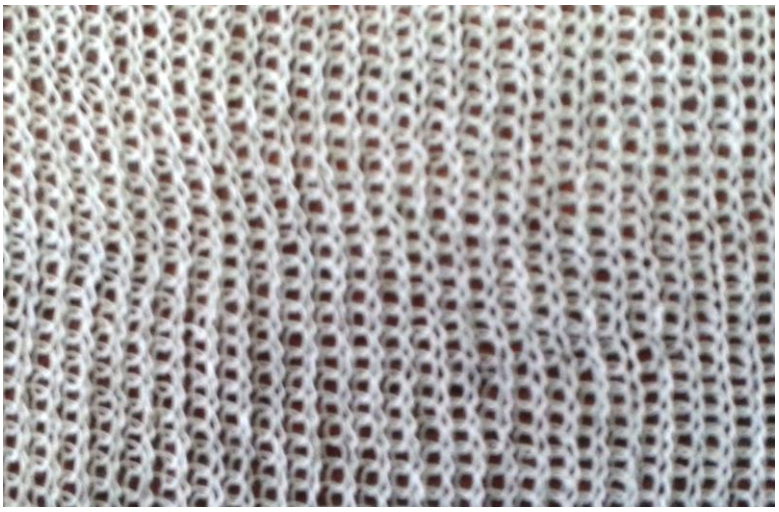

Figure 4.14: Image for fabric 7 knitted from yarn sample 7

4.2.2 Fabric weight:

The weight in grams was determined for each fabric sample. Although different yarns having different counts were used, the number of courses in each knitted fabric sample was nearly the same and the average was taken as 18 courses. The length used to knit 18 courses is equivalent to 20 meters. The results obtained are given in appendix I.

4.2.3 Fabric weight spectrograms:

The spectrograms for each fabric sample are plotted. The x-axis presents the weight in grams and the y-axis presents the length of the yarn consuming in meter which is equivalent for the length used in the yarn samples. Figures 4.15, 4.16, 4.17, 4.18, 4.19, 4.20 and 4.21 show the spectrograms of variations in fabric weight for sample 1, 2, 3, 4, 5, 6 and 7 respectively. As can be seen in figures the curves behavior is nearly the yarn diameter variation curves. See Appendexs A to G.

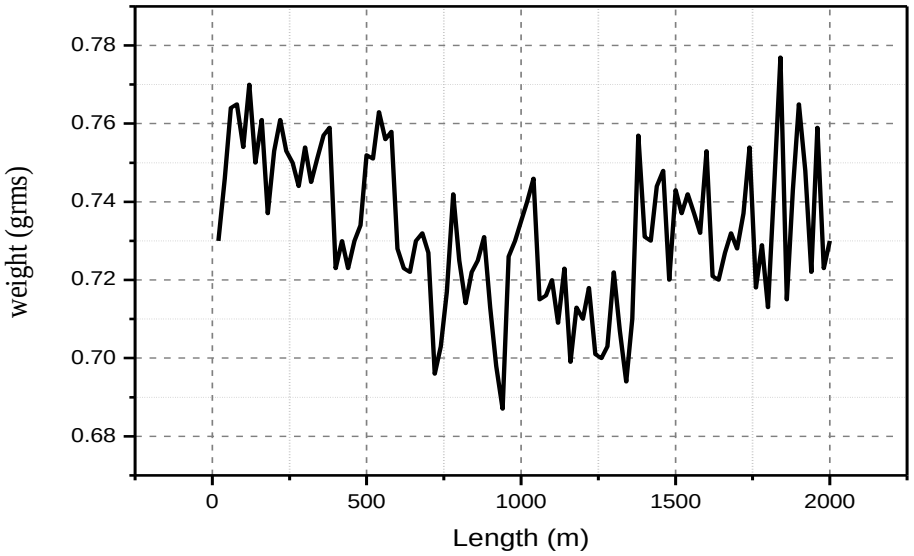

Figure 4.15: The variations in the fabric weight for fabric sample 1.

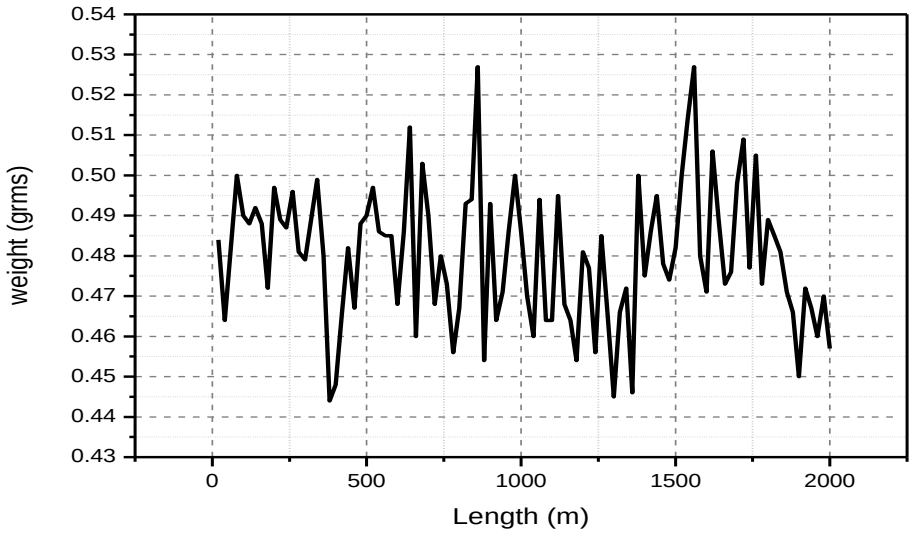

Figure 4.16: The variations in the fabric weight for fabric sample 2.

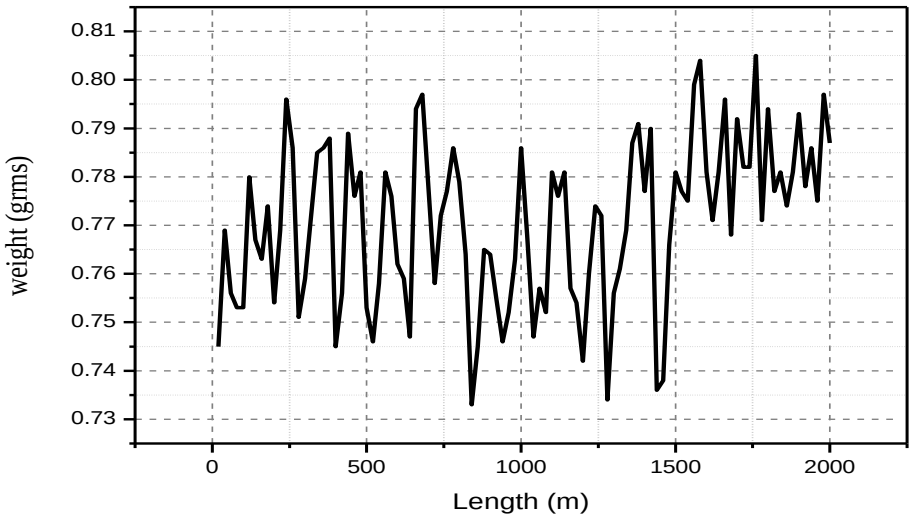

Figure 4.17: The variations in the fabric weight for fabric sample 3.

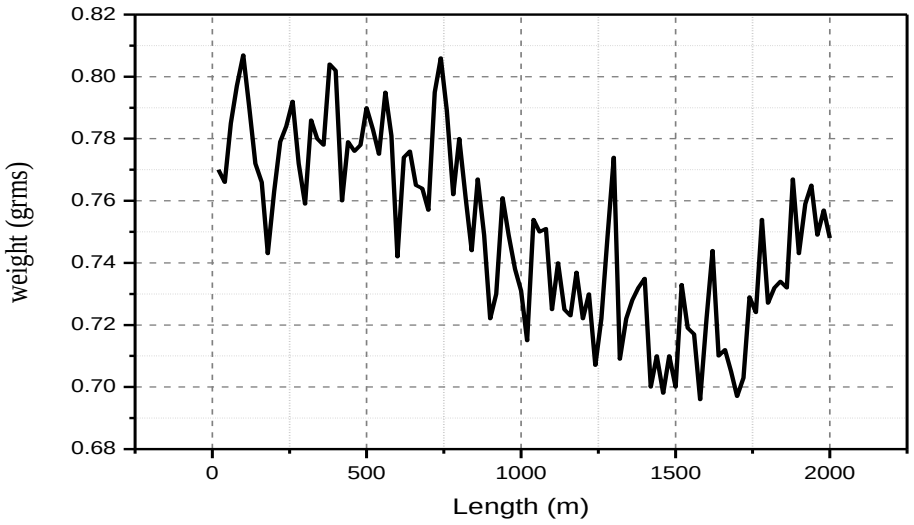

Figure 4.18: The variations in the fabric weight for fabric sample 4.

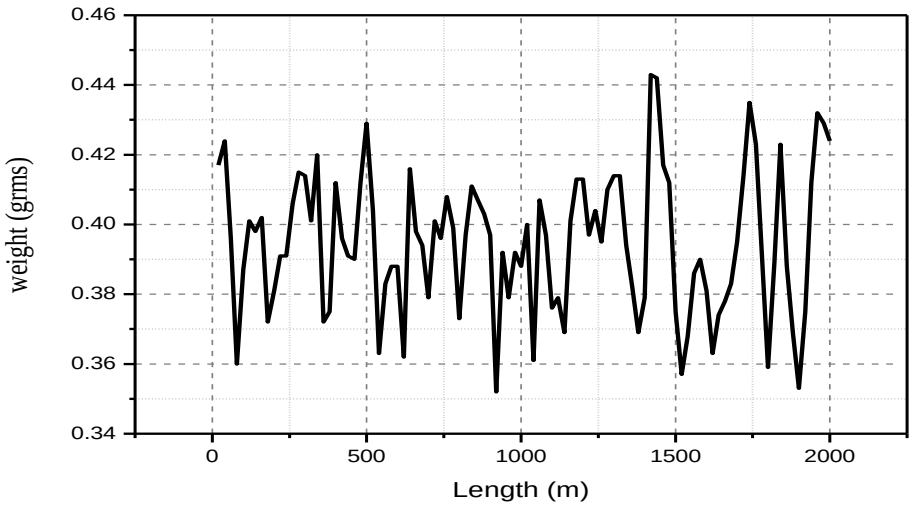

Figure 4.19: The variations in the fabric weight for fabric sample 5.

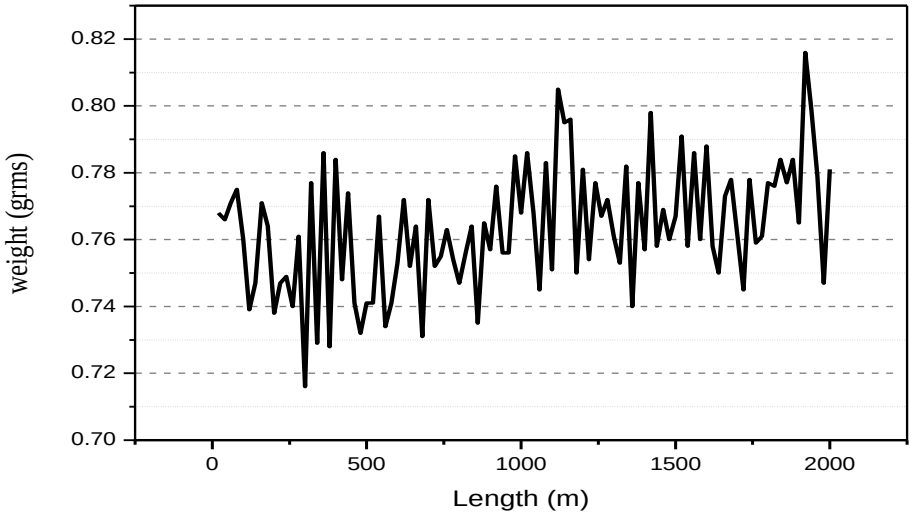

Figure 4.20: The variations in the fabric weight for fabric sample 6.

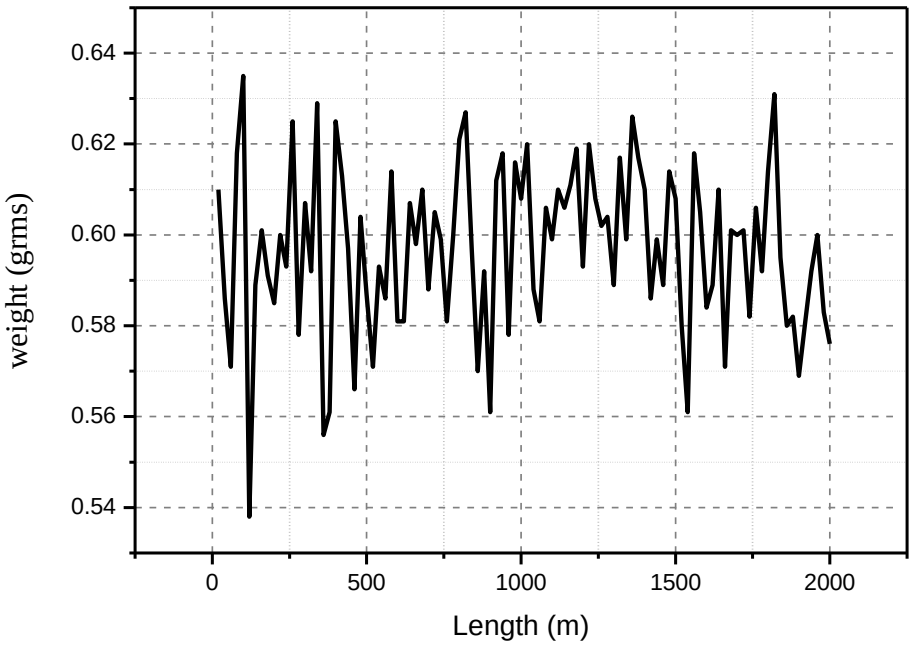

Figure 4.21: The variations in the fabric weight for fabric sample 7.

4.3 Models:

From the data given in table 4.8 and 4.9, the final CVs for yarn and fabric are calculated. The Origin 8.5 program is used to establish an equation (model) that could better correlate the data obtained from the yarn and fabric for each sample. Nonlinear regression analysis curve fit is used to choose the best model.

4.3.1 Origin 8.5 **program:**

Origin 8.5 is a proprietary computer program for interactive scientific graphing and data analysis. It is produced by OriginLab Corporation, and runs on Microsoft Windows. It has inspired several platform-independent open-source clones like QtiPlot or SciDAVis. Graphing support in Origin 8.5 includes various 2D/3D plot types. Data analyses in Origin 8.5 include statistics, signal processing, curve fitting and peak analysis. Origin's curve fitting is performed by the nonlinear least squares fitter which is based on the Levenberg–Marquardt algorithm. Origin 8.5 imports data files in various formats such as ASCII text, Excel, NI TDM, DIADem, NetCDF, SPC, etc. It also exports the graph to various image file formats such as JPEG, GIF, EPS, TIFF, etc. There is also a built-in query tool for accessing database data via ADO.

4.3.2 Sine function:

A periodic function occurs when a specific horizontal shift, *P*, results in the original function; where $f(x + P) = f(x)$ for all values of x. When this occurs the horizontal shift is termed the period of the function. The sine is a periodic and it takes the formula:

$$f(x) = A\sin(Bt) + k \qquad (4.1)$$

Where;

$A \equiv$ the vertical stretch and it is the amplitude of the function.

$K \equiv$ the vertical shift and it determines the midline of the function.

$B \equiv$ the horizontal stretch/compression, and is related to the period, P, by the following equation;

$$P = \frac{2\pi}{B} \qquad (4.2)$$

And figure 4.29 shows the function curve.

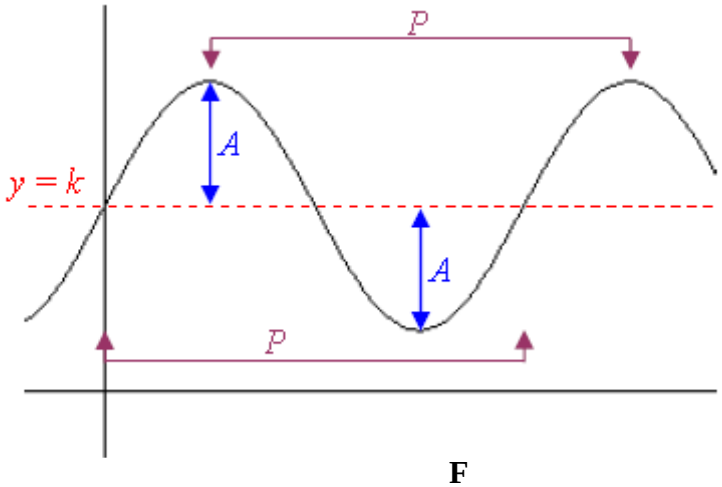

F

Figure 4.22: the sine function curve

Recalling that when the inside of the function is factored, it reveals the horizontal shift and given is by the following equation;

$$f(x) = A\sin[B(x - h)] + k \qquad (4.3)$$

where;

$h \equiv$ the horizontal shift of the function.

Steps to build the model:

Many steps are followed to build the models using Origin program. These steps are as follow:

First step:

Open program from start menu.

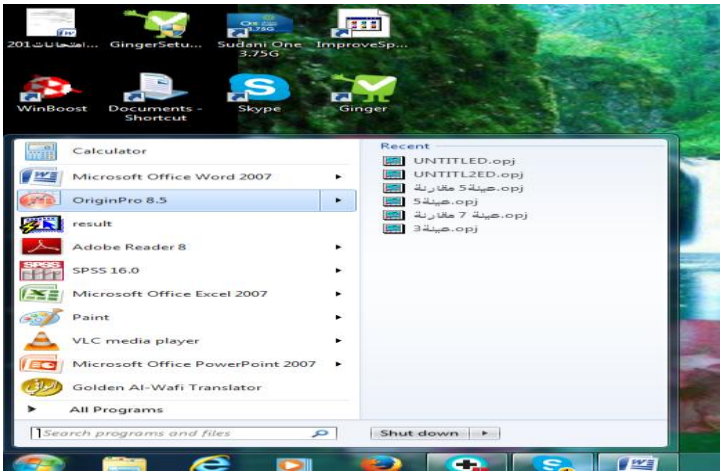

Second step:

The data is inserted on the data sheet (which is open automatically on the window).

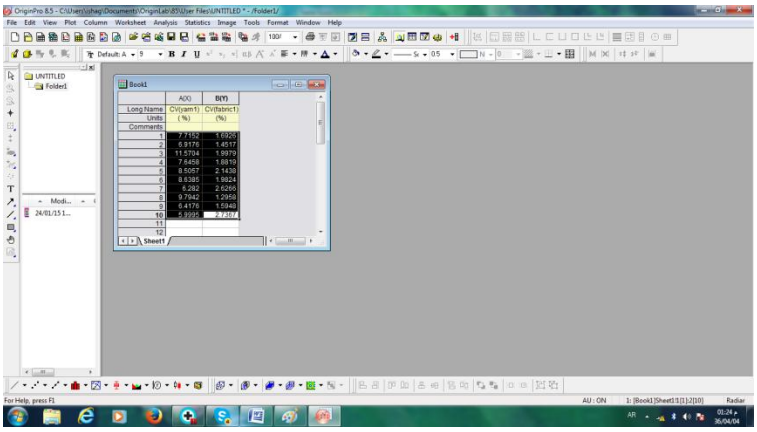

Third step:

Select Non-linear curve fit selected from analysis fitting menu.

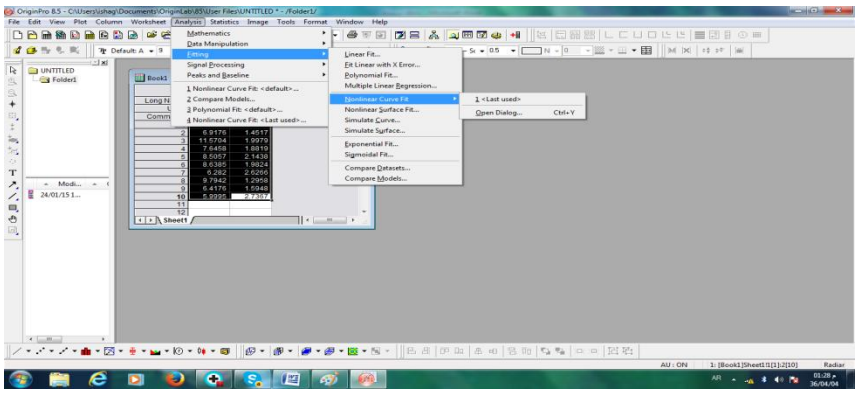

Fourth step:

On the non-linear fitting box all necessary setting (data selection, function selection and all parameters need to display) are done.

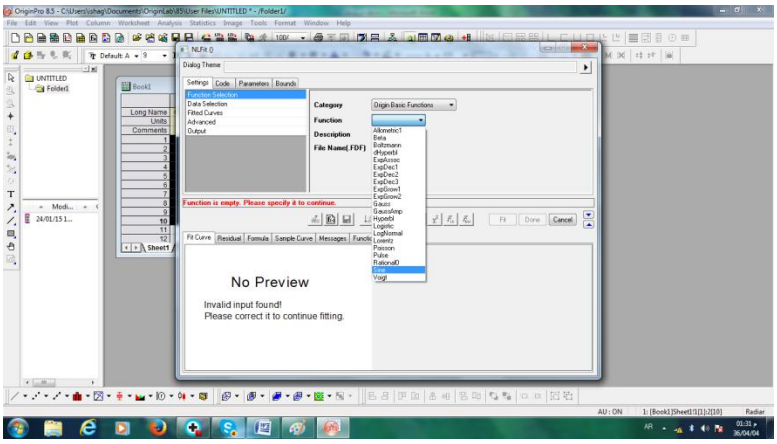

Finally: Pressing the fitting button will display the results. Many functions tested to obtain the mathematical model.

4.3.3 Establishment of the proposed models:

The mean CV% for each yarn and fabric sample is calculated from the tables given in Appendix H and I respectively in order to establish the proposed models. The *Non-linear fit* functions are tested in order to select best model for each sample. For all samples the correlation coefficient R, mean square error MSE and the significant value (Prop>F) are used to choose the best model.

4.3.3.1 Proposed model for sample 1 (Ne 14 polyester/viscose (65/35) yarn):

The calculated CV% for yarn and fabric for samle1 are shown in table 4.10.

Table 4.10: The calculated yarn and fabric CV's for sample1

CV (yarn) (%)	CV (fabric) (%)
7.7152	1.6926
6.9176	1.4517
11.5704	1.9979
7.6458	1.8819
8.5057	2.1438
8.6385	1.9824
6.2820	2.6266
9.7942	1.2958
6.4176	1.5948
5.9995	2.7367

The values obtained from origin 8.5 program for sample 1 are given in table 4.11.

Table 4.11: The results obtained for sample 1

Errors / Model	R	MSE	Prob>F
Sine**	79	0.35	0.00003**
Polynomial	91	0.33	0.24
Exponential	70	0.37	0.00001

From table 4.11 it can be seen that the Polynomial model is not suitable because, it is insignificant (Prob>F = 0.24). On the other hand, for the Exponential the correlation coefficient R is less than sine model and mean squared error MSE values are more than the Sine. Therefore the

model chosen is the Sine model. The best curve that fits for sample1is illustrated in figure 4.23.

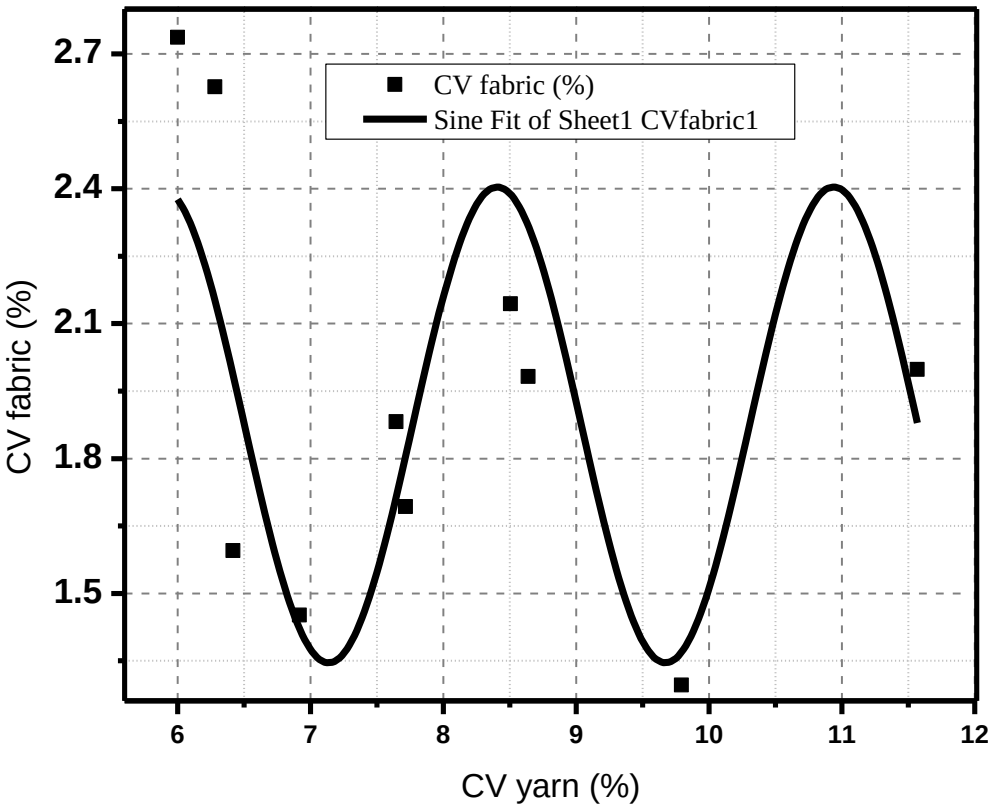

Figure4.23: Best curve that fit for sample 1

The mathematical model for sample1 is as follows:

$$Y_1 = 1.87 + 0.53\sin(2.49X_1 - 6.69) \qquad (4.4)$$

Where Y_1 is the CV (%) for fabric sample 1

X_1 is the CV (%) for yarn sample 1

Comparing model with the data:

Predicted value is calculated from equation (4.4) and compared with the actual data. The result is shown in table 4.12.

Table 4.12: Calculated & predicted fabric CV for sample 1

CV (fabric) (%)	CV (predicted) (%)
1.6926	1.42144
1.4517	1.87929
1.9979	1.71383
1.8819	2.38764
2.1438	2.31761
1.9824	2.15014
2.6266	1.36941
1.2958	1.98563
1.5948	2.37672
2.7367	1.42144

The CV curve for the calculated and predicted values for sample 1 are plotted in figure 4.24 which represents the relation between actual value and predicted value calculated using equation (4.4). Figure 4.24 shows the relation between the measured values and those calculated using equation (4.4). As can be seen from the figure 4.24, the trends are nearly the same. The correlation is 79%.

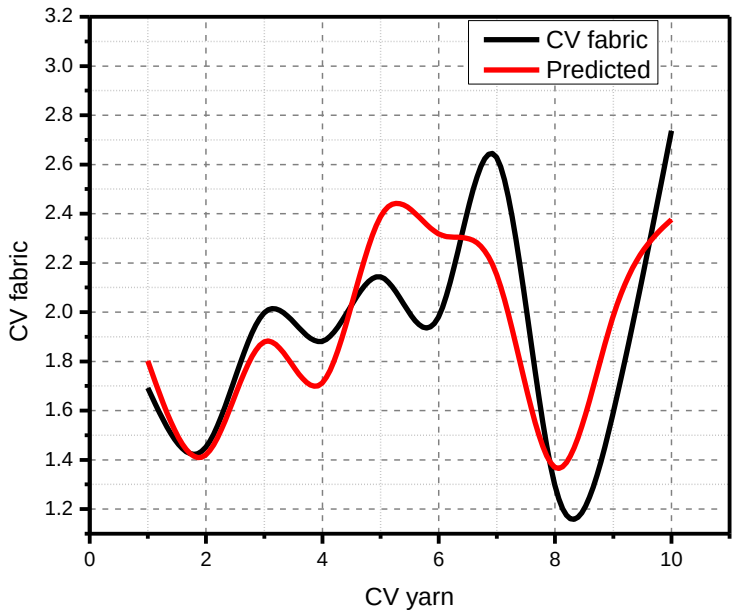

Figure 4.24: CV curve for the actual and predicted values for sample

4.3.3.2 Proposed model for sample 2 (Ne 24 cotton yarn):

The calculated CV% for yarn and fabric for sample 2 are shown in table 4.13.

Table 4.13: The calculated yarn and fabric CV's for sample 2

CV (yarn) (%)	CV (fabric) (%)
13.3065	3.09853
11.6431	3.9001
13.3533	2.2248
16.9288	3.8231
16.2588	3.2668
10.8987	2.9753
12.1718	3.6378
9.0008	3.7245
14.2775	2.9278
11.8850	2.2538

The results obtained from Origin 8.5 program for sample 2 are given in table 4.14.

Table 4.14: The results obtained for sample 2

Errors / Model	R	MSE	Prob>F
Sine**	86**	0.37**	0.000003**
Polynomial	54	0.58	0.31
Exponential	31	0.65	0.00002

From table 4.14, the Polynomial model is insignificant. Therefore it is discarding. For exponential the correlation coefficient R value less and the mean squared error MSE value is more than the Sine model. Therefore the Sine model is chosen because it best fits the data. The best curve that fits for sample 2 is illustrated in figure 4.25.

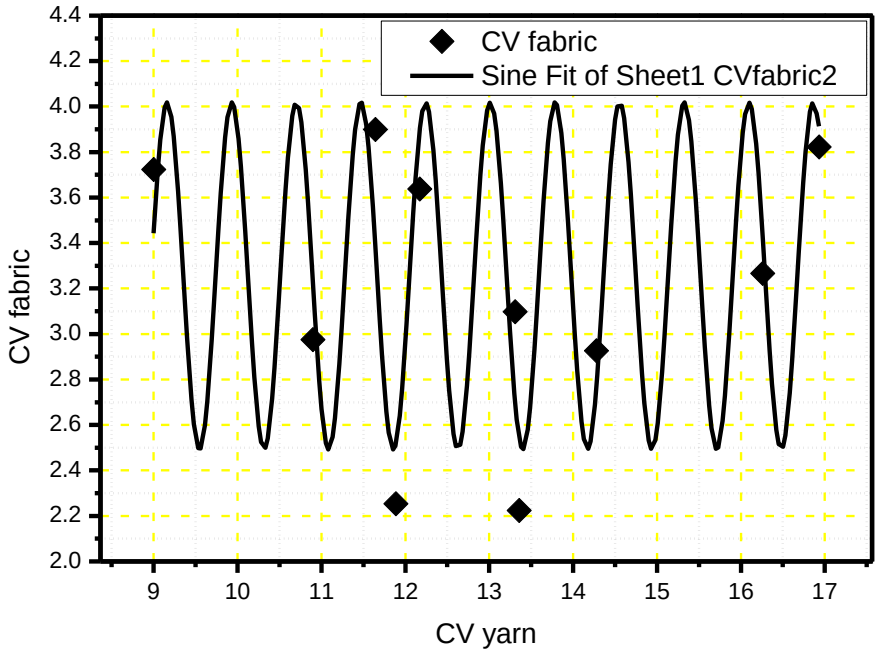

Figure 4.25: Best curve that fit for sample 2

The mathematical model for sample 2 is given by;

$$Y_2 = 3.26 + 0.76\sin(8.16X_2 - 60.63) \qquad (4.5)$$

Where Y_2 is the CV (%) for fabric sample 2

X_2 is the CV (%) for yarn sample 2

Comparing model with the data:

The predicted values calculated from equation two is compared with the actual data obtained from experimental data and the results are shown in table 4.15.

Table 4.15: Calculated & predicted fabric CV for sample 2

CV (fabric) (%)	CV (predicted) (%)
3.09853	2.69675
3.9001	3.39544
2.2248	2.54323
3.8231	3.91358
3.2668	3.42388
2.9753	3.2364
3.6378	3.89338
3.7245	3.44308
2.9278	2.77574
2.2538	2.51064

The CV curve for the calculated and predicted values for sample 2 are plotted in figure 4.26 which represents the relation between actual and predicted values calculated using equation (4.5). The figure shows the relation between the measured values and those calculated using equation (4.5). As can be seen from the figure, the trends are nearly the same with correlation of 86%.

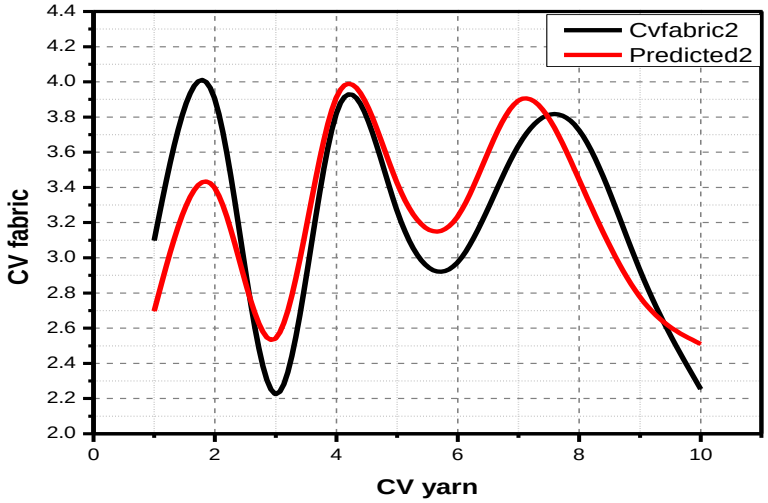

Figure 4.26: CV curve for the calculated and predicted values for sample 2

4.3.3.3 Proposed model for sample 3 (Ne 15 polyester/cotton (50/50) yarn):

The calculated CV% for yarn and fabric for sample 2 are shown in table 4.16.

Table 4.16: Yarn and fabric calculated CV's for sample 3

CV (yarn) (%)	CV (fabric) (%)
6.1491	1.4456
4.0678	2.2437
6.1414	1.8902
4.0581	2.0779
5.1285	1.9227
5.7735	1.8522
3.4967	2.1423
5.7287	2.9461
4.3280	1.5673
5.3165	0.9847

The model values obtained from Origin 8.5 program for sample 3 are given in table 4.17.

Table 4.17: The results obtained for sample 3

Errors / Model	R	MSE	Prob>F
Sine**	73**	0.4**	0.0001**
Polynomial	62	0.6	0.8
Exponential	27	0.6	0.0002

As can be seen from table 4.17, the Polynomial model is not suitable because, it is insignificant. On the other hand the Exponential is not suitable because the correlation coefficient R is less and mean squared error MSE is more than the Sine. Therefore the Sine model is chosen because it best fits with the data. The best curve that fits for sample 3 is illustrated in figure 4.27.

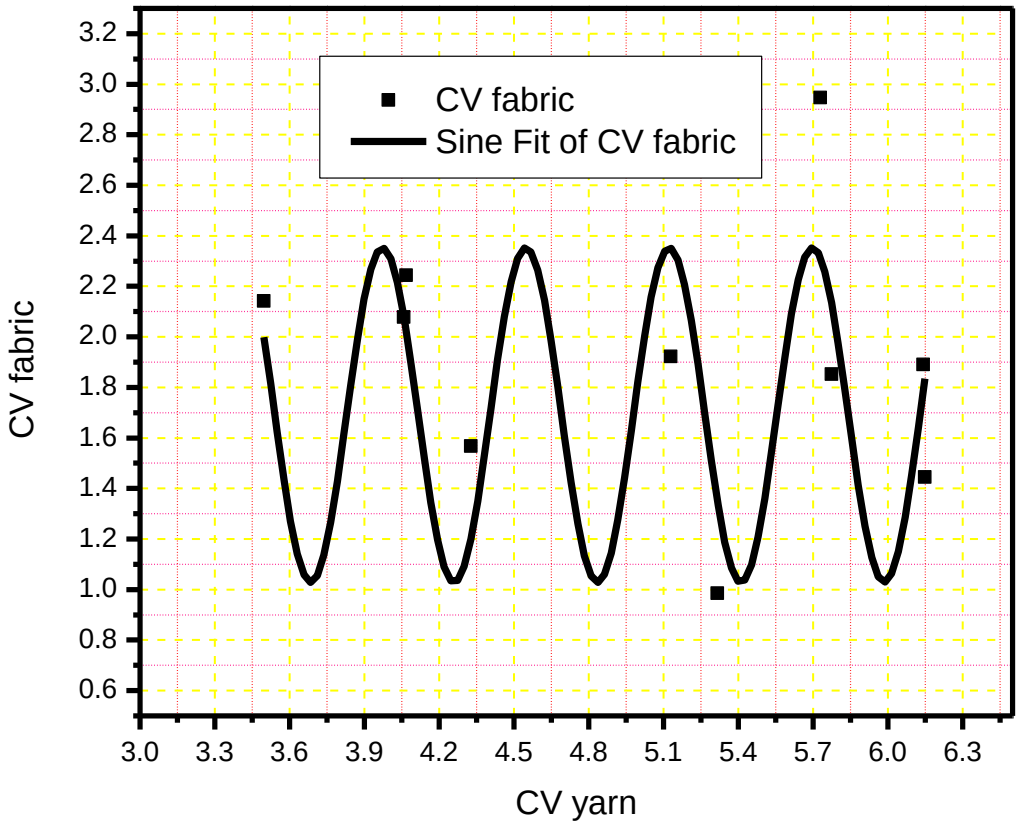

Figure4.27: best curve that fit for sample 3

The model for sample 3 is:

$$Y_3 = 1.69 + 0.66\sin(10.92X_3 - 4.13) \qquad (4.6)$$

Where Y_3 is the CV (%) for fabric sample 3

X_3 is the CV (%) for yarn sample 3

Comparing model with the data:

Predicted value, calculated from equation (4.6) compared with the actual data is show in table 4.18.

Table 4.18: Actual & predicted fabric CV for sample 3

CV (fabric) (%)	CV (predicted) (%)
2.2437	2.02422
1.8902	1.77899
2.0779	2.08282
1.9227	2.35122
1.8522	2.13873
2.1423	1.99867
2.9461	2.31517
1.5673	1.20334
0.9847	1.34628
2.2437	2.02422

The CV curve for the calculated and predicted values for sample 3 are plotted in figure 4.28 which represents the relation between actual and predicted values calculated using equation (4.6). The figure shows the relation between the measured values and those calculated using equation 3. As can be seen from the figure, the trends are nearly the same. The correlation is 73%.

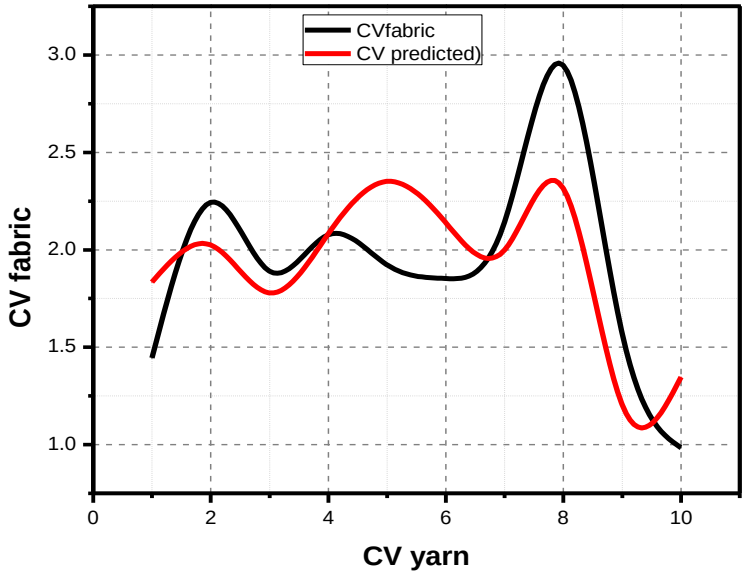

Figure 4.28: CV curve for the calculated and predicted values for sample 3

4.3.3.4 Proposed model for sample 4 (Ne 15 polyester/viscose (65/35) bended yarn):

The calculated CV% for yarn and fabric for sample 4 are given in table 4.19.

Table 4.19: Yarn and fabric calculated CV's for sample 4

CV (yarn) (%)	CV (fabric) (%)
4.0303	2.4260
10.5781	1.7208
7.8331	1.9484
7.0244	2.0425
5.7998	2.0142
5.7531	1.9142
8.0407	2.6545
8.6047	1.7177
7.5300	2.0200
10.1374	1.7713

The values obtained from Origin 8.5 program for sample 4 are given in table 4.20.

Table 4.20: The results obtained for sample 4

Errors / Model	R	MSE	Prob>F
Sine**	78**	0.2**	0.000002
Polynomial	68	0.3	0.7
Exponential	47	0.3	0.000002

From the values obtained in table 4.20 the sine model is chosen because the result obtained from the polynomial is not significant. In the case of the exponential, the value of R is less and that for the MSE is larger than the Sine. The best curve fits for sample 4 is shown in figure 4.29.

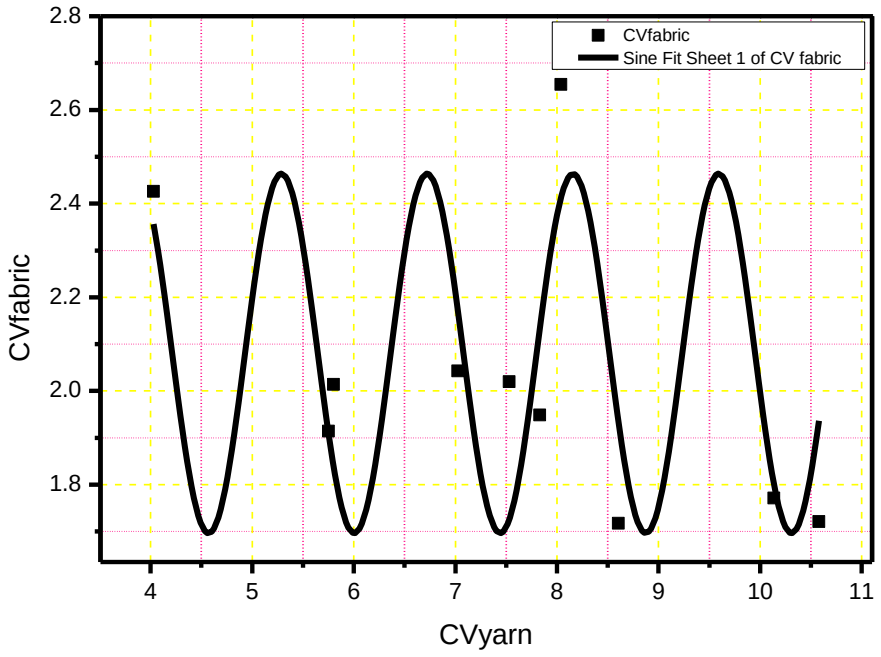

Figure 4.29: Best curve that fit for sample 4

The mathematical model for sample 4 is as follows:

$$Y_4 = 2.08 + 0.38\sin(4.38X_4 - 2.76) \qquad (4.7)$$

Where Y_4 is the CV (%) for fabric sample 4

X_4 is the CV (%) for yarn sample 4

Comparing model with the data:

Predicted value calculated from equation (4.7) compared with the actual data is show in table 4.21.

Table 4.21: Calculated & predicted CV fabric for sample 4

CV (fabric) (%)	CV (predicted) (%)
2.4260	2.3566
1.7208	1.9362
1.9484	2.1384
2.0425	2.1749
2.0142	1.8426
1.9142	1.9089
2.6545	2.4153
1.7177	1.9332
2.0200	1.7258
1.7713	1.7978

The CV curve for the calculated and predicted values for sample 4 are plotted in figure 4.30 which represents the relation between calculated value and predicted value calculate using the equation (4.7). The figure shows the relation the measured values and those calculated using equation (4.7). As can be seen from the figure, the trends are nearly the same. The correlation coefficient is 78%.

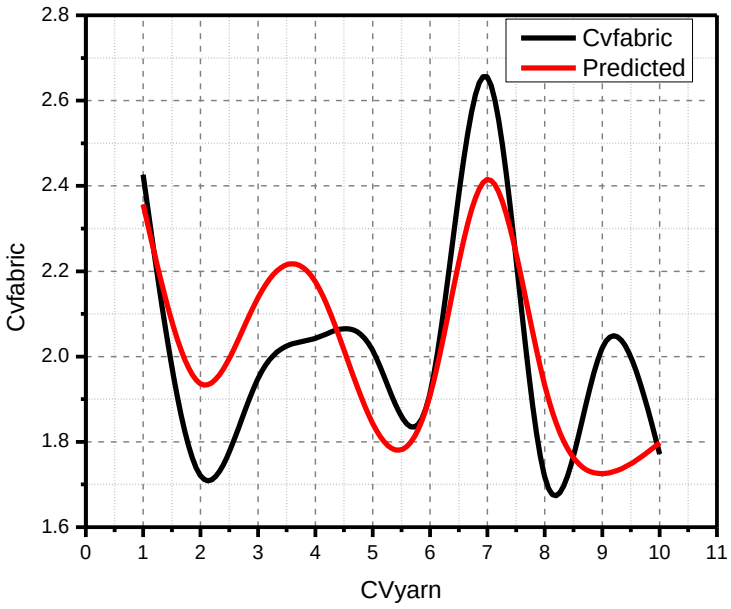

Figure 4.30: CV curve for the calculated and predicted values for sample 4

4.3.3.5 Proposed model for sample 5 (Ne 30 polyester yarn):

The calculated CV% for yarn and fabric for sample 5 are given in table 4.22.

Table 4.22: The calculated yarn and fabric CV's for sample 5

CV (yarn) (%)	CV (fabric) (%)
6.9502	4.9361
14.3057	4.2295
11.5332	4.4964
9.0346	4.1977
10.4044	4.2891
12.8304	4.8079
11.2259	3.8846
6.4581	4.7789
14.3497	4.1990
14.3459	4.5227

The model values obtained from origin 8.5 program for sample 4 are given in table 4.23.

Table 4.23: The model values obtained for sample 5

Errors / Model	R	MSE	Prob>F
Sine**	81**	0.2**	2.888E-8
Polynomial	73	0.3	0.2
Exponential	60	0.3	7.64593E-9

As can be seen from table 4.23, the Polynomial model is not suitable because, it insignificant (Prob>F=0.2). On the other hand for the Exponential, the correlation coefficient R is less and mean squared error MSE is large than the Sine. Therefore the Sine Model chosen because it best fits the data. The best curve that fits for sample 5 is in figure 4.31.

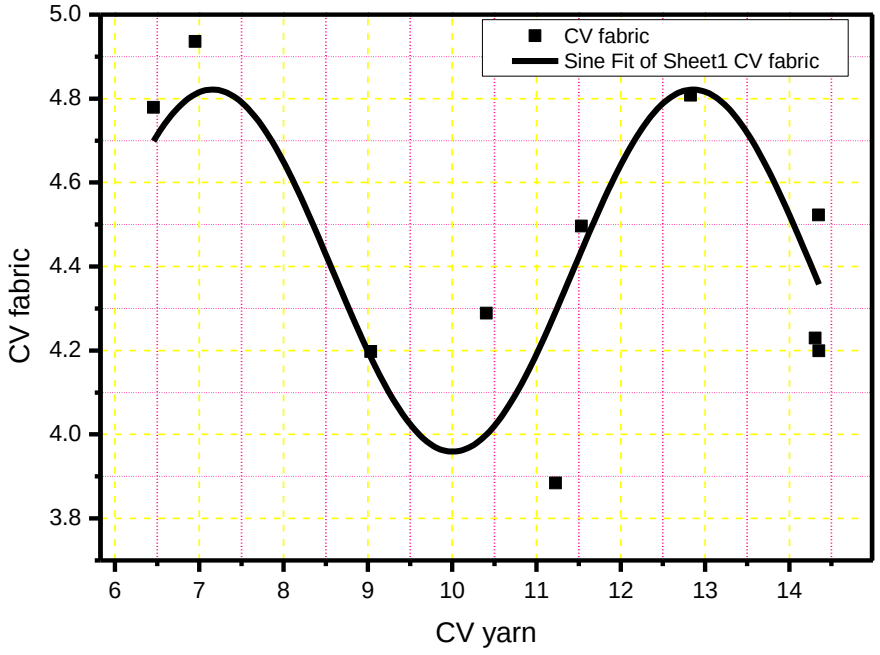

Figure 4.31: Best curve that fit for sample 5

The mathematical model for sample 5 is as follows:

$$Y_5 = 4.39 + 0.43\sin(1.10X_5 - 12.61) \qquad (4.8)$$

Where Y_5 is the CV (%) for fabric sample 5

X_5 is the CV (%) for yarn sample 5

Comparing model with the data:

Predicted value calculated from equation (4.8) and compared with the measure data the result show in table 4.24.

Table 4.24: Calculated & predicted CV fabric for sample 5

CV (fabric) (%)	CV (predicted) (%)
4.9361	4.5931
4.2295	4.0701
4.4964	4.5143
4.1977	3.9782
4.2891	4.6070
4.8079	4.7991
3.8846	4.3576
4.7789	4.8152
4.1990	4.2402
4.5227	4.2235

The CV curve for the calculated and predicted values for sample 5 are plotted in figure 4.32 which represents the relation between actual value and predicted value calculate using the equation (4.8). The figure shows the relation between the measured values and those calculated using equation (4.8). As can be seen from the figure, the trends are nearly the same. The correlation is 81%.

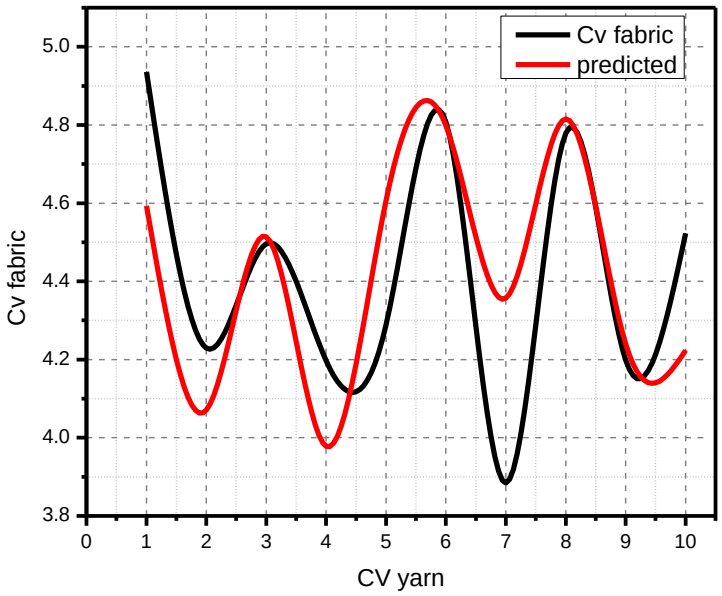

Figure 4.32: CV curve for the calculated and predicted values for sample 5

4.3.3.6 Proposed model for sample 6 (Ne 16 cotton yarn):

The calculated CV% for yarn and fabric for sample 6 are given in table 4.25.

Table 4.25: The calculated yarn and fabric CV's for sample 6

CV (yarn) (%)	CV (fabric) (%)
13.6712	1.7963
12.5010	3.2779
11.9595	1.8413
12.8946	1.6301
13.3331	1.7696
12.1710	2.7512
11.7261	1.7397
14.8898	2.0123
15.4105	1.5564
16.2147	2.3475

The model values obtained from origin 8.5 program for sample 4 are given in table 4.26.

Table 4.26: The model values obtained for sample 6

Errors / Model	R	MSE	Prob>F
Sine**	82	0.4	0.00004
Polynomial	77	0.5	0.5
Exponential	0	0.7	0.0004

From table 4.26, the Polynomial model was not chosen because, it is insignificant. The exponential was not chosen because the correlation coefficient R was zero. Therefore the Sine model was chosen because it best fits the data. The best curve that fits for sample 6 is illustrated in figure 4.33.

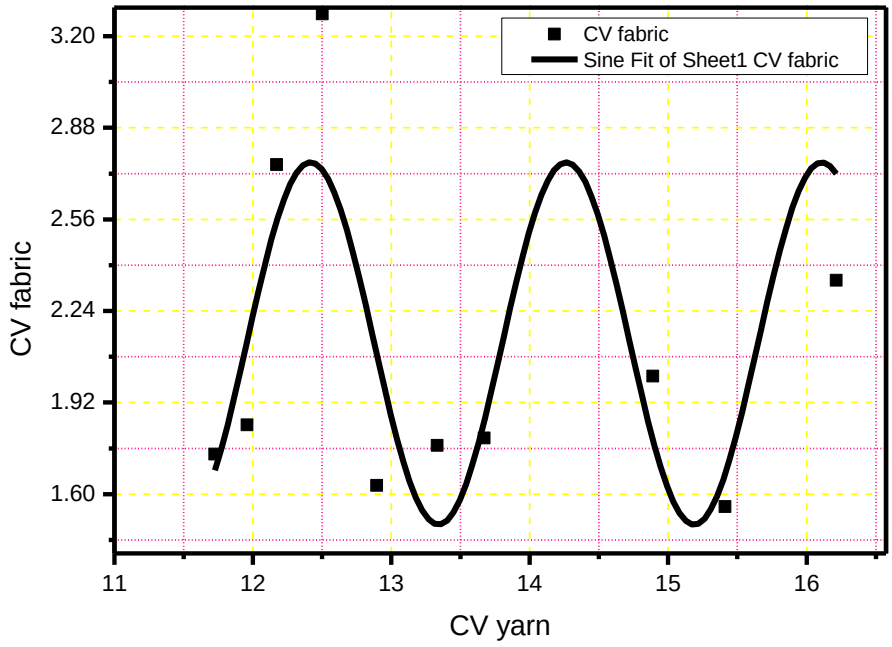

Figure 4.33: Best curve that fit for sample 6

The mathematical model for sample 6 is as follows:

$$Y_6 = 2.13 + 0.63\sin(3.4X_6 - 3.32) \qquad (4.9)$$

Where Y_6 is the CV (%) for fabric sample 6

X_6 is the CV (%) for yarn sample 6

Comparing model with the data:

Predicted value calculated from equation (4.9) and compared with the measured data the result shown in table 4.27.

Table 4.27: Calculated & predicted CV% fabric for sample 6

CV (fabric) (%)	CV (predicted) (%)
1.7963	1.6762
3.2779	2.7583
1.8413	1.9208
1.6301	2.3083
1.7696	1.5363
2.7512	2.3663
1.7397	1.5553
2.0123	1.9927
1.5564	1.5467
2.3475	2.7594

The CV curve for the calculated and predicted values for sample 6 are plotted in figure 4.34 which represents the relation between measured value and predicted value calculated using the equation (4.9). The figure shows the relation the measured values and those calculated using equation (4.9). As can be seen from the figure, the trends are nearly the same. The correlation was 82%.

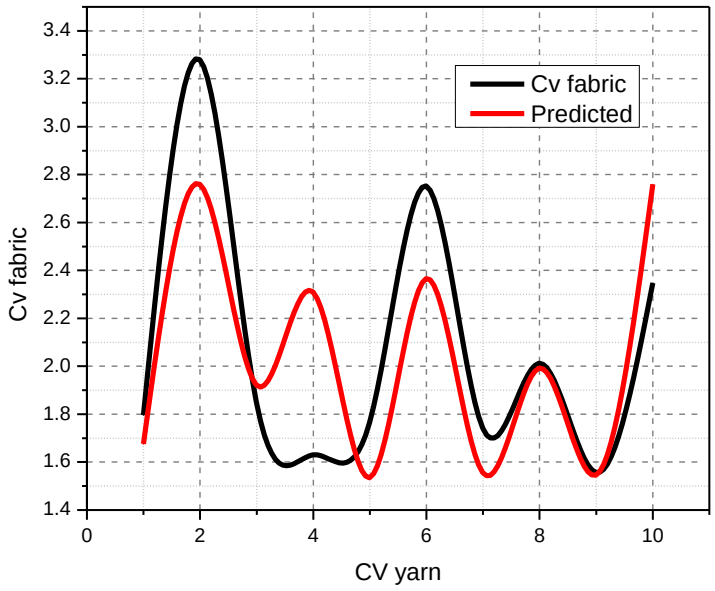

Figure 4.34: CV curve for the calculated and predicted for sample 6

4.3.3.7 Proposed model for sample 7 (Ne 20 cotton yarn):

The calculated CV% for yarn and fabric for sample 7 are given in table 4.28.

Table 4.28: Yarn and fabric CV's for sample 7

CV (yarn) (%)	CV (fabric) (%)
4.3539	4.4946
14.1311	4.356
8.8286	2.755
10.6681	2.1379
12.9351	3.7194
6.6398	2.14
14.827	1.8259
16.2207	2.9623
11.1281	2.2127
10.8708	2.9569

The model values obtained from origin 8.5 program for sample 7 are given in table 4.29.

Table 4.29: The model values obtained for sample 7

Errors / Model	R	MSE	Prob>F
Sine**	73**	0.8**	0.0003
Polynomial	68	1.04	0.7
Exponential	57	0.9	0.0002

From the values obtained in table 4.29 the sine model was chosen because the result obtained from the polynomial was not significant. In the case of the exponential, the value of R was less and that for the MSE was large than the sine. The best curve fit for sample 7 is shown in figure 4.35.

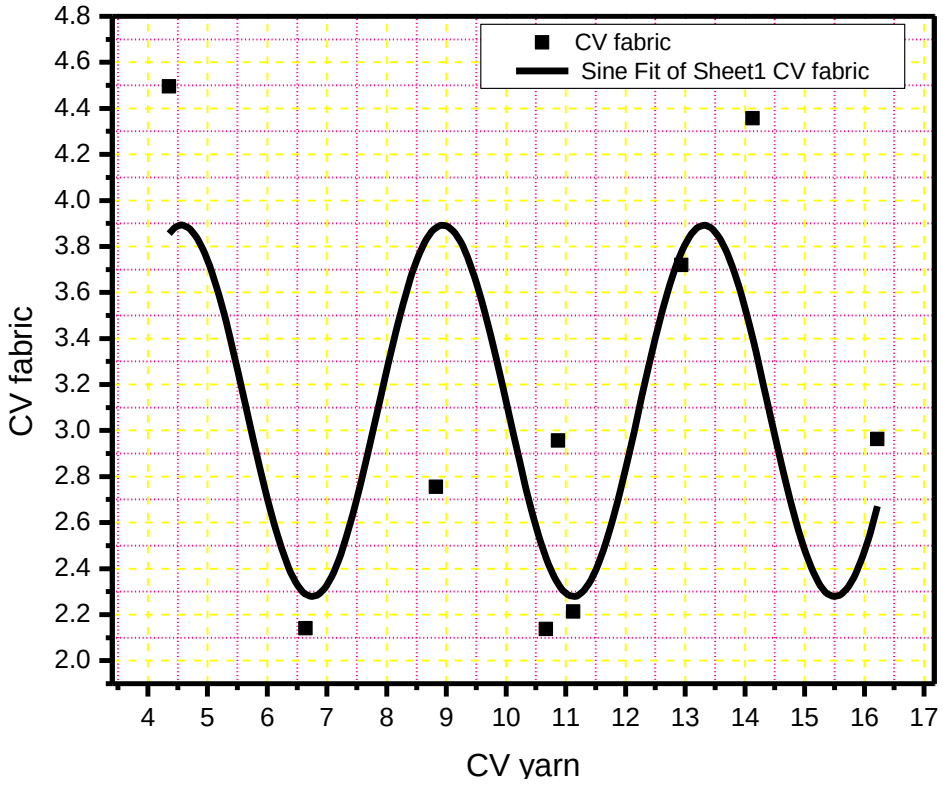

Figure 4.35: Best curve that fit for sample 7

The mathematical model for sample 7 is as follows:

$$Y_7 = 3.09 + 0.81\sin(1.44X_7 - 4.99) \qquad (4.10)$$

Where Y_7 is the CV (%) for fabric sample 7

X_7 is the CV (%) for yarn sample 7

Comparing model with the data:

Predicted values calculated from equation (4.10) and compared with the measured data the result shown in table 4.30.

Table 4.30: Calculated & predicted fabric CV for sample 7

CV (fabric) (%)	CV (predicted) (%)
4.4946	2.5616
4.3560	3.3984
2.7550	3.8824
2.1379	2.4476
3.7194	3.7758
2.1400	2.2890
1.8259	2.6289
2.9623	2.6717
2.2127	2.2785
2.9569	2.3326

The CV curve for the calculated and predicted values for sample 7 are plotted in figure 4.36 which represents the relation between measured value and predicted value calculated using equation (4.10). The figure shows the relation between the measured values and those calculated using equation (4.10). As can be seen from the figure, the trends are nearly the same. The correlation was 73 %.

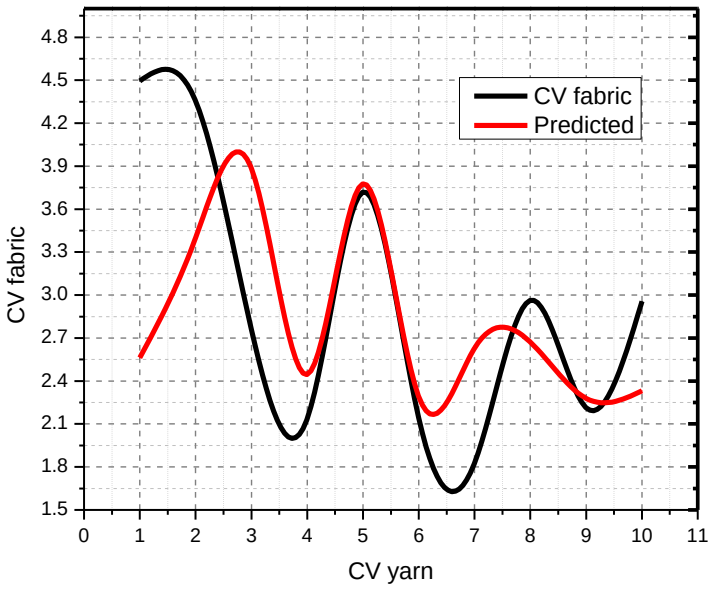

Figure 4.36: CV curve for the calculated and predicted values for sample 7

4.4 Proposed specifications for knitted fabrics:

Grading specification system for knitted fabrics CV% proposed is based on CV% of the yarn used. The Uster statistic for knitted fabric appearance is used. The range of the yarn CV given in Uster statistic guide is substituted in the proposed model equations to give the predicted specifications of a fabric knitted with a specific yarn. The obtained results are given in table 4.31

Table 4.31: Proposed specifications for knitted fabric

Material (yarn)	Fabric CV (%)	specification
Polyester/viscose	2.02	v. good
(65/35)%	2.04	good
Ne 14	2.07	Acceptable
	Above 2.07	fail
100% cotton	3.78	excellent
Ne 24	3.85	v. good
	3.91	good
	3.96	Acceptable
	4.00	fail
Polyester/cotton	2.02	v.good
(50/50)%	2.19	good
Ne 15	2.29	Acceptable
	Above 2.02	fail
Polyester/Viscose	2.31	v.good
(65/35)%	2.34	good
Ne 15	2.36	Acceptable
	Above 2.36	fail
100% Polyester	4.39	excellent
Ne 30	4.40	v. good
	4.41	good
	4.42	Acceptable
	4.43	fail
100% Cotton	2.51	excellent
Ne 16	2.54	v. good
	2.56	good
	2.59	Acceptable
	2.62	fail
100% Cotton	3.27	excellent
Ne 20	3.29	v. good
	3.31	good
	3.33	Acceptable
	3.35	fail

CHAPTER FIVE

Conclusions and Future work

5.1 Conclusions

- The knitting fabric process adds positively to the yarn regularity.
- The knitted fabric mass irregularities show smaller values than the yarn mass irregularities.
- The polyester/ cotton yarns and polyester/ viscose blended yarns are more regular than pure polyester and pure cotton yarns.
- The yarn mass variation (CVym) and the knitted fabric mass variation (CVfm) curves follow a sinusoidal curve. Its behavior coincides with the sine function curve.
- The sine function is the best model to estimate the knitted fabric mass variations (CVfm) from the yarn mass variations (CVm). This fact emphasis by the high correlation coefficients obtained.
- Mass variation (CVfm) of the fabric knitted from blended polyester/viscous (65/35) yarn having Ne 14 can be predicted using equation (4.4).
- Equation (4.5) predicts the mass variation (CVfm) of the fabric knitted from carded cotton yarn having Ne 24.
- From equation (4.6) predict mass variation (CVfm) of the fabric knitted from blended polyester/cotton (50/50) yarn having Ne 15.
- Equation (4.7) can be used to predict mass variation (CVfm) of the fabric knitted from blended polyester/viscous (65/35) yarn having Ne 15.
- Equation (4.8) predicts mass variation (CVfm) of the fabric knitted from carded polyester yarn having Ne 30.

- From equation (4.9) mass variation (CVfm) of the fabric knitted from carded cotton yarn having Ne 16 can be predicted.
- Equation (4.10) predicts mass variation (CVfm) of the fabric knitted from carded yarn having Ne 20.
- The proposed mathematical equations (models) in this research are tested and proved a high degree of agreement with experimental data.
- The research concludes a prediction specification system for seven different knitted fabrics based on yarn specification.

5.1 Future work:

In this study the yarn CVm is used to predict the CVm of knitted fabrics. Future work is needed in woven fabrics, also other yarn properties such as hairiness; slubs… can have some effect on the fabric (knitted or woven) properties. These aspects need tackling by other researchers.

REFERENCES

1. Characterization and Quantification of Woven Fabric Irregularities using 2-D Anisotropy Measures. (Under the direction of Dr. Warren J. Jasper and Dr. Moon W. Suh.), North Carolina state university, july2005.
2. Alberto Barella. The inuence of twist on the regularity of the apparent diameter of worsted yarns. Journal of the Textile Institute, 43:P734{P741, 1952.
3. Physical testing of textile , B P Saville,Textile institute , Cambridge England , 2000.
4. J. W. S. Hearle, P. Grosberg, and S. Backer. Structural Mechanics of Fibers, Yarns, and Fabrics. Wiley-Interscience, New York, NY, 1969.
5. Uster Technologies AG, Switzerland. Uster Tester 4-SX, 2004.
6. T. Vijayakumar. Textile technology. http://www.geocities.com/vijayakumar777/, March 2003.
7. I. S. Tsai and W. C. Chu. The measurement of yarn diameter and the effect of shape error factor (sef) on the measurement of yarn evenness. Journal of the Textile Institute, 87(3):496{508, 1996.
8. Keissokki Kogo Co. Ltd., Japan. Keisokki Laserspot Hairiness Diameter Tester and KET-80 Evenness Tester, 2004.
9. You Huh and Moon W. Suh. Measuring thickness variations in fiber bundles with a ying laser spot scanning method. Textile Research Journal, 73:767{773, 2003.
10. Eric W. Weisstein. World of mathematics. http://mathworld.wolfram.com/, December 2004. From Math World {a Wolfram Web Resource.
11. Mario Bona. Textile Quality. Texilia, Torino, Italy, 2nd edition, 1994.
12. R. Further. Evenness testing in yarn production. part ii. The Textile Institute, 1982.
13. M. W. H. Townsend and D. R. Cox. The use of correlograms for measuring yarn irregularities. Journal of the Textile Institute, 42:P145{151, 1951.
14. J. L. Spencer-Smith and H. A. C. Todd. A time series met with in textile research. Supplement to the Journal of the Royal Statistical Society, 7(2):131{145, 1941.

15. H. Catling. Some effects of sinusoidal periodic yarn thickness variations on the appearance of woven cloth. Journal of Textile Institute, page T232, 1958.
16. R. Foster. Weaving investigations: Periodic patterning in fabrics. Journal of the Textile Institute, 43(9):P742, 1952.
17. W. Wegener. The irregularity of woven and knitted fabrics. Journal of the Textile Institute, 77(2):69{75, March-April 1986.
18. M. C. Moyer. Using Variance Length Curve Analysis to Determine the Impact of Medium Term Yarn Variations on Fabric Appearance. Institute of Textile Technology, 1992.
19. A. D. Sule and M. K. Bardhan. Objective evaluation of feel and handle appearance and tailorability of fabrics, Part-II The KES-FB System of Kawabata. Colourage, 46(12):P23, December 1999. 130
20. Brian T. Snyder. Development of a yarn quality rating system for visual fabric qualities. Master's thesis, NCSU, College of Textiles, Raleigh, 2000.
21. Zweigle. Zweigle: G 580-CYROS yarn quality control system. Textile World, 147(4):82, April 1997.
22. Avishai Nevel and Filiz Avsar. Measuring yarn appearance using the new EIB.Technical report, Lawson-Hemphill, 2001.
23. Moon W. Suh and et. al. 3-D Electronic imaging of fabric qualities by on-line yarn data. Technical report, National Textile Center, 2003.
24. J. G. Martindale. A new method of measuring the irregularity of yarns with some observations on the origin of irregularities in worsted slivers and yarns. Journal of the Textile Institute, 36:T35{47, March 1945.
25. P. Grosberg. Correlation between mean fiber length and yarn irregularity. Journal of the Textile Institute, 47:T179, 1956.
26. E. Dyson. Some observations on yarn irregularity. Journal of the Textile Institute, 65:215{217, 1974.
27. Mishu I. Zeidman, Moon W. Suh, and Subhash K. Batra. A new perspective on yarn evenness: Components and determinants of general unevenness. Textile Research Journal, pages 1{6, January 1990.
28. W. L. Balls. Studies of Quality in Cotton. Macmillan, London, 1928.

29. G. A. Foster. The investigation of periodicities in the products of cotton spinning:The drafting wave. Journal of the Textile Institute, 36:T229{T242, 1945. 126
30. D. R. Cox and J. Ingham. Some cause of irregularity in worsted drawing and. Journal of the Textile Institute, 41:P376, 1950.
31. Sung H. Jeong and Moon W. Suh. Sequential channelling of mass variances in spun yarn manufacturing processes. Textile Research Journal, 72:721{726, 2002.
32. W. S. Hearle, P. Grosberg, and S. Backer. Structural Mechanics of Fibers, Yarns, and Fabrics. Wiley-Interscience, New York, NY, 1969. 127
33. M. W. H. Townsend and D. R. Cox. The analysis of yarn irregularity. Journal of the Textile Institute, 42:P107{113, 1951.
34. Jooyong Kim. On-line Measurement and Characterization of Yarn and Fabric Qualities using a Wavelet-Stothastic Hybrid Method. PhD thesis, North Carolina State University, Fiber and Polymer Science, Raleigh/USA, 1998.
35. H. Breny. The calculation of the variance-length curve from the length distribution of fibers. Journal of the Textile Institute, 44:P1{9, 1953.
36. Moon W. Suh. Probabilistic assessment of irregularity in random fiber arrayse effect of fiber length distribution on 'variance-length curve'. Textile Research Journal, 46(4):291{298, April 1976.
37. Lieve V. Langenhove. Simulating the mechanical properties of a yarn based on the properties and arrangement of its fibers. Part I: Finite element model. Textile Research Journal, 67:263{268, 4 1997.
38. Maria Cybulska. Assessing yarn structure with image analysis methods. Textile Research Journal, 69(5):369{373, 1999.
39. A.Lachkar R.Benslimane and et. al. Genetic-based inverse voting hough transform for the assessment of yarn twist level. The restoration of ancient textiles is a projected funded by European Union.
40. B. Xu, B. Pourdeyhimi, and J. Sobus. Fiber cross-sectional shape analysis using image processing techniques. Textile Research Journal, 63:717{730, 1993.
41. F. T. Peirce. The geometry of cloth structure. Journal of the Textile Institute, 28(3):T45{95, 1937. var.
42. Alberto Barella. Law of critical yarn diameter and twist. Textile Research Journal, pages 249{258, April 1950.

43. J. E. Booth. Textile Mathematics. Part III. The Textile Institute, Manchester, 1977. p408.
44. A. Mukhopadhyay, V. K. Kothari, and M. Poddar. Optical measurement of yarn faults. The Indian Textile Journal, pages p13{19, December 2002.
45. Brian T. Snyder. Development of a yarn quality rating system for visual fabric qualities. Master's thesis, NCSU, College of Textiles ,Raleigh, 2000.
46. R. G. Fargher, H. M. Taylor, and F. W. Thomas. Some effects of yarn irregularity in dyeing and finishing. Journal of the Textile Institute, 41:P591{P605, 1950.
47. Dong Han. Development of fabric image models and invariance property of variance-area curve within fabric. Master's thesis, NCSU, College of Textiles, Raleigh, 2002.
48. J. Scharcanski and C. T. J. Dodson. Stochastic texture image estimators for local spatial anisotropy and its variability. IEEE Transactions on Instrumentation and Measurement, 49(5):971{9, 2000.
49. J. Scharcanski and C. T. J. Dodson. Texture analysis for estimating spatial variability and anisotropy in planar stochastic structures. Optical Engineering Journal, 35(8):2302{2309, August 1996.
50. Avishai Nevel and Filiz Avsar. Measuring yarn appearance using the new EIB.Technical report, Lawson-Hemphill, 2001.
51. E. J. Wood. Applying Fourier and associated transforms to pattern characterization in textiles. Textile Research Journal, 60:212{220, 1990.
52. Y. Wu, B. Pourdeyhimi, and M. S. Spivak. Textural evaluation of carpets using image analysis. Textile Research Journal, 61:407{419, 1991.
53. Arkady Cherkassky. Analysis and simulation of nonwoven irregularity and nonhomegenity. Textile Research Journal, 68:242{253, April 1998.
54. Arkady Cherkassky. Evaluating nonwoven fabric irregularity on the basis of linnik functionals. Textile Research Journal, 69:701{708, October 1999.
55. Akio Sakaguchi and et. al. Image analysis of woven fabric surface irregularity.Textile Research Journal, 71:666{671, 2001.

APPENDIXES

Appendix A: Spectrograms, mass wavelength for yarn sample1, Ne 14, polyester/viscose(65/35)

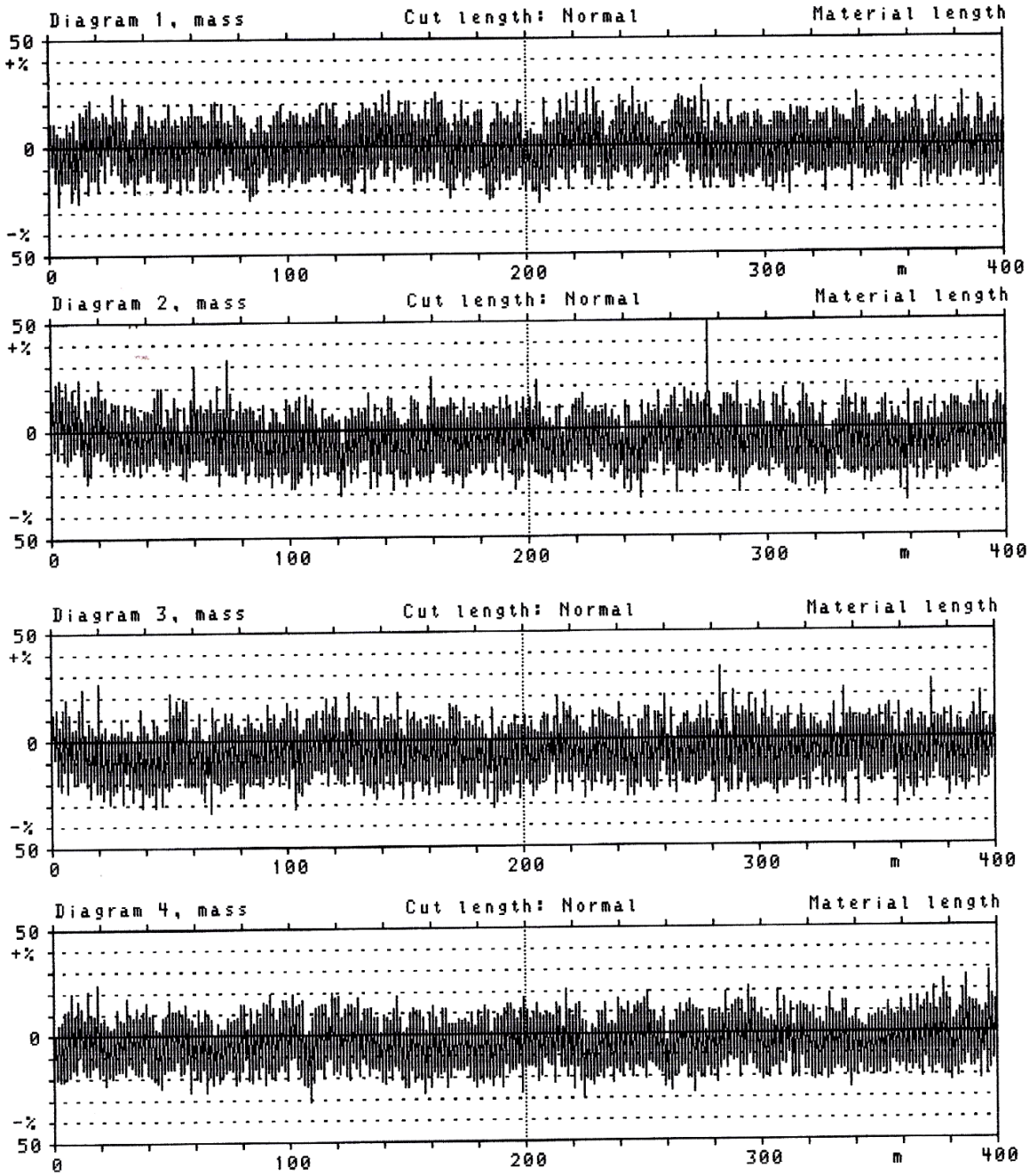

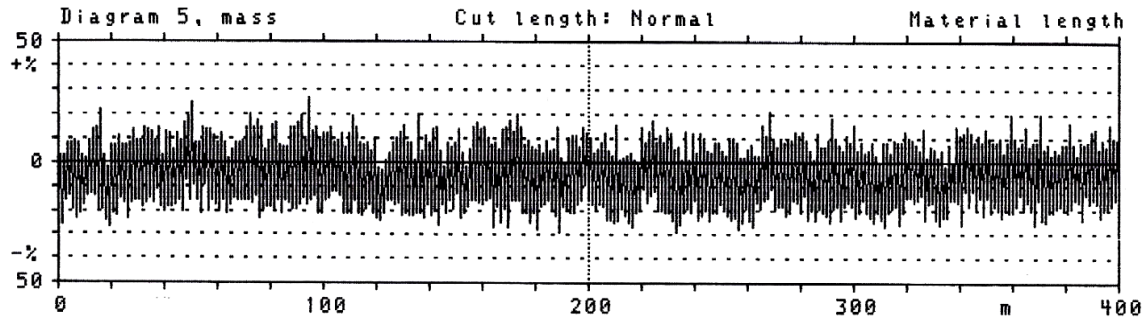
Diagram 5, mass
Cut length: Normal
Material length
50
+%
0
-%
50
0
100
200
300
m
400

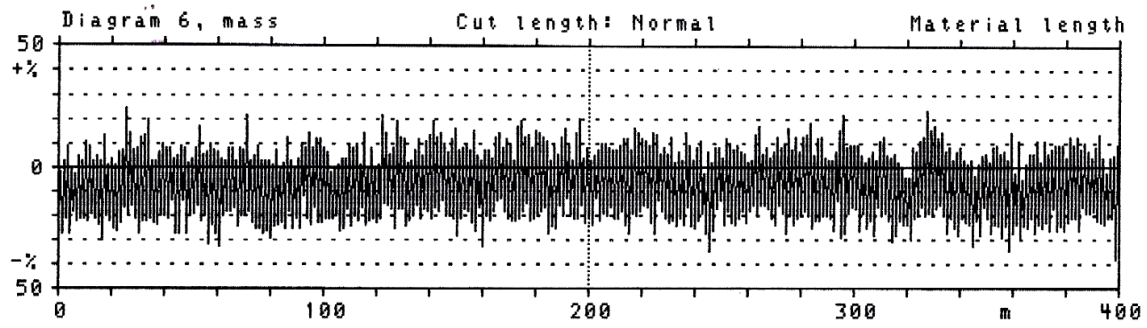
Diagram 6, mass
Cut length: Normal
Material length
50
+%
0
-%
50
0
100
200
300
m
400

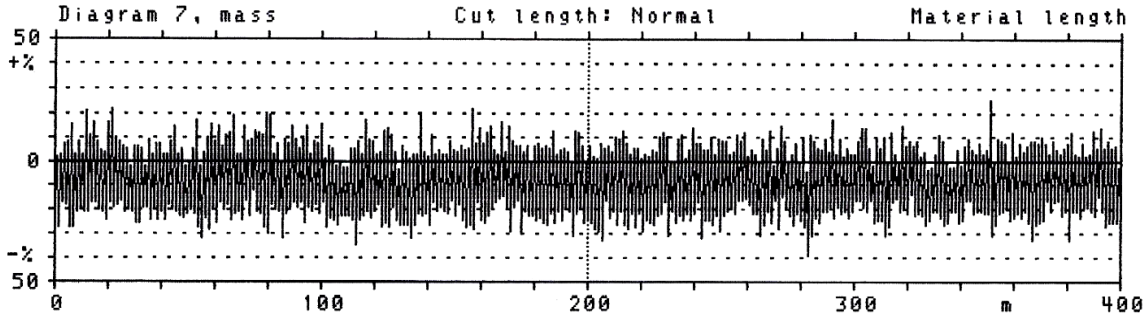
Diagram 7, mass
Cut length: Normal
Material length
50
+%
0
-%
50
0
100
200
300
m
400

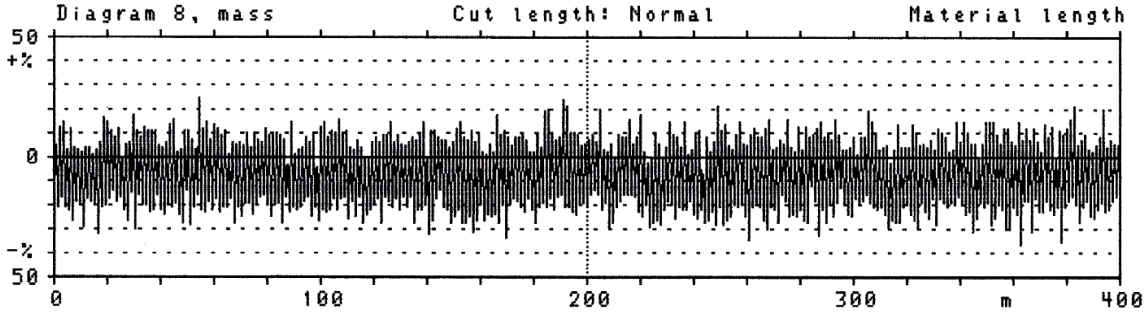
Diagram 8, mass
Cut length: Normal
Material length
50
+%
0
-%
50
0
100
200
300
m
400

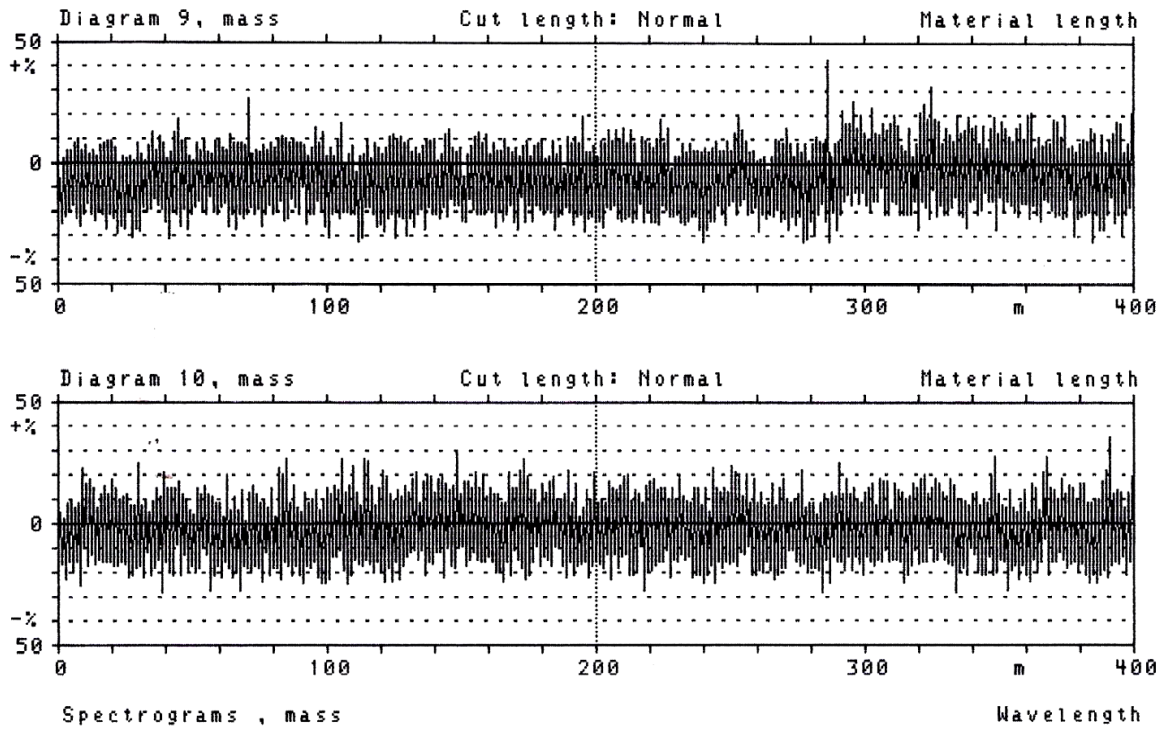

Appendix B: Spectrograms, mass wavelength for Ne 24 cotton yarn.

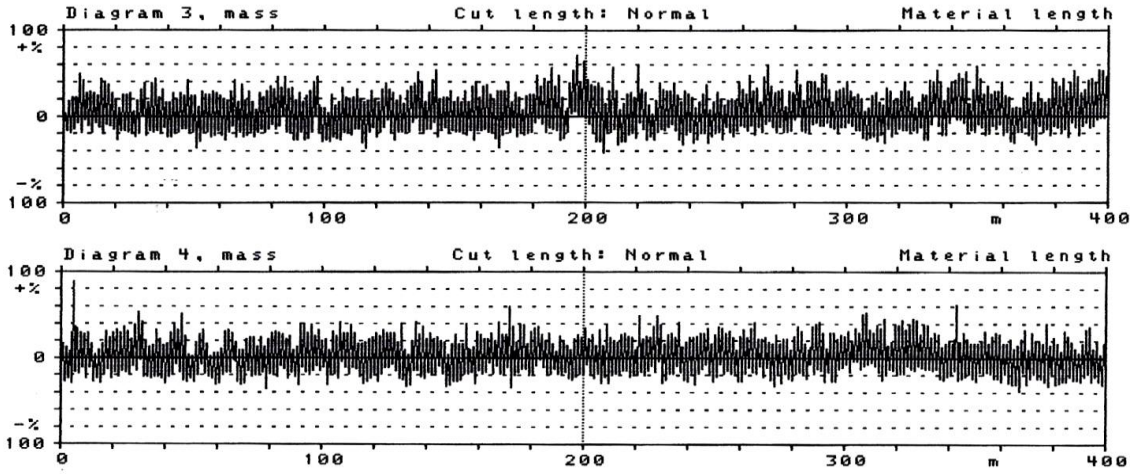

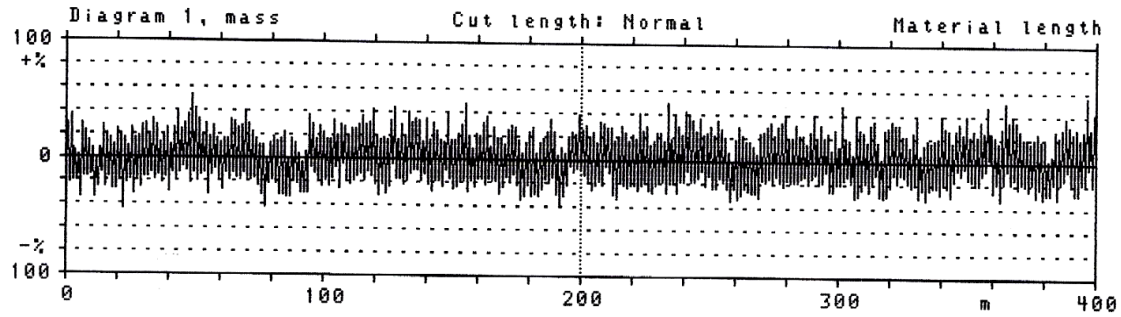
Diagram 1, mass
Cut length: Normal
Material length
100
+%
0
-%
100
0
100
200
300
m
400

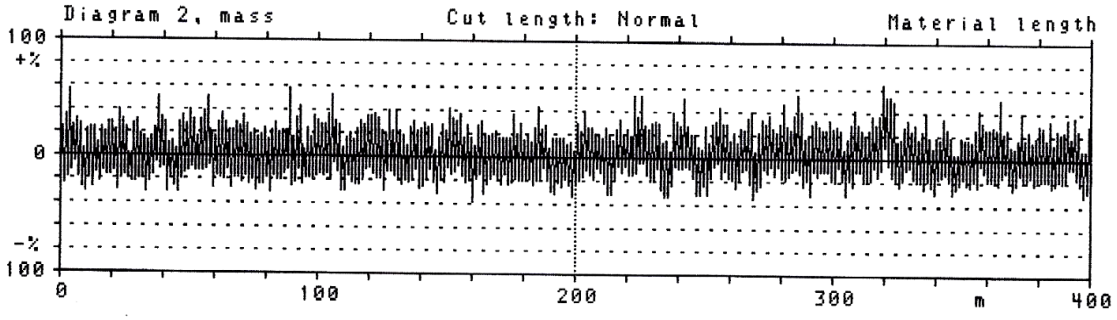
Diagram 2, mass
Cut length: Normal
Material length
100
+%
0
-%
100
0
100
200
300
m
400

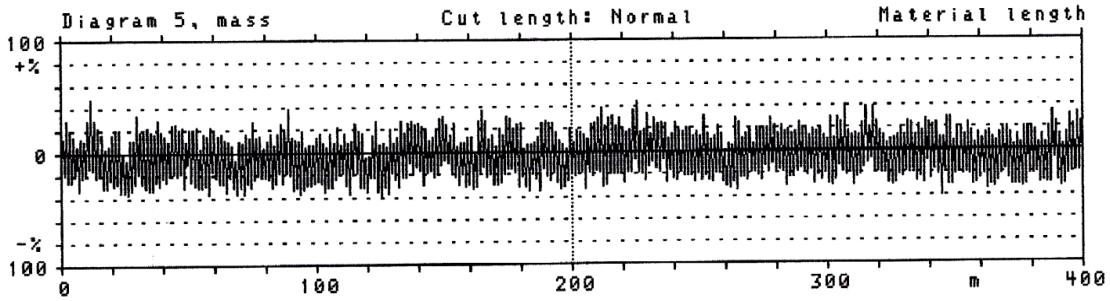
Diagram 5, mass
Cut length: Normal
Material length
100
+%
0
-%
100
0
100
200
300
m
400

Appendix C: Spectrograms, mass wavelength for Ne 15 polyester/viscose (65/35) yarn.

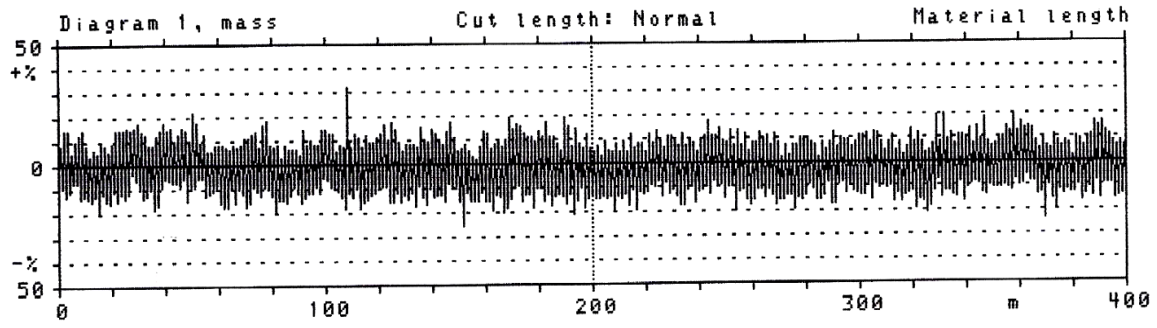

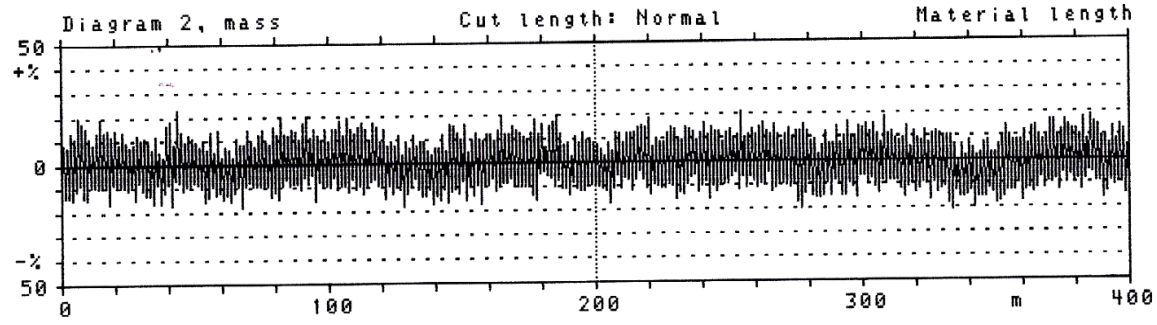

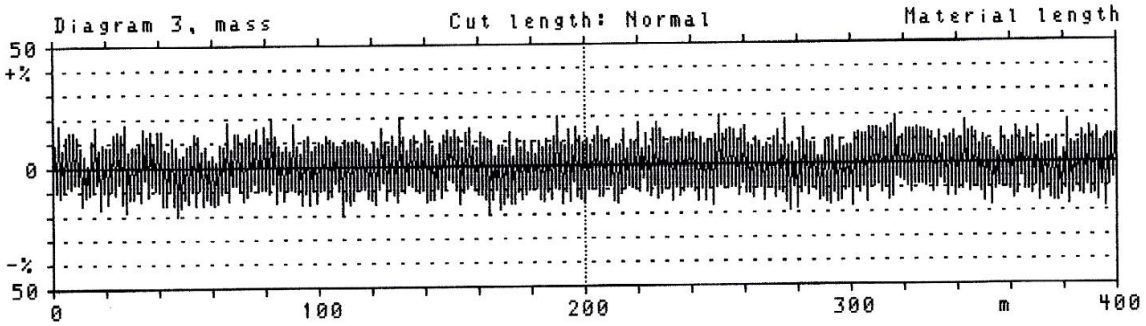

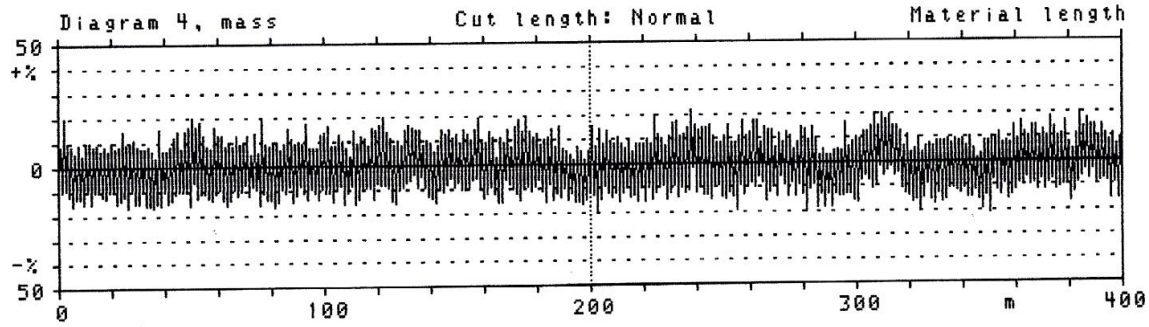

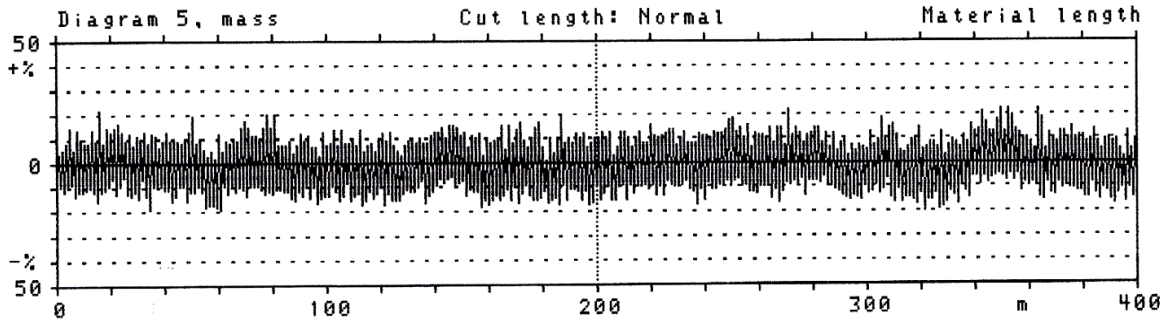

Appendix D: Total result for 15Ne polyester/viscose (65/35) yarn.

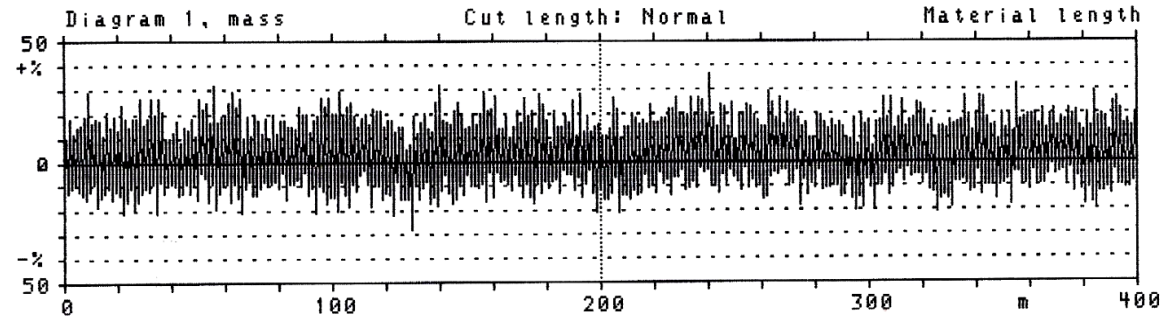

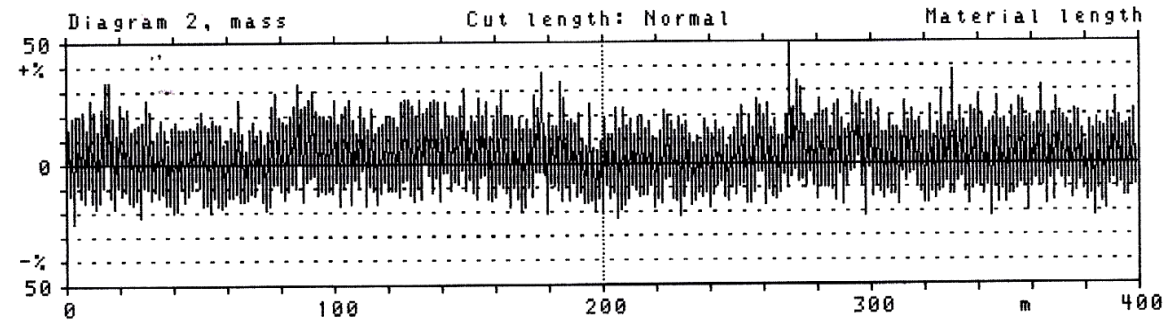

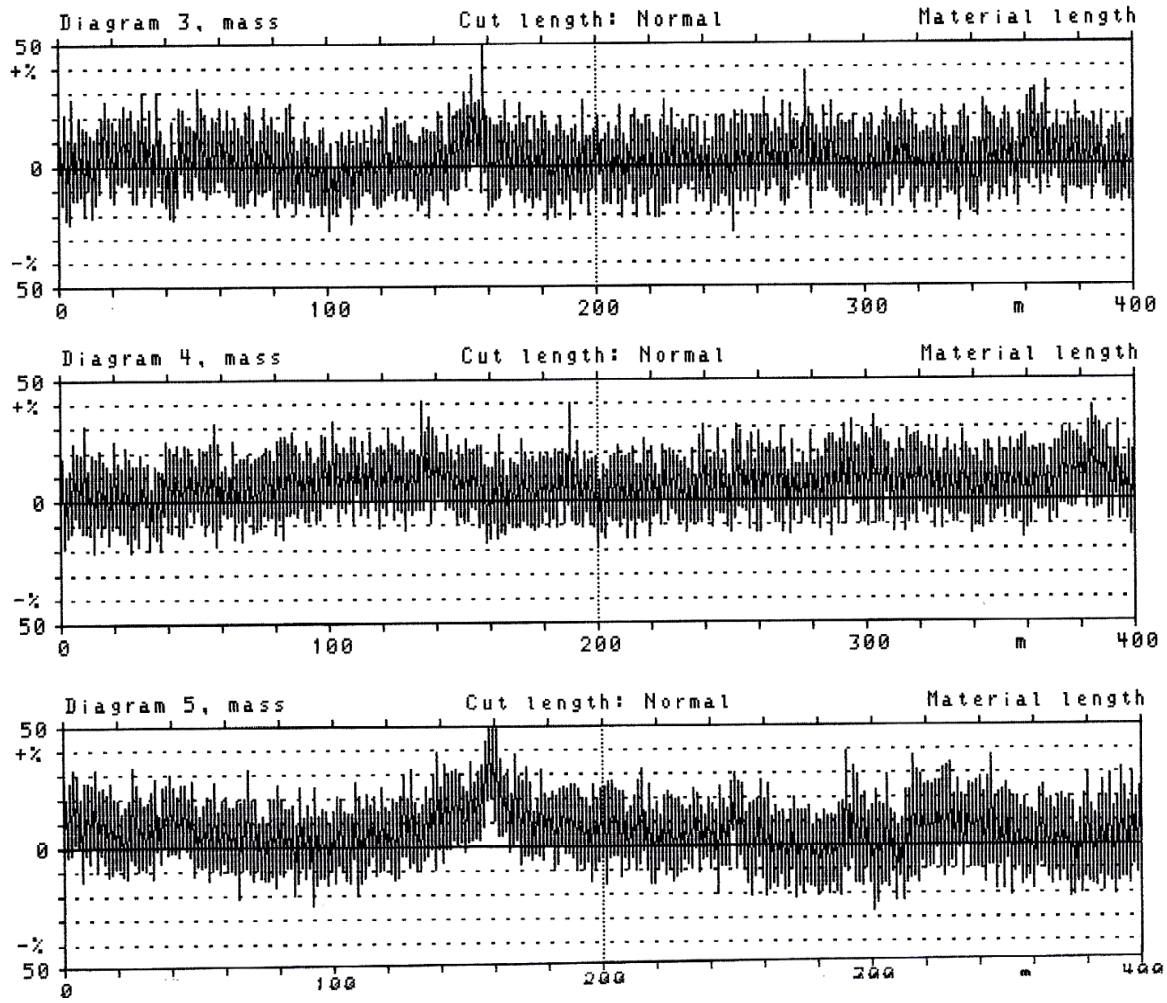

Appendix E: Spectrograms, mass wavelength for 30Ne polyester yarn.

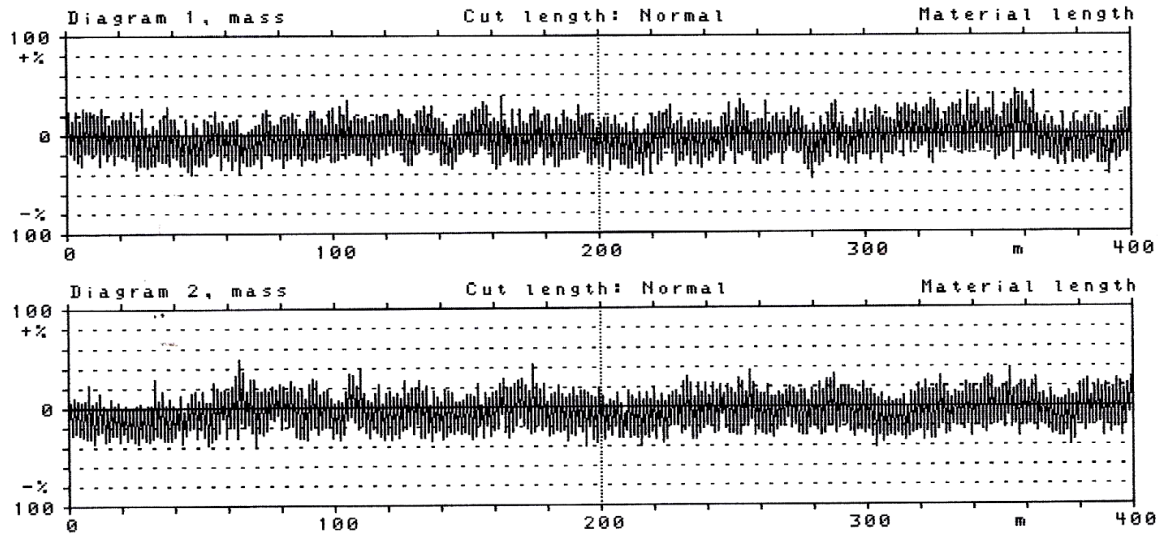

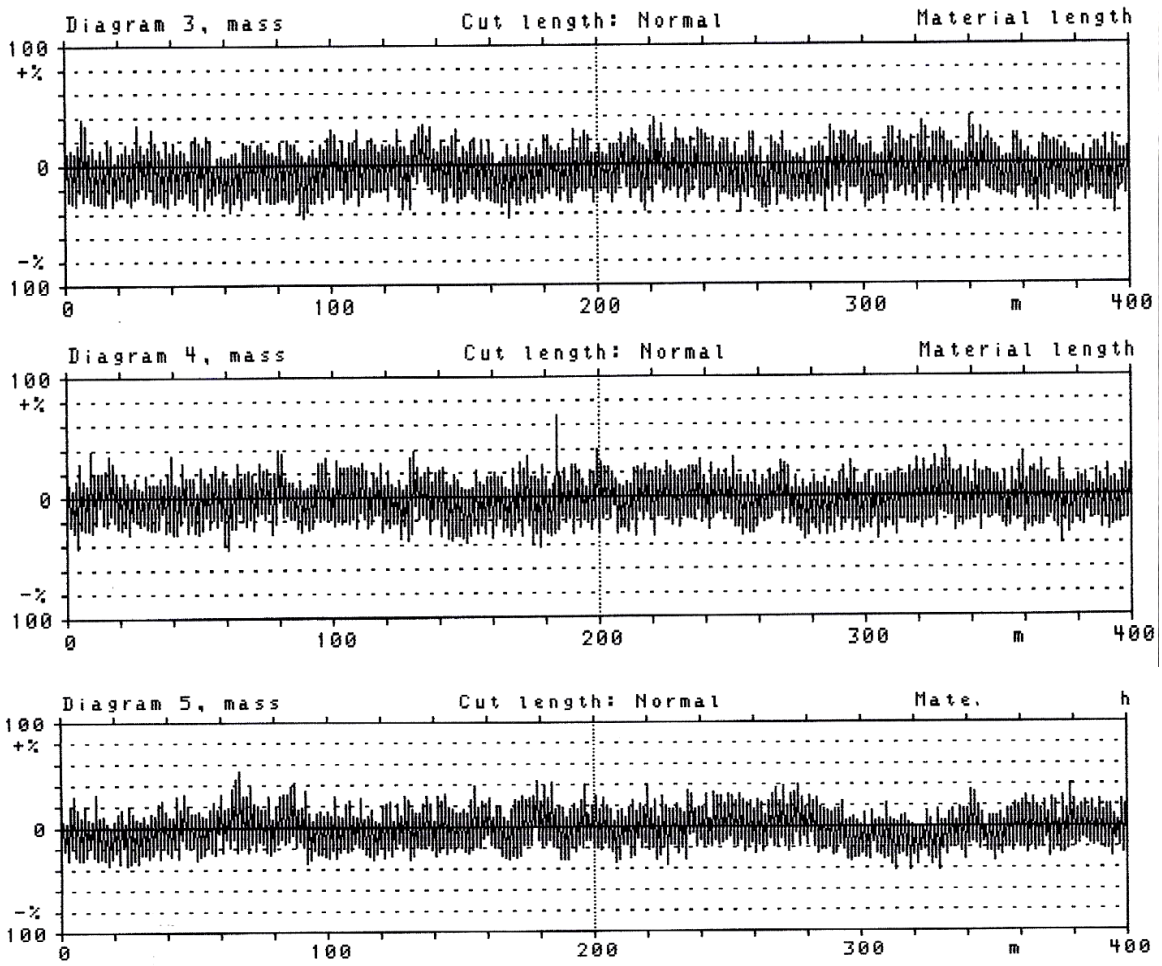

Appendix F: Spectrograms, mass wavelength for Ne 16 cotton yarn.

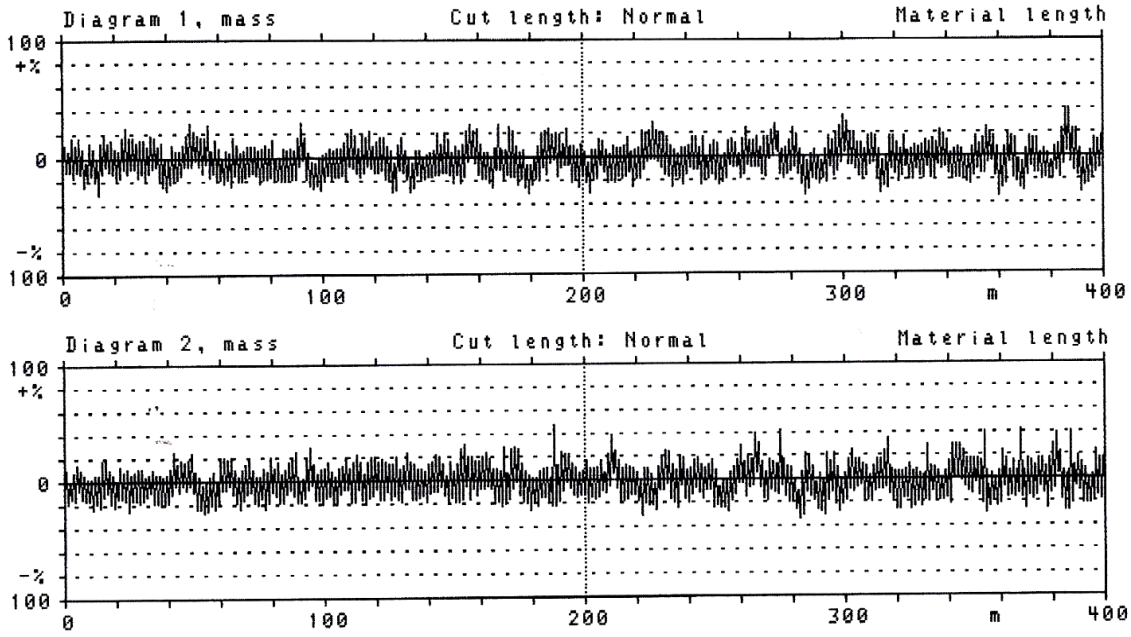

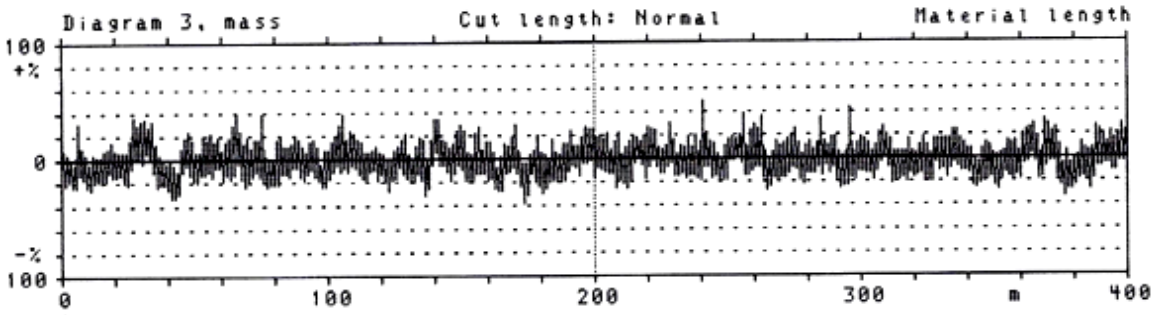
Diagram 3, mass
Cut length: Normal
Material length
100
+%
0
-%
100
0
100
200
300
m
400

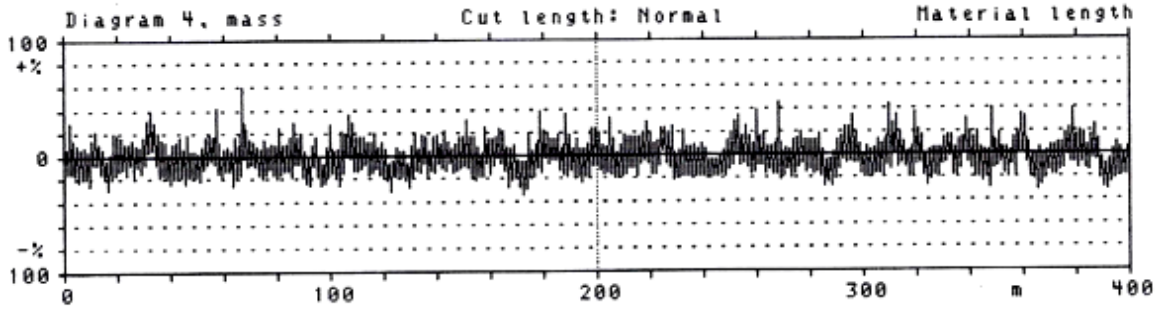
Diagram 4, mass
Cut length: Normal
Material length
100
+%
0
-%
100
0
100
200
300
m
400

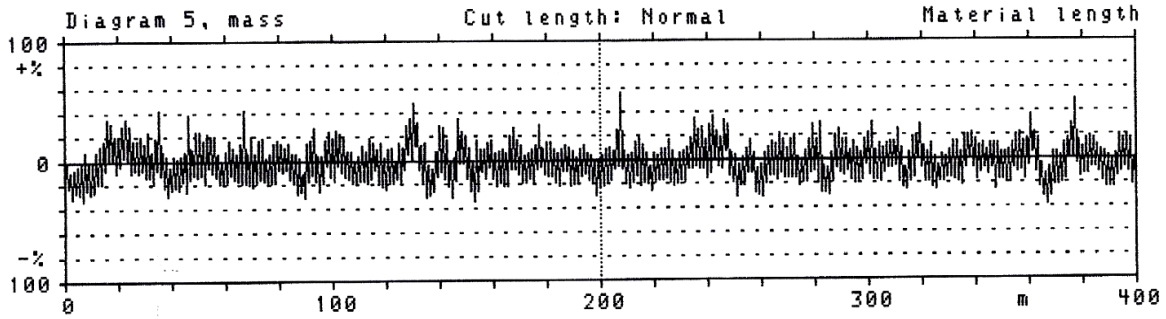
Diagram 5, mass
Cut length: Normal
Material length
100
+%
0
-%
100
0
100
200
300
m
400

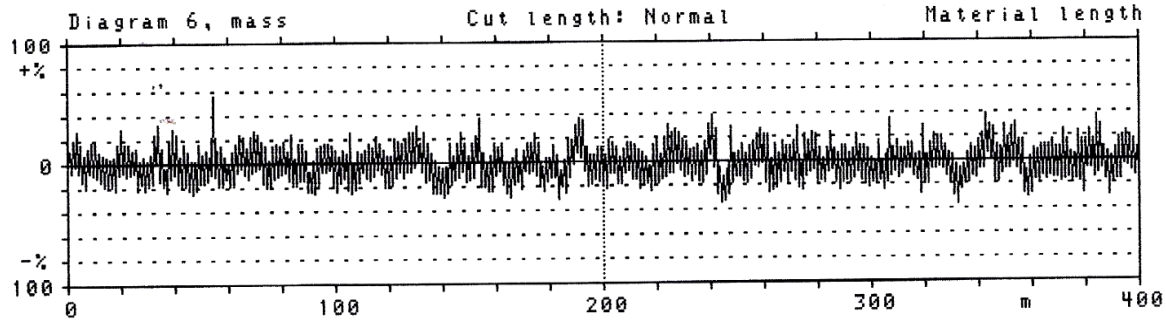
Diagram 6, mass
Cut length: Normal
Material length
100
+%
0
-%
100
0
100
200
300
m
400

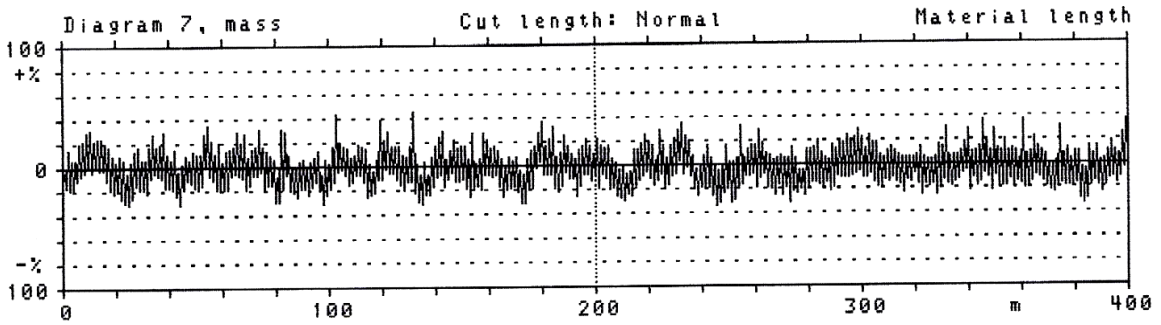
Diagram 7, mass
Cut length: Normal
Material length
100
+%
0
-%
100
0
100
200
300
m
400

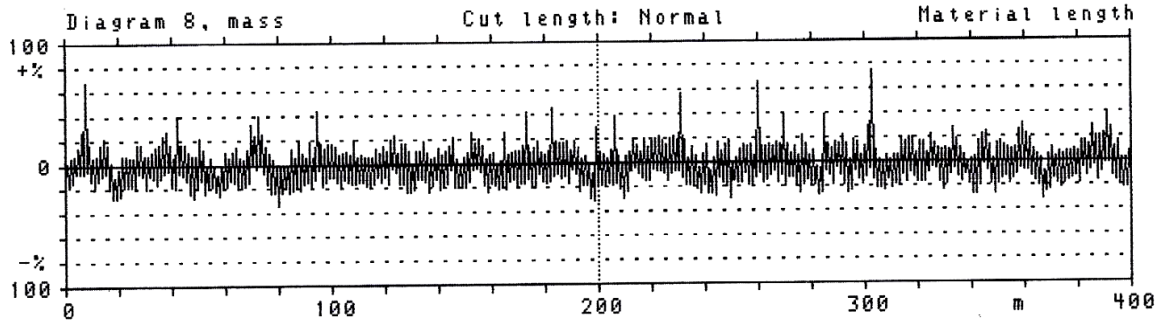
Diagram 8, mass
Cut length: Normal
Material length
100
+%
0
-%
100
0
100
200
300
m
400

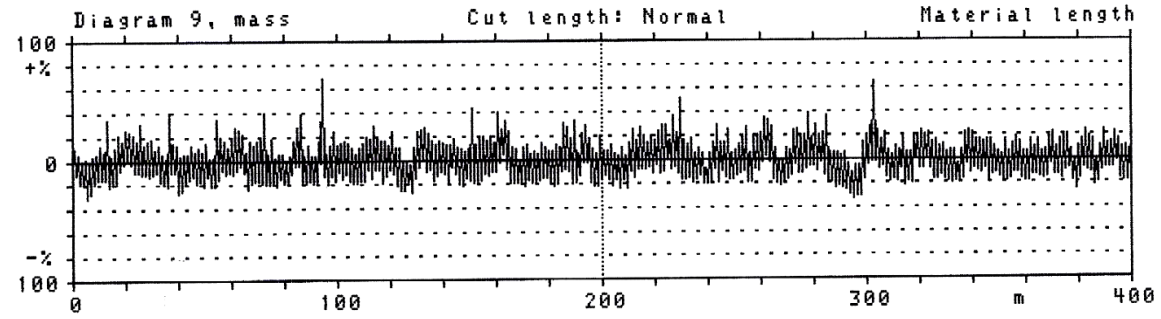
Diagram 9, mass
Cut length: Normal
Material length
100
+%
0
-%
100
0
100
200
300
m
400

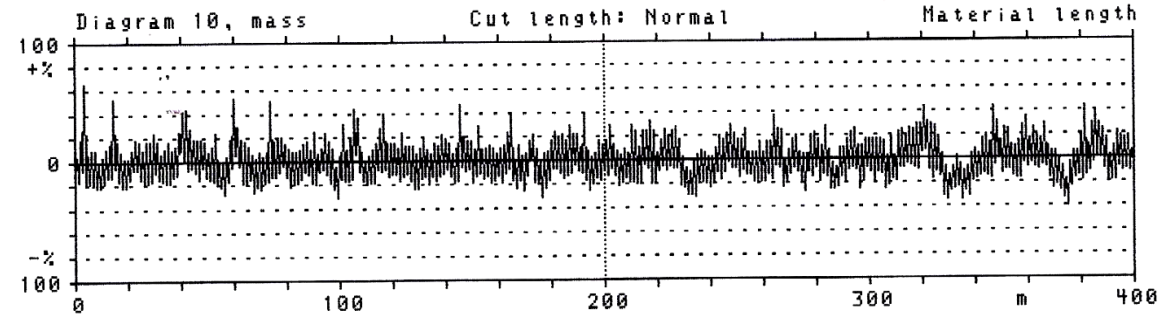
Diagram 10, mass
Cut length: Normal
Material length
100
+%
0
-%
100
0
100
200
300
m
400

Appendix G: Spectrograms, mass wavelength for Ne 20 cotton yarn.

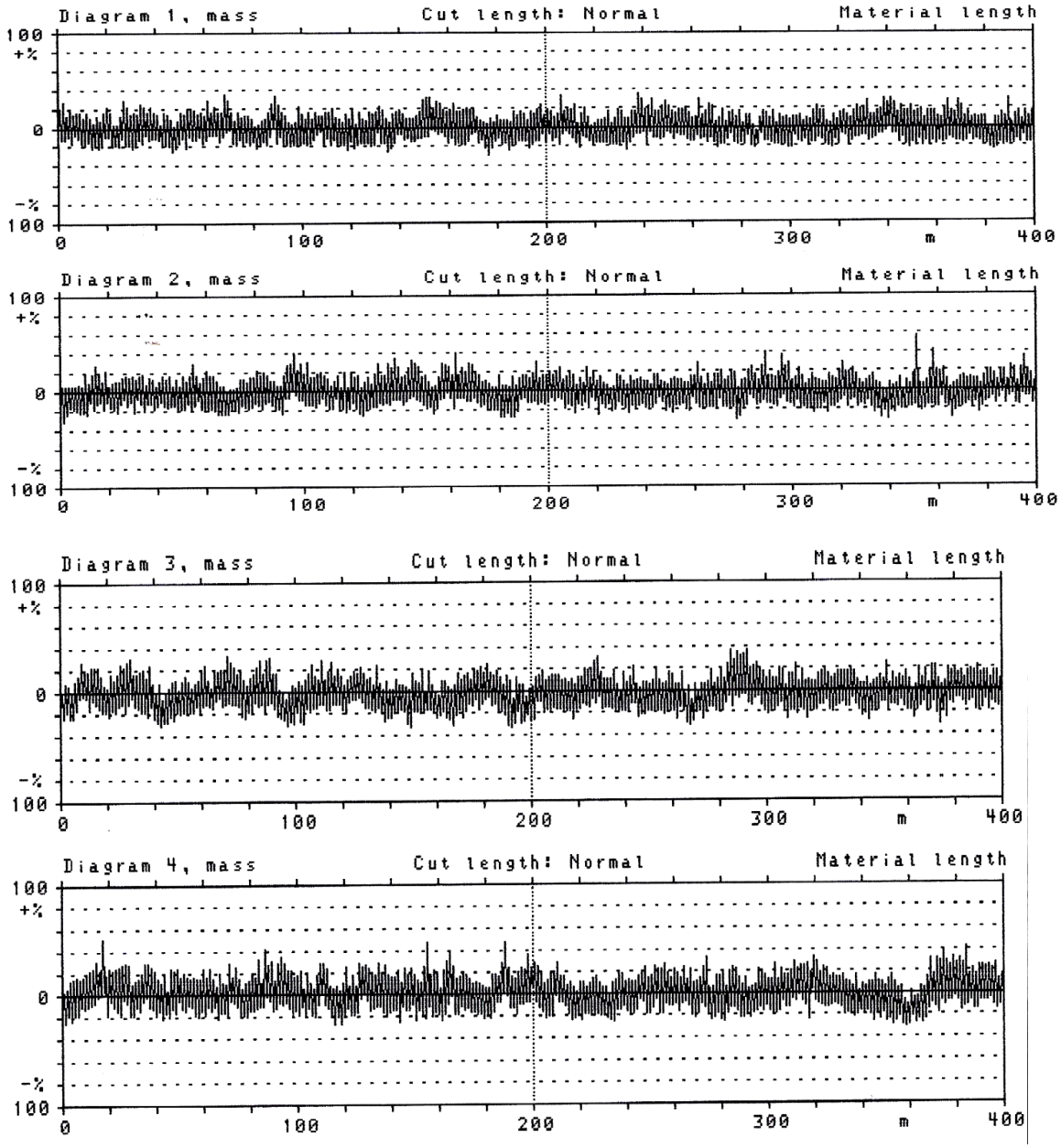

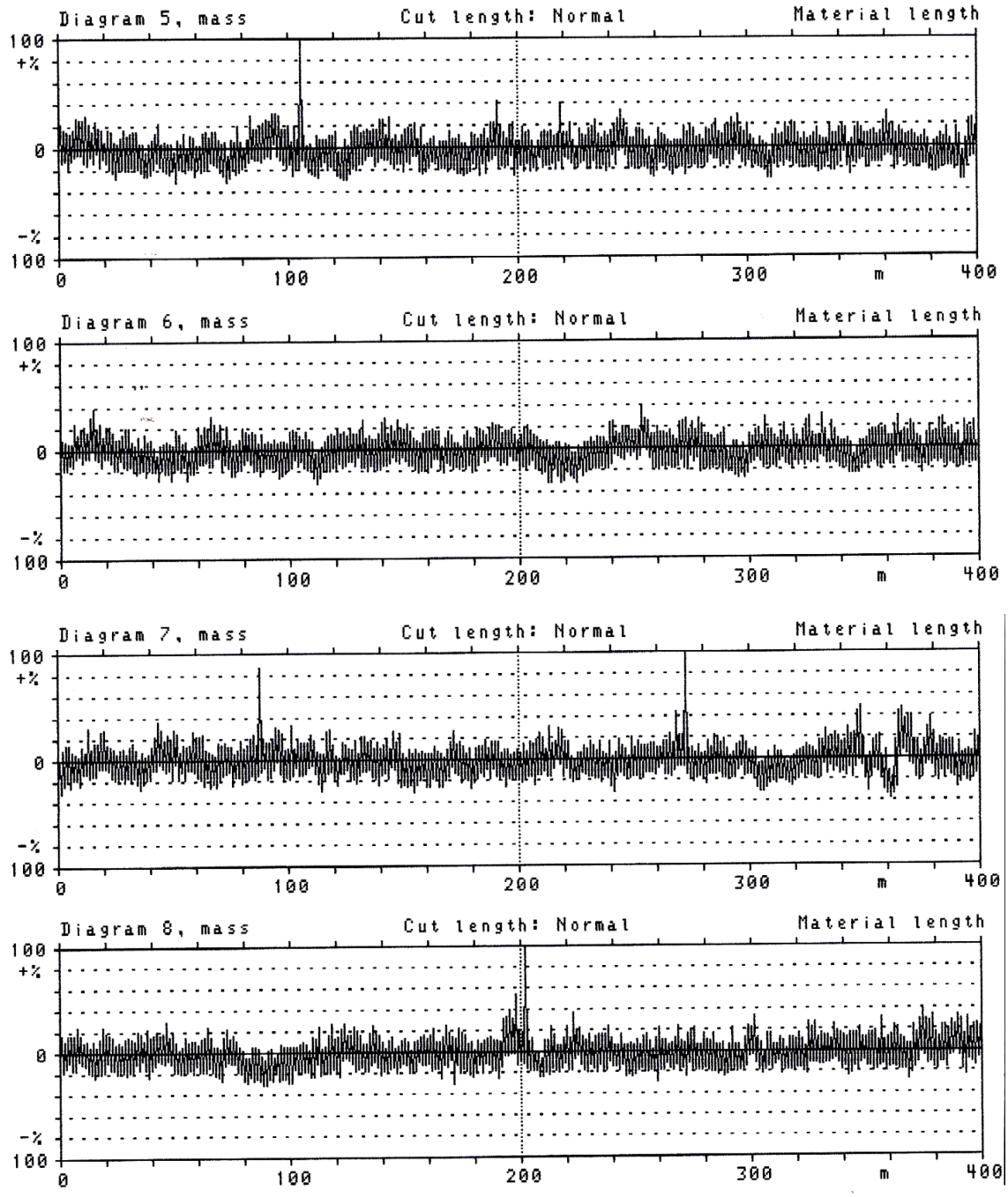
Diagram 5, mass
Cut length: Normal
Material length
100
+%
0
-%
100
0
100
200
300
m
400
Diagram 6, mass
Cut length: Normal
Material length
100
+%
0
-%
100
0
100
200
300
m
400
Diagram 7, mass
Cut length: Normal
Material length
100
+%
0
-%
100
0
100
200
300
m
400
Diagram 8, mass
Cut length: Normal
Material length
100
+%
0
-%
100
0
100
200
300
m
400

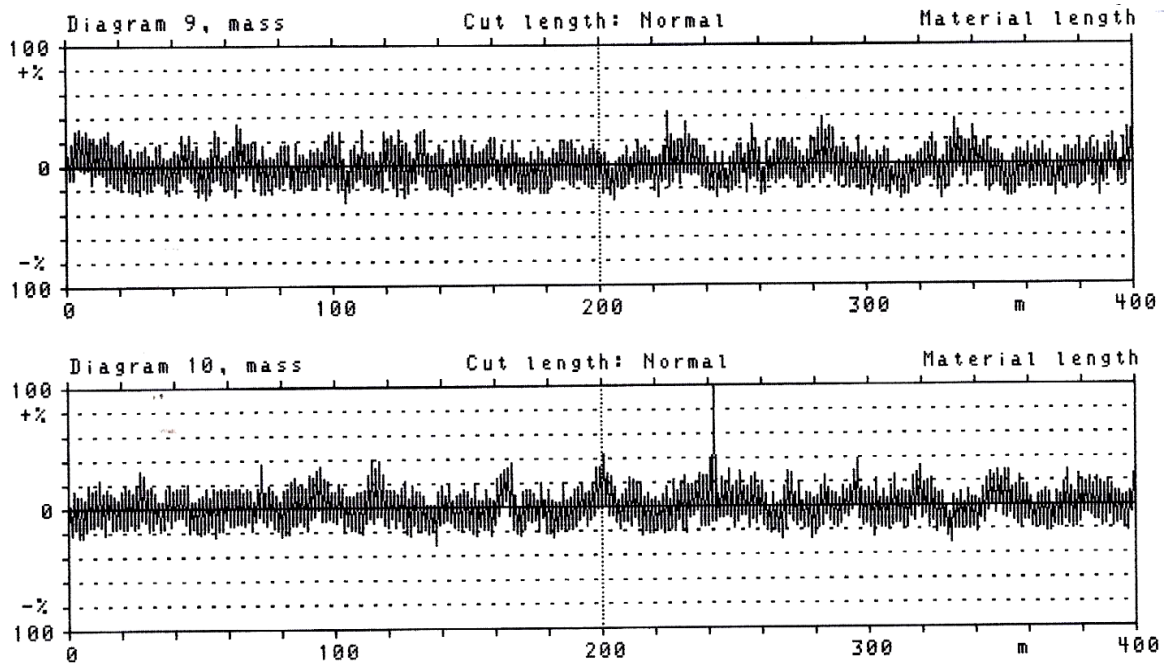

Appendix H: Measured yarns diameter

Length (m)	Diameter (mm)						
	Sample 1	Sample 2	Sample 3	Sample 4	Sample 5	Sample 6	Sample 7
20	0.225472	0.170353	0.222503	0.238898	0.154039	0.199581	0.223129
40	0.261838	0.148133	0.264661	0.243582	0.157352	0.170097	0.219072
60	0.254565	0.162946	0.229529	0.257635	0.144101	0.199581	0.212987
80	0.242443	0.181463	0.222503	0.236556	0.147414	0.226797	0.196759
100	0.249716	0.194424	0.252950	0.245924	0.170602	0.188241	0.202844
120	0.261838	0.149984	0.236556	0.231871	0.165633	0.231333	0.217044
140	0.269112	0.235161	0.236556	0.262319	0.140788	0.190509	0.217044
160	0.240019	0.199979	0.231871	0.248266	0.140788	0.247208	0.204873
180	0.254565	0.199979	0.241240	0.257635	0.145757	0.158758	0.200816
200	0.206077	0.235161	0.217818	0.243582	0.144101	0.215457	0.202844
220	0.254565	0.185166	0.217818	0.248266	0.132507	0.185973	0.174446
240	0.266687	0.222199	0.229529	0.311504	0.159008	0.208653	0.251527
260	0.247292	0.174056	0.215476	0.234213	0.139132	0.213189	0.192702
280	0.235170	0.229606	0.227187	0.231871	0.137476	0.229065	0.196759
300	0.215774	0.177759	0.234213	0.252950	0.168946	0.312979	0.174446
320	0.240019	0.203683	0.236556	0.259977	0.16729	0.233600	0.192702
340	0.261838	0.212941	0.215476	0.271688	0.173915	0.222261	0.253556
360	0.237594	0.183314	0.238898	0.231871	0.207042	0.174633	0.192702

380	0.240019	0.166649	0.224845	0.217818	0.140788	0.174633	0.182560
400	0.218199	0.222199	0.215476	0.262319	0.168946	0.244940	0.202844
420	0.273961	0.203683	0.248266	0.264661	0.124225	0.192777	0.190674
440	0.220623	0.224051	0.250608	0.222503	0.122569	0.199581	0.186617
460	0.278809	0.166649	0.215476	0.213134	0.147414	0.226797	0.206901
480	0.244867	0.194424	0.229529	0.252950	0.170602	0.249476	0.200816
500	0.230321	0.207386	0.231871	0.271688	0.124225	0.204117	0.184588
520	0.201228	0.229606	0.245924	0.255293	0.140788	0.254012	0.219072
540	0.235170	0.185166	0.220161	0.231871	0.137476	0.215457	0.202844
560	0.261838	0.146281	0.248266	0.245924	0.152383	0.258548	0.237328
580	0.208501	0.175908	0.259977	0.234213	0.129194	0.188241	0.182560
600	0.213350	0.185166	0.229529	0.229529	0.157352	0.242672	0.219072
620	0.240019	0.203683	0.250608	0.227187	0.157352	0.206385	0.172418
640	0.203652	0.212941	0.241240	0.215476	0.173915	0.204117	0.182560
660	0.220623	0.183314	0.241240	0.241240	0.152383	0.276692	0.202844
680	0.225472	0.248122	0.243582	0.241240	0.163977	0.201849	0.186617
700	0.218199	0.194424	0.250608	0.262319	0.154039	0.192777	0.180532
720	0.198803	0.296266	0.231871	0.220161	0.162321	0.181437	0.239356
740	0.210925	0.175908	0.227187	0.257635	0.142445	0.226797	0.176475
760	0.240019	0.192573	0.220161	0.257635	0.168946	0.226797	0.204873
780	0.247292	0.203683	0.238898	0.227187	0.16729	0.249476	0.215015
800	0.242443	0.199979	0.238898	0.229529	0.197104	0.224529	0.186617
820	0.254565	0.201831	0.231871	0.243582	0.140788	0.204117	0.170389
840	0.206077	0.168501	0.243582	0.213134	0.14907	0.170097	0.194731
860	0.213350	0.194424	0.210792	0.252950	0.110974	0.195045	0.202844
880	0.218199	0.237012	0.245924	0.238898	0.14907	0.176901	0.190674
900	0.220623	0.148133	0.236556	0.210792	0.168946	0.229065	0.152133
920	0.240019	0.175908	0.227187	0.238898	0.162321	0.219993	0.200816
940	0.206077	0.203683	0.245924	0.238898	0.152383	0.301639	0.158219
960	0.196379	0.192573	0.224845	0.236556	0.14907	0.222261	0.158219
980	0.196379	0.190721	0.234213	0.248266	0.155695	0.170097	0.210958
1000	0.215774	0.259232	0.217818	0.238898	0.154039	0.238136	0.152133
1020	0.230321	0.244419	0.252950	0.231871	0.182197	0.244940	0.192702
1040	0.227896	0.194424	0.238898	0.241240	0.162321	0.224529	0.198788
1060	0.264263	0.211089	0.252950	0.238898	0.124225	0.258548	0.198788
1080	0.215774	0.199979	0.215476	0.236556	0.124225	0.233600	0.202844
1100	0.193954	0.233309	0.227187	0.236556	0.145757	0.247208	0.182560
1120	0.206077	0.188869	0.241240	0.241240	0.14907	0.197313	0.182560
1140	0.223048	0.203683	0.227187	0.210792	0.152383	0.226797	0.170389
1160	0.227896	0.214793	0.229529	0.262319	0.159008	0.226797	0.200816
1180	0.244867	0.240716	0.215476	0.252950	0.124225	0.170097	0.215015
1200	0.235170	0.259232	0.241240	0.229529	0.14907	0.260816	0.186617
1220	0.213350	0.194424	0.224845	0.267003	0.137476	0.229065	0.204873

1240	0.240019	0.164798	0.234213	0.257635	0.182197	0.195045	0.202844
1260	0.206077	0.138875	0.236556	0.255293	0.129194	0.192777	0.206901
1280	0.235170	0.190721	0.222503	0.259977	0.226918	0.235868	0.194731
1300	0.225472	0.188869	0.241240	0.257635	0.140788	0.242672	0.204873
1320	0.242443	0.192573	0.243582	0.281056	0.165633	0.188241	0.212987
1340	0.235170	0.179611	0.224845	0.290425	0.168946	0.231333	0.202844
1360	0.218199	0.203683	0.227187	0.231871	0.14907	0.224529	0.174446
1380	0.208501	0.209238	0.241240	0.231871	0.14907	0.260816	0.172418
1400	0.242443	0.218496	0.241240	0.229529	0.18054	0.260816	0.283982
1420	0.179408	0.170353	0.229529	0.227187	0.165633	0.231333	0.182560
1440	0.227896	0.181463	0.243582	0.283398	0.165633	0.204117	0.186617
1460	0.196379	0.174056	0.243582	0.269345	0.140788	0.276692	0.210958
1480	0.225472	0.185166	0.238898	0.276372	0.155695	0.222261	0.198788
1500	0.215774	0.214793	0.220161	0.278714	0.155695	0.185973	0.202844
1520	0.227896	0.222199	0.210792	0.295109	0.162321	0.272156	0.247470
1540	0.218199	0.183314	0.234213	0.245924	0.145757	0.238136	0.194731
1560	0.244867	0.190721	0.243582	0.252950	0.175571	0.306175	0.141991
1580	0.230321	0.192573	0.210792	0.295109	0.162321	0.240404	0.259641
1600	0.254565	0.207386	0.241240	0.245924	0.165633	0.226797	0.202844
1620	0.193954	0.177759	0.245924	0.262319	0.134163	0.249476	0.192702
1640	0.223048	0.177759	0.227187	0.297451	0.159008	0.167829	0.182560
1660	0.215774	0.188869	0.220161	0.257635	0.182197	0.197313	0.152133
1680	0.244867	0.161094	0.241240	0.267003	0.137476	0.256280	0.174446
1700	0.223048	0.172204	0.222503	0.234213	0.144101	0.231333	0.202844
1720	0.213350	0.111100	0.234213	0.262319	0.140788	0.181437	0.186617
1740	0.210925	0.198128	0.234213	0.274030	0.132507	0.258548	0.227186
1760	0.235170	0.162946	0.215476	0.374741	0.190478	0.229065	0.168361
1780	0.213350	0.190721	0.241240	0.281056	0.173915	0.231333	0.184588
1800	0.227896	0.185166	0.234213	0.281056	0.182197	0.181437	0.172418
1820	0.252141	0.174056	0.248266	0.241240	0.202073	0.192777	0.194731
1840	0.235170	0.185166	0.220161	0.257635	0.168946	0.231333	0.186617
1860	0.206077	0.135171	0.234213	0.234213	0.154039	0.154222	0.160247
1880	0.223048	0.194424	0.245924	0.220161	0.165633	0.272156	0.204873
1900	0.237594	0.166649	0.215476	0.206108	0.124225	0.244940	0.219072
1920	0.235170	0.196276	0.241240	0.269345	0.124225	0.235868	0.204873
1940	0.225472	0.214793	0.250608	0.278714	0.16729	0.224529	0.200816
1960	0.242443	0.168501	0.238898	0.222503	0.165633	0.254012	0.231243
1980	0.213350	0.181463	0.224845	0.269345	0.173915	0.213189	0.176475
2000	0.237594	0.188869	0.224845	0.264661	0.157352	0.181437	0.223129

Appendix I: Weight of knitted fabrics

Length Of Yarn Consumed (m)	Weight (grams)						
	Sample 1	Sample 2	Sample 3	Sample 4	Sample 5	Sample 6	Sample 7
20	0.730	0.484	0.745	0.770	0.417	0.768	0.610
40	0.746	0.464	0.769	0.766	0.424	0.766	0.586
60	0.764	0.482	0.756	0.785	0.396	0.771	0.571
80	0.765	0.500	0.753	0.797	0.360	0.775	0.618
100	0.754	0.490	0.753	0.807	0.387	0.760	0.635
120	0.770	0.488	0.780	0.790	0.401	0.739	0.538
140	0.750	0.492	0.767	0.772	0.398	0.747	0.589
160	0.761	0.488	0.763	0.766	0.402	0.771	0.601
180	0.737	0.472	0.774	0.743	0.372	0.764	0.591
200	0.753	0.497	0.754	0.763	0.381	0.738	0.585
220	0.761	0.489	0.769	0.779	0.391	0.747	0.600
240	0.753	0.487	0.796	0.784	0.391	0.749	0.593
260	0.750	0.496	0.786	0.792	0.406	0.740	0.625
280	0.744	0.481	0.751	0.772	0.415	0.761	0.578
300	0.754	0.479	0.759	0.759	0.414	0.716	0.607
320	0.745	0.489	0.772	0.786	0.401	0.777	0.592
340	0.751	0.499	0.785	0.780	0.420	0.729	0.629
360	0.757	0.480	0.786	0.778	0.372	0.786	0.556
380	0.759	0.444	0.788	0.804	0.375	0.728	0.561
400	0.723	0.448	0.745	0.802	0.412	0.784	0.625
420	0.730	0.466	0.756	0.760	0.396	0.748	0.613
440	0.723	0.482	0.789	0.779	0.391	0.774	0.597
460	0.730	0.467	0.776	0.776	0.390	0.741	0.566
480	0.734	0.488	0.781	0.778	0.412	0.732	0.604
500	0.752	0.490	0.753	0.790	0.429	0.741	0.587
520	0.751	0.497	0.746	0.783	0.404	0.741	0.571
540	0.763	0.486	0.758	0.775	0.363	0.767	0.593
560	0.756	0.485	0.781	0.795	0.383	0.734	0.586
580	0.758	0.485	0.776	0.781	0.388	0.741	0.614
600	0.728	0.468	0.762	0.742	0.388	0.753	0.581
620	0.723	0.486	0.759	0.774	0.362	0.772	0.581
640	0.722	0.512	0.747	0.776	0.416	0.752	0.607
660	0.730	0.460	0.794	0.765	0.398	0.764	0.598
680	0.732	0.503	0.797	0.764	0.394	0.731	0.610

700	0.727	0.490	0.778	0.757	0.379	0.772	0.588
720	0.696	0.468	0.758	0.795	0.401	0.752	0.605
740	0.703	0.480	0.772	0.806	0.396	0.755	0.599
760	0.717	0.473	0.777	0.789	0.408	0.763	0.581
780	0.742	0.456	0.786	0.762	0.399	0.754	0.600
800	0.725	0.467	0.779	0.780	0.373	0.747	0.621
820	0.714	0.493	0.764	0.761	0.397	0.756	0.627
840	0.722	0.494	0.733	0.744	0.411	0.764	0.597
860	0.725	0.527	0.745	0.767	0.407	0.735	0.570
880	0.731	0.454	0.765	0.749	0.403	0.765	0.592
900	0.713	493	0.764	0.722	0.397	0.757	0.561
920	0.698	0.464	0.755	0.730	0.352	0.776	0.612
940	0.687	0.471	0.746	0.761	0.392	0.756	0.618
960	0.726	0486	0.752	0.749	0.379	0.756	0.578
980	0.730	0.500	0.763	0.738	0.392	0.785	0.616
1000	0.735	0.486	0.786	0.731	0.388	0.768	0.608
1020	0.740	0.470	0.768	0.715	0.400	0.786	0.620
1040	0.746	0.460	0.747	0.754	0.361	0.768	0.588
1060	0.715	0.494	0.757	0.750	0.407	0.745	0.581
1080	0.716	0.464	0.752	0.751	0.397	0.783	0.606
1100	0.720	0.464	0.781	0.725	0.376	0.751	0.599
1120	0.709	0.495	0.776	0.740	0.379	0.805	0.610
1140	0.723	0.468	0.781	0.725	0.369	0.795	0.606
1160	0.699	0.464	0.757	0.723	0.401	0.796	0.611
1180	0.713	0.454	0.754	0.737	0.413	0.750	0.619
1200	0.710	0.481	0.742	0.722	0.413	0.781	0.593
1220	0.718	0.477	0.760	0.730	0.397	0.754	0.620
1240	0.701	0.456	0.774	0.707	0.404	0.777	0.608
1260	0.700	0.485	0.772	0.722	0.395	0.767	0.602
1280	0.703	0.466	0.734	0.748	0.410	0.772	0.604
1300	0.722	0.445	0.756	0.774	0.414	0.761	0.589
1320	0.707	0.466	0.761	0.709	0.414	0.753	0.617
1340	0.694	0.472	0.769	0.722	0.394	0.782	0.599
1360	0.710	0.446	0.787	0.728	0.382	0.740	0.626
1380	0.757	0.500	0.791	0.732	0.369	0.777	0.617
1400	0.731	0.475	0.777	0.735	0.379	0.757	0.610
1420	0.730	0.486	0.790	0.700	0.443	0.798	0.586
1440	0.744	0.495	0.736	0.710	0.442	0.758	0.599
1460	0.748	0.478	0.738	0.698	0.417	0.769	0.589

1480	0.720	0.474	0.766	0.710	0.412	0.760	0.614
1500	0.743	0.482	0.781	0.700	0.375	0.767	0.608
1520	0.737	0.500	0.777	0.733	0.357	0.791	0.580
1540	0.742	0.514	0.775	0.719	0.368	0.758	0.561
1560	0.737	0.527	0.799	0.717	0.386	0.786	0.618
1580	0.732	0.480	0.804	0.696	0.390	0.760	0.605
1600	0.753	0.471	0.781	0.722	0.381	0.788	0.584
1620	0.721	0.506	0.771	0.744	0.363	0.758	0.589
1640	0.720	0.489	0.781	0.710	0.374	0.750	0.610
1660	0.727	0.473	0.796	0.712	0.378	0.773	0.571
1680	0.732	0.476	0.768	0.705	0.383	0.778	0.601
1700	0.728	0.498	0.792	0.697	0.395	0.762	0.600
1720	0.737	0.509	0.782	0.703	0.414	0.745	0.601
1740	0.754	0.477	0.782	0.729	0.435	0.778	0.582
1760	0.718	0.505	0.805	0.724	0.423	0.759	0.606
1780	0.729	0.473	0.771	0.754	0.391	0.761	0.592
1800	0.713	0.489	0.794	0.727	0.359	0.777	0.614
1820	0.745	0.485	0.777	0.732	0.389	0.776	0.631
1840	0.777	0.481	0.781	0.734	0.423	0.784	0.595
1860	0.715	0.471	0.774	0.732	0.388	0.777	0.580
1880	0.743	0.466	0.781	0.767	0.369	0.784	0.582
1900	0.765	0.450	0.793	0.743	0.353	0.765	0.569
1920	0.748	0.472	0.778	0.759	0.375	0.816	0.581
1940	0.722	0.467	0.786	0.765	0.412	0.799	0.592
1960	0.759	0.460	0.775	0.749	0.432	0.779	0.600
1980	0.723	0.470	0.797	0.757	0.429	0.747	0.583
2000	0.730	457	0.787	0.748	0.424	0.781	0.576

Appendix J: Non-linear curve fit for model

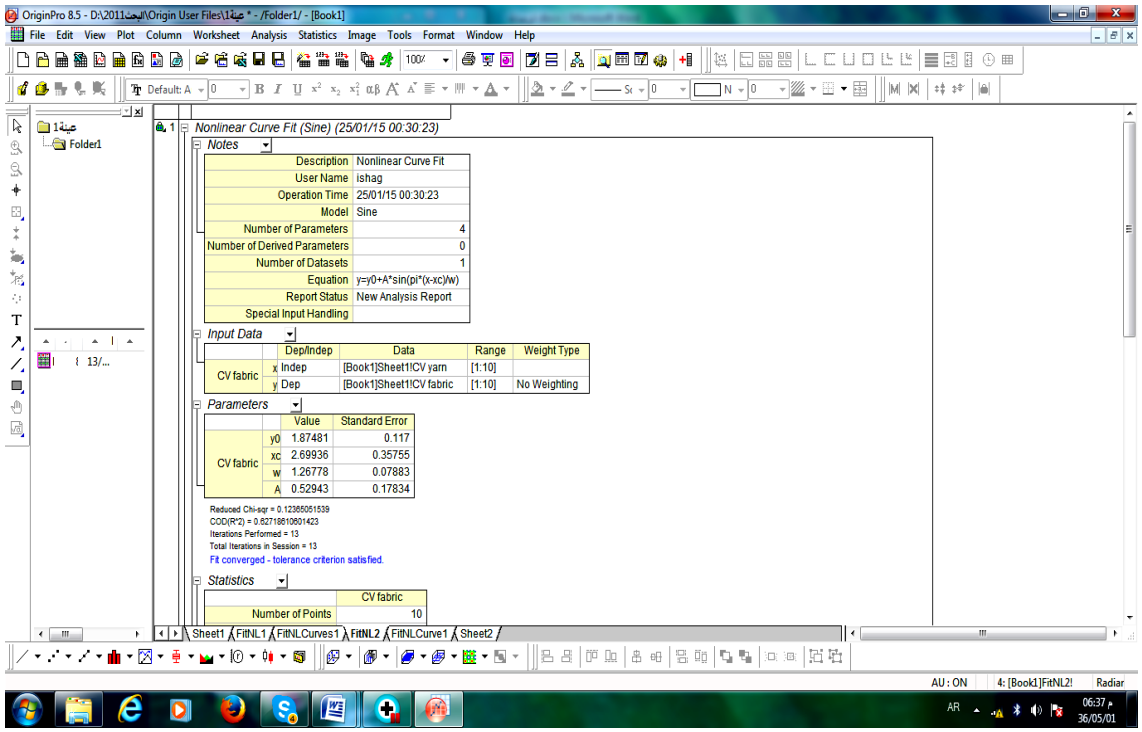

Nonlinear Curve Fit (Sine) (25/01/15 00:30:23)

Notes

Description	Nonlinear Curve Fit
User Name	ishag
Operation Time	25/01/15 00:30:23
Model	Sine
Number of Parameters	4
Number of Derived Parameters	0
Number of Datasets	1
Equation	y=y0+A*sin(pi*(x-xc)/w)
Report Status	New Analysis Report
Special Input Handling	

Input Data

		Dep/Indep	Data	Range	Weight Type
CV fabric	x	Indep	[Book1]Sheet1!CV yarn	[1:10]	
	y	Dep	[Book1]Sheet1!CV fabric	[1:10]	No Weighting

Parameters

		Value	Standard Error
CV fabric	y0	1.87481	0.117
	xc	2.69936	0.35755
	w	1.26778	0.07883
	A	0.52943	0.17834

Reduced Chi-sqr = 0.12365051539
COD(R^2) = 0.62718610801423
Iterations Performed = 13
Total Iterations in Session = 13
Fit converged - tolerance criterion satisfied.

Statistics

	CV fabric
Number of Points	10

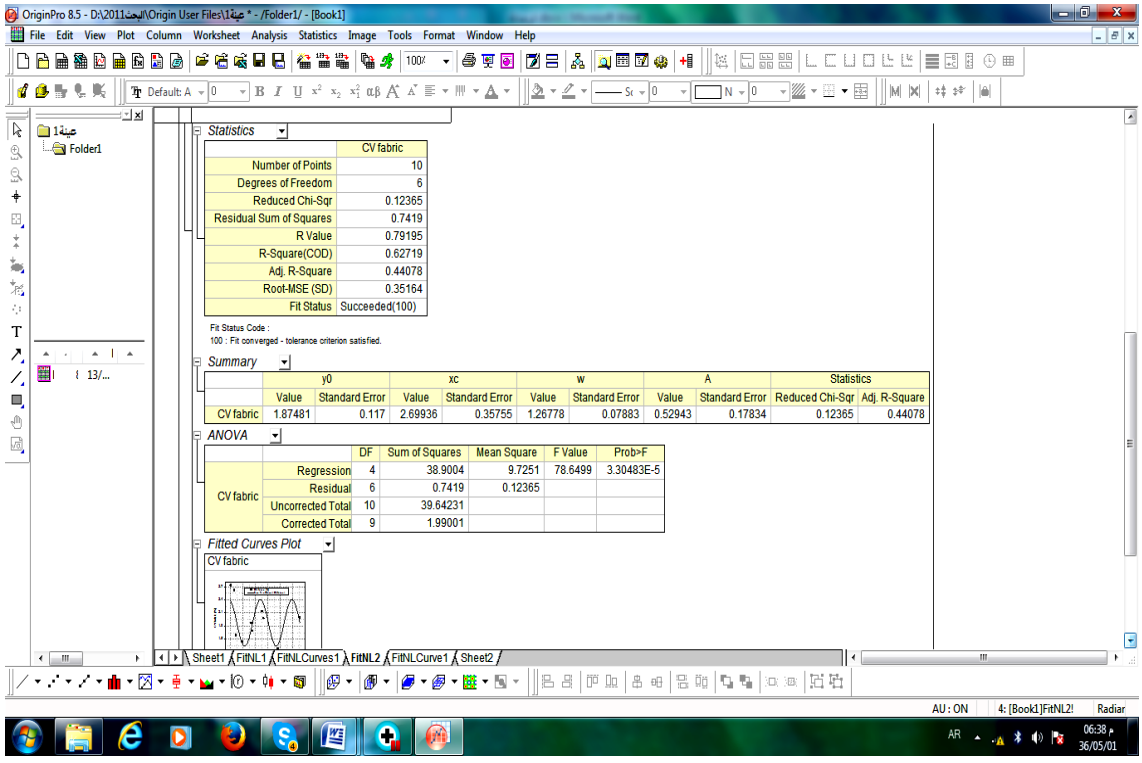

Statistics

	CV fabric
Number of Points	10
Degrees of Freedom	6
Reduced Chi-Sqr	0.12365
Residual Sum of Squares	0.7419
R Value	0.79195
R-Square(COD)	0.62719
Adj. R-Square	0.44078
Root-MSE (SD)	0.35164
Fit Status	Succeeded(100)

Fit Status Code :
100 : Fit converged - tolerance criterion satisfied.

Summary

	y0		xc		w		A		Statistics	
	Value	Standard Error	Value	Standard Error	Value	Standard Error	Value	Standard Error	Reduced Chi-Sqr	Adj. R-Square
CV fabric	1.87481	0.117	2.69936	0.35755	1.26778	0.07883	0.52943	0.17834	0.12365	0.44078

ANOVA

		DF	Sum of Squares	Mean Square	F Value	Prob>F
CV fabric	Regression	4	38.9004	9.7251	78.6499	3.30483E-5
	Residual	6	0.7419	0.12365		
	Uncorrected Total	10	39.64231			
	Corrected Total	9	1.99001			

Fitted Curves Plot

CV fabric

Appendix K: Non-linear curve fit for model 2

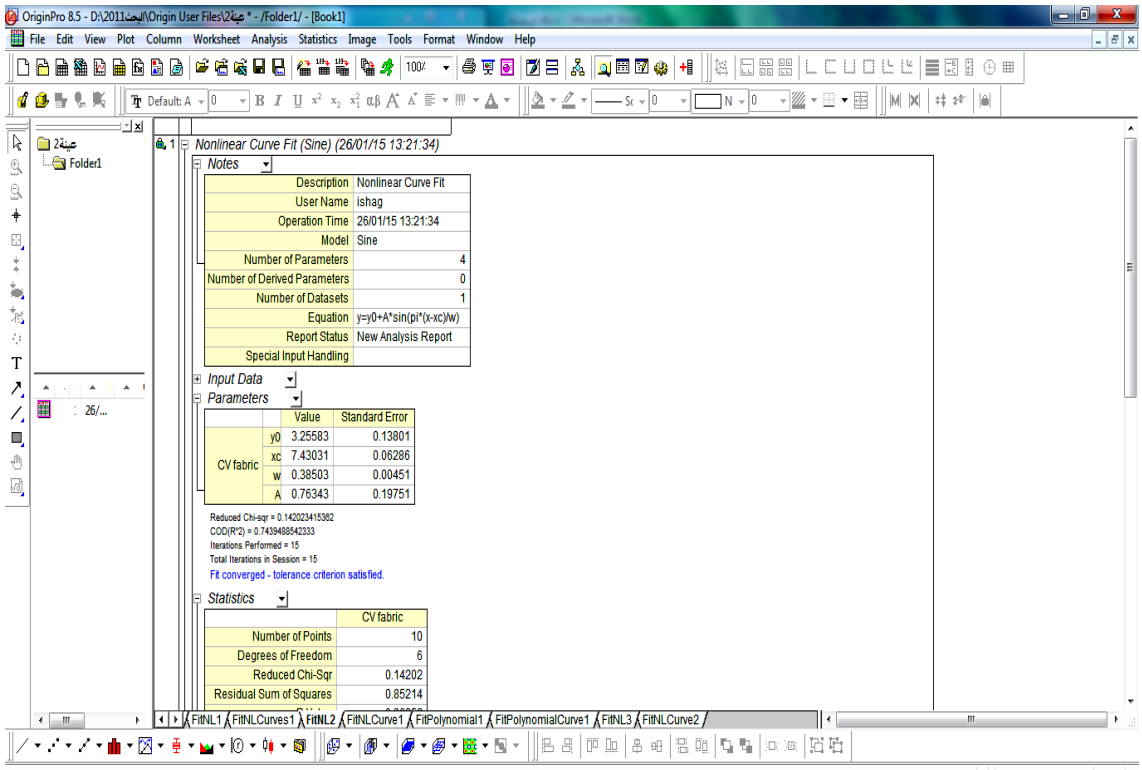
OriginPro 8.5 - D:\2011البحث\Origin User Files\عينة2 * - /Folder1/ - [Book1]
File Edit View Plot Column Worksheet Analysis Statistics Image Tools Format Window Help
عينة2
Folder1
Nonlinear Curve Fit (Sine) (26/01/15 13:21:34)
Notes
Description Nonlinear Curve Fit
User Name ishag
Operation Time 26/01/15 13:21:34
Model Sine
Number of Parameters 4
Number of Derived Parameters 0
Number of Datasets 1
Equation y=y0+A*sin(pi*(x-xc)/w)
Report Status New Analysis Report
Special Input Handling
Input Data
Parameters
Value Standard Error
CV fabric y0 3.25583 0.13801
xc 7.43031 0.06286
w 0.38503 0.00451
A 0.76343 0.19751
Reduced Chi-sqr = 0.142023415362
COD(R^2) = 0.743948842333
Iterations Performed = 15
Total Iterations in Session = 15
Fit converged - tolerance criterion satisfied.
Statistics
CV fabric
Number of Points 10
Degrees of Freedom 6
Reduced Chi-Sqr 0.14202
Residual Sum of Squares 0.85214
FitNL1 FitNLCurves1 FitNL2 FitNLCurve1 FitPolynomial1 FitPolynomialCurve1 FitNL3 FitNLCurve2
AU : ON
4: [Book1]FitNL2!
Radiar

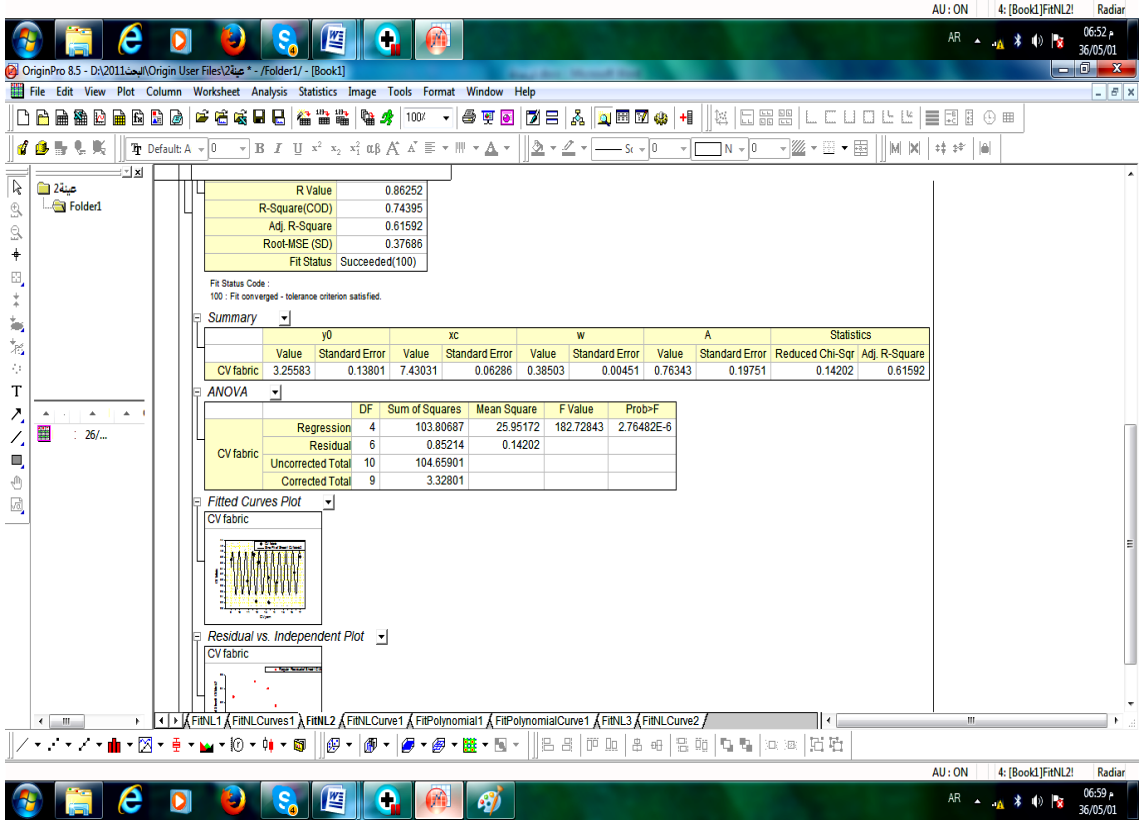
OriginPro 8.5 - D:\2011البحث\Origin User Files\عينة2 * - /Folder1/ - [Book1]
R Value 0.86252
R-Square(COD) 0.74395
Adj. R-Square 0.61592
Root-MSE (SD) 0.37686
Fit Status Succeeded(100)
Fit Status Code :
100 : Fit converged - tolerance criterion satisfied.
Summary
y0 xc w A Statistics
Value Standard Error Value Standard Error Value Standard Error Value Standard Error Reduced Chi-Sqr Adj. R-Square
CV fabric 3.25583 0.13801 7.43031 0.06286 0.38503 0.00451 0.76343 0.19751 0.14202 0.61592
ANOVA
DF Sum of Squares Mean Square F Value Prob>F
CV fabric Regression 4 103.80687 25.95172 182.72843 2.76482E-6
Residual 6 0.85214 0.14202
Uncorrected Total 10 104.65901
Corrected Total 9 3.32801
Fitted Curves Plot
CV fabric
Residual vs. Independent Plot
CV fabric
FitNL1 FitNLCurves1 FitNL2 FitNLCurve1 FitPolynomial1 FitPolynomialCurve1 FitNL3 FitNLCurve2
AU : ON
4: [Book1]FitNL2!
Radiar

Appendix L: Non-linear curve fit for model 3

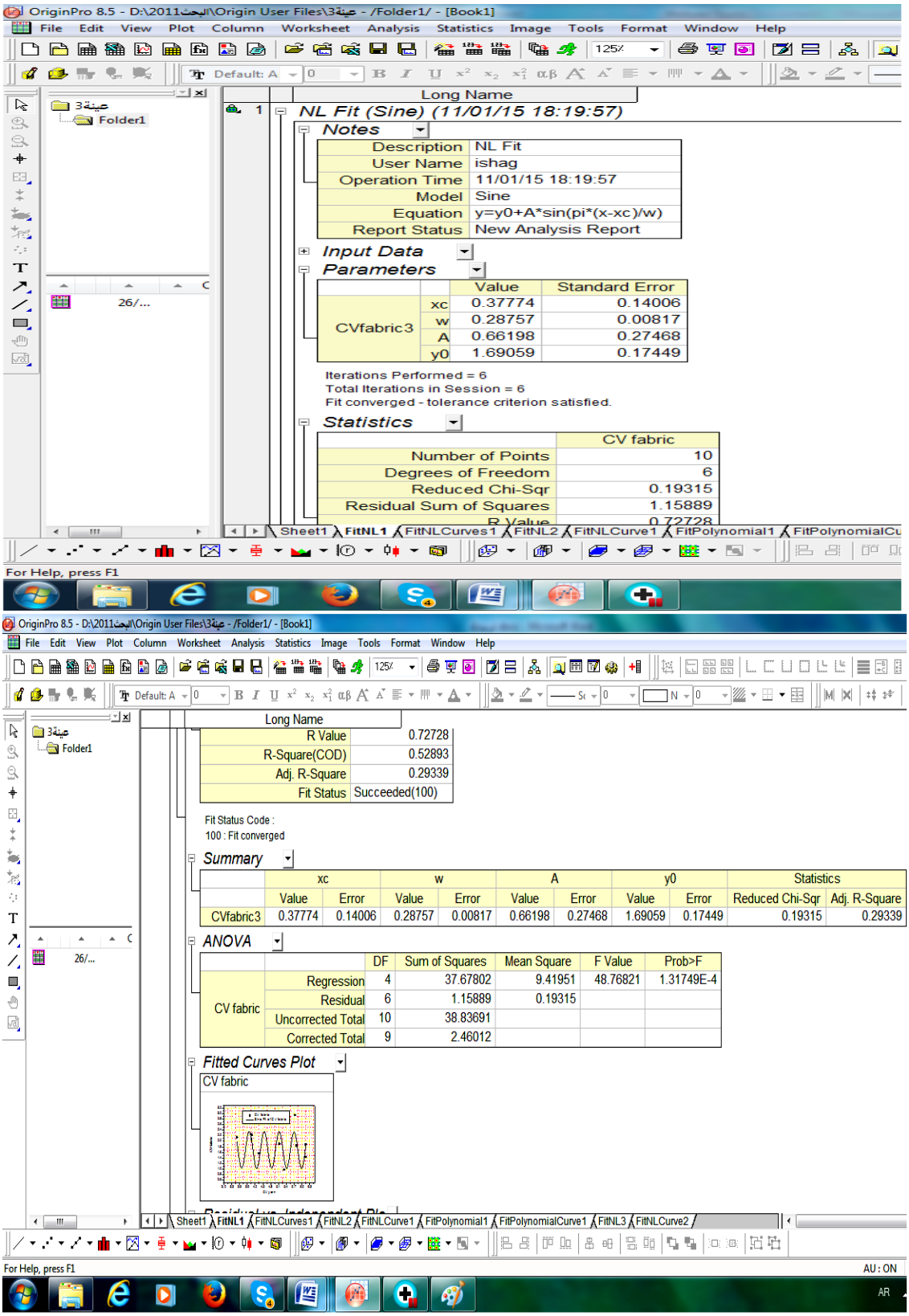

Appendix M: Non-linear curve fit for model 4

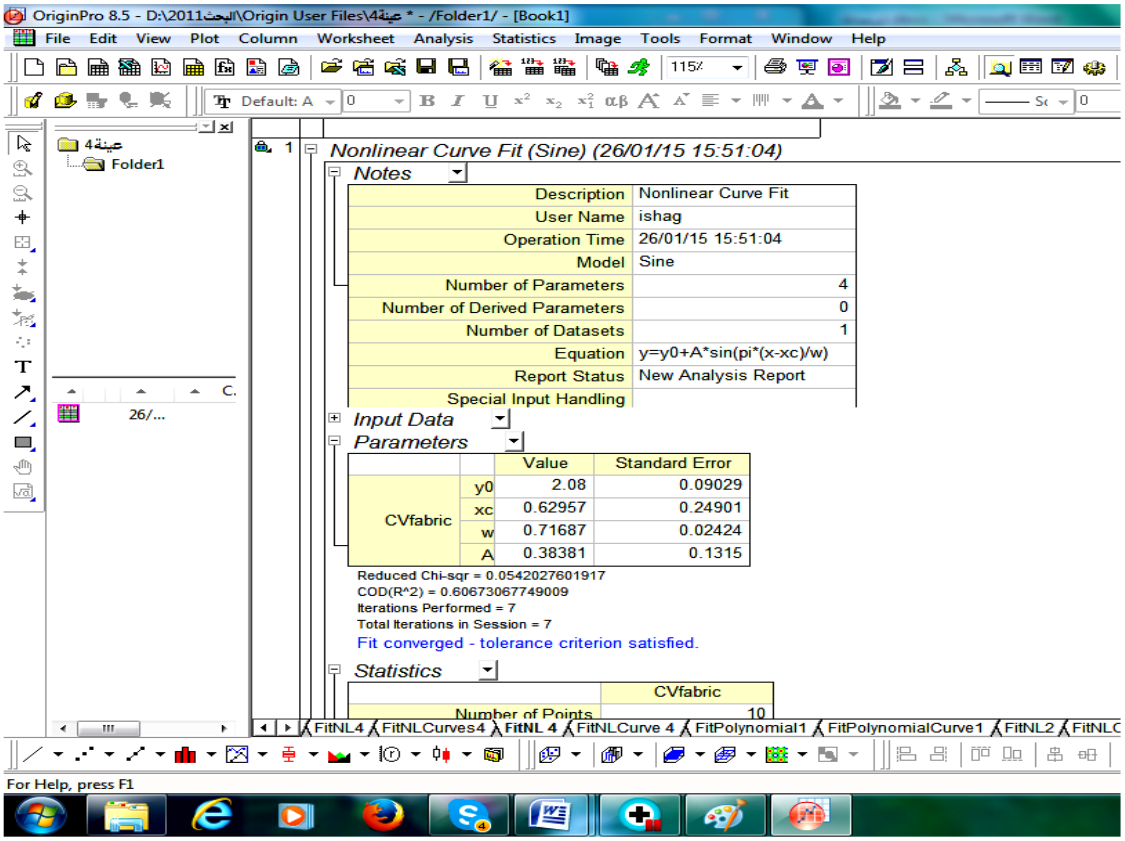

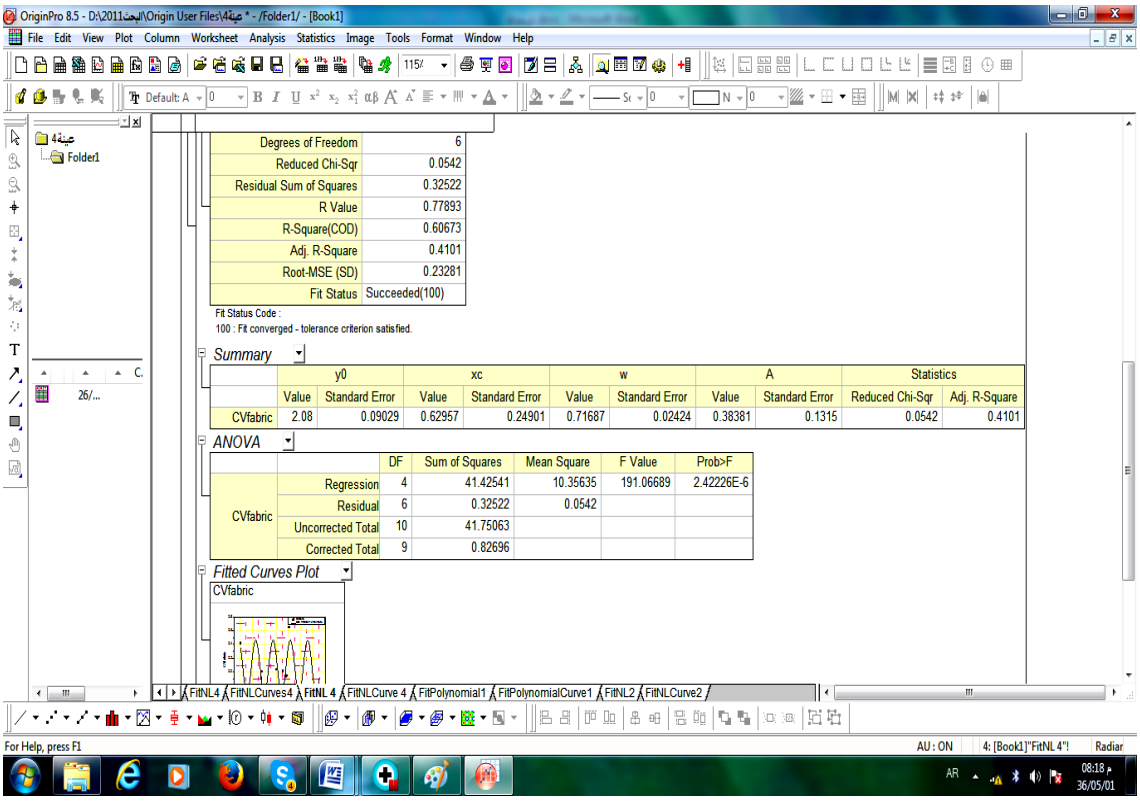

Appendix N: Non-linear curve fit for model 5

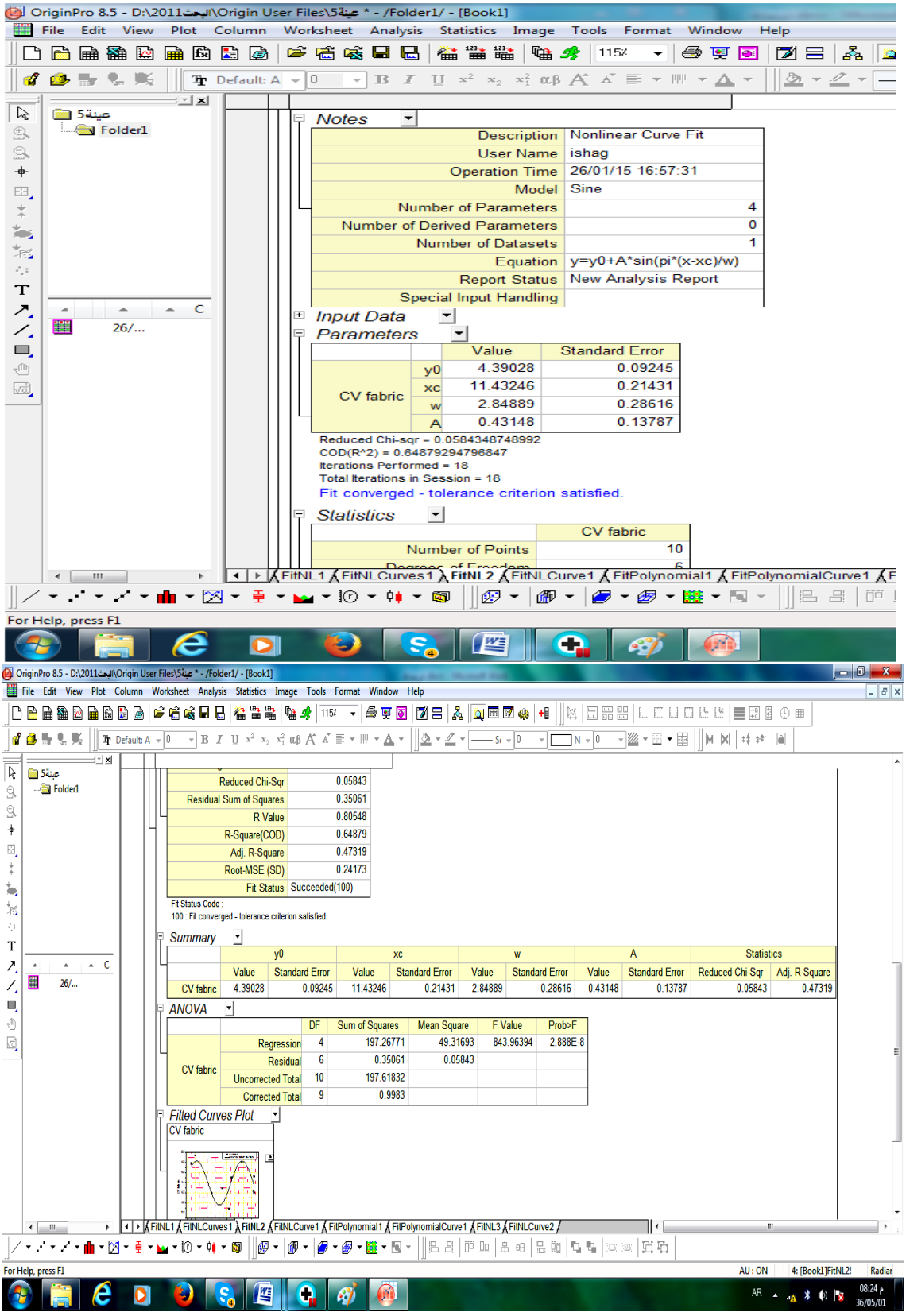

Notes

Description	Nonlinear Curve Fit
User Name	ishag
Operation Time	26/01/15 16:57:31
Model	Sine
Number of Parameters	4
Number of Derived Parameters	0
Number of Datasets	1
Equation	y=y0+A*sin(pi*(x-xc)/w)
Report Status	New Analysis Report
Special Input Handling	

Input Data

Parameters

		Value	Standard Error
CV fabric	y0	4.39028	0.09245
	xc	11.43246	0.21431
	w	2.84889	0.28616
	A	0.43148	0.13787

Reduced Chi-sqr = 0.0584348748992
COD(R^2) = 0.64879294796847
Iterations Performed = 18
Total Iterations in Session = 18
Fit converged - tolerance criterion satisfied.

Statistics

	CV fabric
Number of Points	10

Reduced Chi-Sqr	0.05843
Residual Sum of Squares	0.35061
R Value	0.80548
R-Square(COD)	0.64879
Adj. R-Square	0.47319
Root-MSE (SD)	0.24173
Fit Status	Succeeded(100)

Fit Status Code :
100 : Fit converged - tolerance criterion satisfied.

Summary

	y0		xc		w		A		Statistics	
	Value	Standard Error	Value	Standard Error	Value	Standard Error	Value	Standard Error	Reduced Chi-Sqr	Adj. R-Square
CV fabric	4.39028	0.09245	11.43246	0.21431	2.84889	0.28616	0.43148	0.13787	0.05843	0.47319

ANOVA

		DF	Sum of Squares	Mean Square	F Value	Prob>F
CV fabric	Regression	4	197.26771	49.31693	843.96394	2.888E-8
	Residual	6	0.35061	0.05843		
	Uncorrected Total	10	197.61832			
	Corrected Total	9	0.9983			

Fitted Curves Plot

CV fabric

Appendix O: Non-linear curve fit for model 6

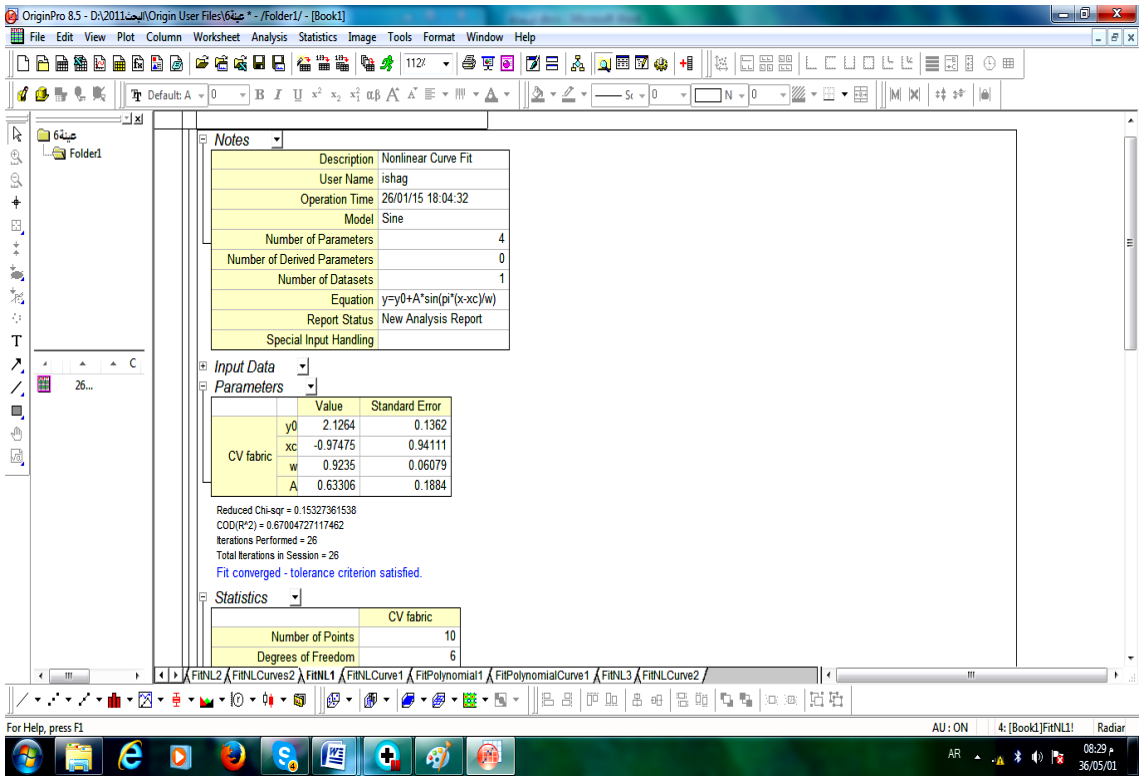

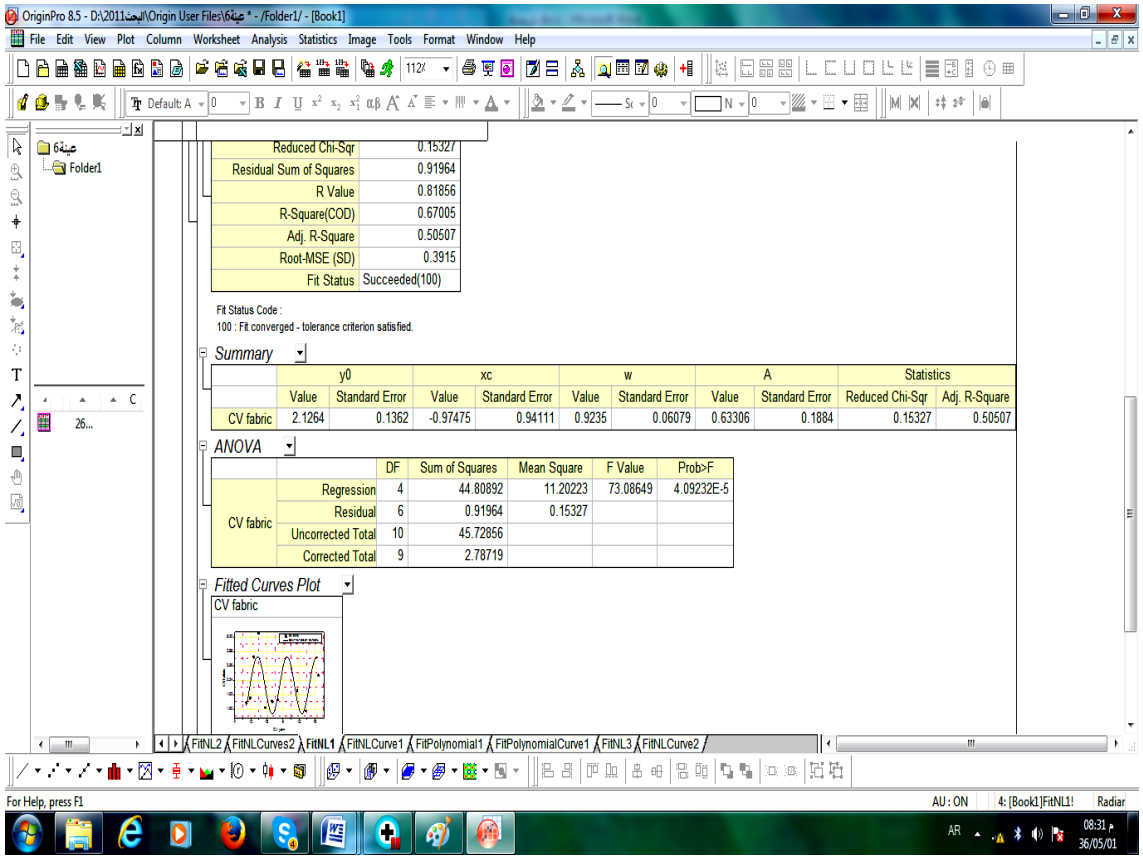

Appendix P: Non-linear curve fit for model 7